TWO-LEVEL OPTIMIZATION OF COMPOSITE WING STRUCTURES BASED ON PANEL GENETIC OPTIMIZATION

By

BOYANG LIU

A DISSERTATION PRESENTED TO THE GRADUATE SCHOOL
OF THE UNIVERSITY OF FLORIDA IN PARTIAL FULFILLMENT
OF THE REQUIREMENTS FOR THE DEGREE OF
DOCTOR OF PHILOSOPHY

UNIVERSITY OF FLORIDA

2001

ACKNOWLEDGMENTS

First I thank Distinguished Professor Raphael T. Haftka, chairman of my advisory committee, for much-needed guidance during my research. He provided the funding necessary to complete my doctoral studies and constantly encouraged me to attend conferences and to publish my work in scientific journals. His help extended beyond problems encountered in the academic world. I sometimes wondered where he found the patience he always had with me. Without it, this work would not have been possible.

I would like to thank my wife, Peining Chen, for the support, patience and encouragement that she gave me during these years.

I would also like to thank the members of my committee: Professors Bhavani V. Sankar, Loc Vu-Quoc, Gale E. Neville and Panagote M. Pardalos. I am grateful for their willingness to serve on my committee, their help whenever required, their involvement with my oral qualifying examination, and their review of this dissertation.

I would also like to thank professors Mehmet A. Akgün from Middle East Technical University, Turkey; Akira Todoroki, from Tokyo Institute of Technology, Tokyo, Japan; Fred Van Keulen, from Delft University of Technology, Delft, The Netherlands and Philippe Trompette, University of Lyon, France. I enjoyed collaborating with them during their stay at the University of Florida.

My colleagues in the Structural and Multidisciplinary Optimization Group at the University of Florida also deserve thanks for their help, and for their many fruitful discussions.

TABLE OF CONTENTS

LIST OF TABLES

LIST OF FIGURES

Abstract of Dissertation Presented to the Graduate School
of the University of Florida in Partial Fulfillment of the
Requirements for the Degree of Doctor of Philosophy

TWO-LEVEL OPTIMIZATION OF COMPOSITE WING STRUCTURES BASED ON PANEL GENETIC OPTIMIZATION

By

Boyang Liu

May 20001

Chairman: Professor Raphael T. Haftka
Major Department: Aerospace Engineering, Mechanics, and Engineering Science

The design of complex composite structures used in aerospace or automotive vehicles presents a major challenge in terms of computational cost. Discrete choices for ply thicknesses and ply angles leads to a combinatorial optimization problem that is too expensive to solve with presently available computational resources. We developed the following methodology for handling this problem for wing structural design: we used a two-level optimization approach with response-surface approximations to optimize panel failure loads for the upper-level wing optimization. We tailored efficient permutation genetic algorithms to the panel stacking sequence design on the lower level. We also developed approach for improving continuity of ply stacking sequences among adjacent panels.

The decomposition approach led to a lower-level optimization of stacking sequence with a given number of plies in each orientation. An efficient permutation genetic

algorithm (GA) was developed for handling this problem. We demonstrated through examples that the permutation GAs are more efficient for stacking sequence optimization than a standard GA. Repair strategies for standard GA and the permutation GAs for dealing with constraints were also developed. The repair strategies can significantly reduce computation costs for both standard GA and permutation GA.

A two-level optimization procedure for composite wing design subject to strength and buckling constraints is presented. At wing-level design, continuous optimization of ply thicknesses with orientations of 0°, 90°, and ±45° is performed to minimize weight. At the panel level, the number of plies of each orientation (rounded to integers) and inplane loads are specified, and a permutation genetic algorithm is used to optimize the stacking sequence. The process begins with many panel genetic optimizations for a range of loads and numbers of plies of each orientation. Next, a cubic polynomial response surface is fitted to the optimum buckling load. The resulting response surface is used for wing-level optimization.

In general, complex composite structures consist of several laminates. A common problem in the design of such structures is that some plies in the adjacent laminates terminate in the boundary between the laminates. These discontinuities may cause stress concentrations and may increase manufacturing difficulty and cost. We developed measures of continuity of two adjacent laminates. We studied tradeoffs between weight and continuity through a simple composite wing design.

Finally, we compared the two-level optimization to a single-level optimization based on flexural lamination parameters. The single-level optimization is efficient and feasible for a wing consisting of unstiffened panels.

CHAPTER 1
INTRODUCTION

Introduction

Because of higher stiffness-to-weight or strength-to-weight ratios compared to isotropic materials, composite laminates are becoming more popular. Composite structures typically consist of laminates stacked from layers with different fiber orientation angles. The layer thickness is normally fixed, and fiber orientation angles are often limited to a discrete set such as 0°, ±45,° and 90°. This leads to an expensive combinatorial optimization for designing composite structures. In addition, design of complex and large aircraft structures, like a wing, requires sizing of local details of stiffened panels in the wing (rib and skin panels). Details include stiffener shape and dimensions, stiffener spacing, and choice of laminates for each part. The design of each panel requires a substantial number of variables to describe geometry, ply composition, and stacking sequence. Designing all the panels simultaneously constitutes a complex optimization problem that requires detailed structural modeling of the entire wing, and appears to be beyond present computational capabilities.

One approach to reducing the complexity of the optimization problem is to decompose it to smaller optimization problems in a process of multilevel optimization. Early studies developed multilevel formulations to wing structural design (Giles 1971; Schmit & Ramannathan 1978, Schmit & Mehrinfar 1982; Sobieszczanski-Sobieski & Leondorf 1972, Sobieszczanski-Sobieski et al. 1985). Multilevel structural optimization in

general consists of lower-level optimization for substructures and coordination optimization, which exchanges information among the lower-level optimizations.

Similar decomposition techniques are naturally applied in multidisciplinary design, which became a popular research area in the last twenty years. Multidisciplinary optimization (MDO) problems involve several disciplines, and often have no clear hierarchy between disciplines. Two popular approaches for MDO problems are concurrent subspace optimization (CSSO) developed by Sobieszczanski-Sobieski (1988) and collaborative optimization (CO) developed by Kroo (1995).

In Schmit's approach for multilevel structural optimization and in CSSO and CO for MDO, equality constraints are used explicitly or implicitly in the coordination process. The use of equality constraints can lead to numerical difficulties (Thareja & Haftka, 1986) and even invalidate some formulations, as recently noted by Alexandrov and Lewis (2000) for the CO approach. Even without the difficulties associated with equality constraints, multilevel optimization can introduce numerical difficulties because lower-level optima are non-smooth and noisy functions of upper-level parameters.

Response surface approaches fit data in the design domain with simple functions, usually polynomials. Response surfaces smooth out noise, are simple, and easily integrate different application packages. The technique therefore seems a promising approach for easing the numerical difficulties in multilevel structural design or MDO problems.

Complex composite structures, such as aircraft wing or fuselage structures or car chassis structures, commonly consist of multiple laminates. Because of different fiber orientation angles of layers, or different layer thickness, or different type of layer materials, discontinuities between adjacent panels or other components are produced. The

discontinuities can cause stress concentration, reduce strength and increase manufacturing difficulty. Even though in many cases discontinuity among adjacent panels is inevitable, we may be able to reduce discontinuity if discontinuity measures are included in the design process.

Two-level Optimization for Composite Wing Structures

Because of the high computational cost of single-level optimization for composite wing box design, current practice is to design composite wing structures at two levels. At the wing level, individual panels are modeled without much detail, and few design variables are assigned to each. Global constraints such as aeroelastic stability are enforced along with simple stress or strain limits using finite element based structural optimization programs such as NASTRAN (CSA/NASTRAN 1995), GENESIS (Vanderplaats 1997) or ADOP (Sharma et al. 1993). The internal load distribution obtained by wing optimization is then used as input to panel-design optimization programs, such as PANDA2 (Bushnell 1987) or PASCO (Stroud & Anderson 1981). These programs obtain detailed geometry and ply compositions for individual panels that satisfy buckling and various local strength failure constraints.

For complex configurations, coordination of the local-level (panel) and upper-level (wing) optimization problems is currently handled largely by ad-hoc methods that are cumbersome and sub optimal. As noted in the previous section, two-level optimization can be ill-conditioned because the lower-level (panel) optima are not smooth functions of upper-level (wing) design variables.

Response surface (RS) techniques offer an attractive way of overcoming both implementation and smoothness difficulties. The RS approach to a two-level optimization

is to perform a large number of lower-level optimizations for different values of the global design variables and loads. Then the results of the lower-level optimizations are fitted with response surfaces, typically low-order polynomials. Finally, upper-level optimization is performed with RS substituting for lower-level optimization. This approach eases implementation problems associated with software integration, as lower-level optimization program can be run independently of the upper-level analysis and optimization. In addition, the RS smoothes out the lower-level optima.

Ragon et al. (1997) demonstrated this approach by fitting a response surface to the optimum weights of stiffened panels designed using PASCO (Stroud et al. 1981) as a function of panel loading and inplane-stiffness constraints specified by the wing-level optimizer. The resulting response surface was used by the wing optimizer, ADOP (Sharma et al. 1993). A similar approach was also used by Balabanov et al. (1999) for a two-level aerodynamic-structural optimization. There the wing structural weight was fitted as a function of aerodynamic shape parameters. The present work extends this technique for the case in which the panel-level design involves discrete or combinatorial optimization, such as stacking sequence design of composite laminates. In addition, Ragon et al. (1997) had trouble with their approach because for some combinations of stiffness constraints, there were no feasible solutions for the panel-optimization problem. Here we overcome this problem by maximizing the load-carrying capacity of the panel for a fixed-weight budget. We demonstrate the methodology for design of a simple wing structure, where a permutation genetic algorithm performs the panel design.

Genetic Algorithms for Panel Optimization

Stacking sequence design of composite laminates is a local problem that is strongly coupled to the overall design of complex composite structures. In complex composite structures, the overall design imposes constraints on individual panel design. The optimization of the overall structure often specifies number of 0°, ±45,° and 90° plies, and inplane loads on each panel. Therefore, the stacking-sequence design is often limited to permutations of a given set of plies. For given inplane loads, and a given number of plies of 0°, ±45° and 90° directions, stacking-sequence optimization is a combinatorial design problem.

Genetic algorithms (GAs) are a popular technique for solving integer and combinatorial optimization problems. In structural optimizations, Genetic algorithms have been applied to integer problems. (Furuya & Haftka 93, Hajela 90, Hajela 1991, Hajela & Lin 1992, Rao 1990, Watabe & Okino 1993). Of course, GAs have been used in composite laminate design (Le Riche & Haftka 1993, 1995; Nagendra et al. 1993).

However, Genetic algorithms are often too expensive when analysis of one candidate solution is computationally expensive, and they do not deal efficiently with constraints. When applied to panel stacking sequence design, constraints on the number of plies come from the wing design. It is possible to use a conventional genetic algorithm. However, available permutation GAs developed mostly for scheduling problems (Michalewicz 1992) are more efficient in the search for an optimal permutation because they reduce the dimensionality of the design space.

Permutation GAs were mostly developed for the traveling salesman problem, which seeks to minimize travel costs for a given list of towns and is insensitive to where

the sequence starts, so that cyclical permutations do not matter. In stacking sequence design, a cyclical permutation moves the outermost ply into the innermost position, and thus greatly influences the bending properties of the laminate.

Therefore, this work seeks to develop permutation GAs more tailored for the stacking sequence design problem. GAs usually handle violations of constraints by penalty functions which are added to the objective function. However, penalty-function approaches often slow down the convergence speed of GAs. In this study, we tested the use of repair strategies that deal with violations of constraints by repairing the laminate to satisfy the constraints (Todoroki & Haftka 1998).

Material Composition Continuity Constraints Between Adjacent Panels

In the design of complex structures, it is customary to divide the structure into panels or regions that may be designed independently or semi-independently (Liu et al. 2000, Ragon et al. 1997, Schmit & Mehrinfar 1982). This is done not only for computational convenience, but because the loads vary from one part of the structure to another, so that structural efficiency dictates variation in structural properties. With this design approach, adjacent laminates may have different total thicknesses, and some plies may terminate at the laminate boundaries. These discontinuities can cause stress concentrations and increase manufacturing difficulty and cost.

While some discontinuities are inevitable if structural efficiency is to be maintained, it is desirable to minimize these discontinuities. It is therefore desirable to add continuity constraints for adjacent laminates in the design process, or to include a measure of continuity in evaluating competing designs. It may be expected that optimization including continuity constraints may lead to designs with fewer and smaller discontinuities.

Kristinsdottir et al. (2001) recently developed a concept named blending rule to measure ply continuity in adjacent composite panels. The basic idea is to follow plies from the region they originate until they terminate. Each ply stems from its key region (the most heavily loaded region) and may cover any number of regions as long as they are adjacent to one another. A ply is allowed to be dropped (discontinued) and is allowed to build up plies at load concentrations. The fiber angle of a ply is held fixed for the entire coverage of that ply. Dropping plies in a consistent manner means that once a ply is dropped, the ply is not added back into the panel.

Comparing results with blending measure and results without blending measure, design with blending is heavier than design without blending but design with blending is easier to manufacture.

The blending approach of Kristinsdottir et al. (2001) is focused on a design approach that limits discontinuities in a prescribed manner. Here the emphasis instead is on measuring the degree of discontinuity so that it can be incorporated as a measure of design performance. One objective of the present work is to develop such measures. Two continuity measures are defined in terms of material composition and stacking sequence. The continuity measures are applied to a simple wing design problem, and trade-off studies between weight and continuity are performed

Single-Level Optimization of Composite Wing Based on Flexural Lamination Parameters.

While the two-level optimization approach makes intuitive sense, we do not have any proof that it will converge to optimal or near optimal designs. Therefore, it is desirable to find an alternative optimization that will check the optimality. We develop a continuous optimization approach based on flexural lamination parameters for this purpose.

This approach, which disregards the discreteness of the problem and some of the constraints, provides a lower bound for the optimal weight.

Lamination parameters, consisting of inplane and flexural lamination parameters (Tsai et al., 1980), provide a compact representation of the stiffness properties of composite laminates. They allow efficient approximate optimization of laminates for desired stiffness properties. Miki (1986) developed a graphical procedure for the design optimization. Miki and Sugiyama (1991, 1993), Fukunaga and Sekine (1992, 1994) graphically solved stacking sequence design problems for stiffness and strength maximization of symmetric laminates using lamination parameters. The simple graphical approach also allows us to see that for many problems the optimal design lies on the boundary of the lamination parameter space, corresponding to angle ply designs (Grenestedt & Gudmandson 1993). Nagendra *et al.* (1996), Todoroki & Haftka (1998), Yamazaki (1996) demonstrated the use of lamination parameters in applications of composite laminate design.

The primary objective for introducing lamination parameters is to provide a single-level continuous optimization to verify optimality of the two-level optimization approach. However, we can also apply ply stacking sequence continuity constraints for multiple adjacent panels based on these lamination parameters.

Objectives

This dissertation develops an approach for design of complex composite structures such as a composite wing based on available technologies. First, efficient and robust permutation GAs characterized random search nature were developed for stacking sequence optimization for composite laminates to maximize buckling failure load. Next,

two-level optimization approach was used for overall wing design, with response surfaces generated from panel optima used as an interface to couple with wing-level design. Third, we developed continuity constraints among adjacent panels to cope with discontinuity, stress concentration and high manufacturing cost. Finally, we developed continuous variable optimization algorithms based on flexural lamination parameters for panel optimization and wing optimization. We constructed response surfaces of continuity constraints of ply stacking sequence based on flexural parameters and checked the optimization results of the two-level approach. The four objectives of the dissertation are as follows:

1) Develop efficient and robust permutation GAs for stacking sequence optimization of composite laminates.
2) Develop a two-level optimization approach for composite wing design based on panel genetic optima.
3) Develop two types of continuity constraints between two adjacent panels and study tradeoff between weight and continuity.
4) Develop a continuous-optimization procedure based on flexural lamination parameters and use them to test the optimality of the two-level optimization results.

Contents

Chapter 2 provides a literature review of two-level optimization and GAs applied in structural design. Chapter 3 discusses the development of an efficient permutation genetic algorithm for stacking sequence design of composite laminates. Chapter 4 describes an algorithm for optimizing an entire composite wing structure by integrating wing optimization with panel optimization via response surface techniques. Chapter 5 describes how to design all panels' stacking sequence together by including material composition continuity constraints among adjacent panels and study tradeoff between weight and continuity. Chapter 6 describes a continuous variable optimization based on

flexural lamination parameters for panel and wing optimization. Chapter 7 provides concluding remarks and recommendations for future work.

CHAPTER 2
BACKGROUND

Multilevel Structural Optimization

Exorbitant computer resources are required for the design of realistic structures carrying a large number of loading cases and having many components that need design variables to describe detailed geometry, direct one-level optimization. The computational resources required for the solution of an optimization problem typically increase with dimensionality of the problem at a rate that is more than linear. That is, if we double the number of design variables in a problem, the cost will typically more than double. One obvious solution is to break up large optimization problems into smaller subproblems and a coordination problem to preserve the couplings among these subproblems.

One important benefit of this approach is that it makes the big problem more tractable and allows simultaneous work on different parts of the problem. The latter advantage also matches the trend of computer technology development, where distributed and parallel processing are becoming more popular. Moreover, to break a big problem into several small problems is natural in engineering optimization because engineers tend to work in teams concentrating on parts of a project in order to develop a broad work front in order to shorten development time.

Early approaches to applying multilevel optimization to minimum weight design of complex structures such as wing and fuselage were based on the fully stressed design (FSD) method. The FSD method is an optimality criteria method. The FSD optimality criterion is that for optimum design, each member of the structure that is not at its minimum

gage is fully stressed by at least one of the design-load conditions. The FSD technique applies to structures that are subject to only stress and minimum gage constraints. The FSD approach implies that we should remove material from members that are not fully stressed unless minimum gage constraints are prevented. This method has been used extensively for aerospace structures (Lansing et al. 1971, Giles 1971). In applying the FSD method, the overall structure (such as fuselage or wing) is represented in a lumped model in which stringers, rings, and skins are represented only in a coarse manner. The detailed design of the lumped-model components is then carried out by mathematical programming with sizing design variables (e.g., skin thickness). This is essential by a two-level approach. Sobieszczanski-Sobieski and Leondorf (1972) developed a mixed-optimization method combining FSD for structure system and mathematical programming for components for preliminary design of fuselages. Giles (1971) developed an automated preliminary program called Design of Aircraft Wing Structures (DAWNS) for wing design. In DAWNS, the external shape, aerodynamics loads, structural geometry, internal loads, and fuel mass were included to obtain optimal wing by a FSD method.

Schmit and Ramannathan (1978) found two main shortcomings to the above approaches: the use of weight as the objective function at the component level and the use of fully stressed type resizing algorithms at the system level. As Sobieszczanski-Sobieski (1972) and Schmit et al. (1978, 1982) noted, the minimum weight structural system is not necessarily made up from a collection of minimum weight components. To cope with this problem, Schmit et al. (1978, 1982) later developed a multilevel approach wherein system-level and component-level design phases are characterized as follows: 1) at the system level, minimize the total structural weight subject to the system level constraints

such as displacements, system buckling, and strength, and 2) for each component, minimize the change in equivalent system stiffness subject to local strength and buckling constraints.

We denote the system design variables as $\underline{S}$ and denote by $\underline{L}$ the concatenation of $\underline{l}_j$, $j=1,\ldots M$, the local design variable vector for all M components. A standard formulation for single-level optimization can be stated as follows:

$$\begin{aligned} &\textbf{Minimize} \quad W(\underline{S}) \\ &\textbf{such that} \quad G_q(\underline{S},\underline{l}) \geq 0; \quad q \in Q \\ &\textbf{and} \\ &\qquad g_{lj}(\underline{l}_j,\underline{S}) \geq 0, \quad \underline{l}_j \in \underline{L}; \quad j \in M \end{aligned} \tag{2-1}$$

Where W is the total system weight and objective function. Here, G_q are system constraints which strongly depend on system design variables $\underline{S}$, like displacement, stress, system buckling constraints, Q represents the set of system level constraints. Component constraints are g_{lj} that primarily depend on the detailed component design variable vector $\underline{l}_j$. Now the design problem (2-1) is decomposed into a multilevel optimization problem as follows:

At system level,

$$\begin{aligned} &\textbf{Minimize} \quad W(\underline{S}) \\ &\textbf{such that} \quad G_q(\underline{S},\underline{l}^*) \geq 0; q \in Q \end{aligned} \tag{2-2}$$

where $\underline{l}^*$ is the detailed design variable vector, which does not change during a system level design modification stage.

For the j_{th} component level, the objective function is to minimize the discrepancy between the component stiffness parameters K_{rj}, $j=1,\ldots R$ which may affect system response. That is, the component level optimization problem is:

$$\begin{aligned} &\textbf{Minimize } c_j = \sum_{r=1}^{R} \left(K_{rj}(\underline{S}_j^*) - K_{rj}(\underline{l}_j) \right)^2 \\ &\textbf{such that } g_{lj}(\underline{l}_j, \underline{S}^*) \geq 0; \quad \underline{l}_j \in \underline{L} \end{aligned} \tag{2-3}$$

where $\underline{S}_j^*$ is the value of the system design variables corresponding to the j_{th} component at the end of the foregoing system stage and is held invariant during the component design modification stage. Equation (2-3) essentially was a quadratic penalty function to enforce the equality constraints $K_{rj}(\underline{S}_j^*) = K_{rj}(\underline{l}_j)$

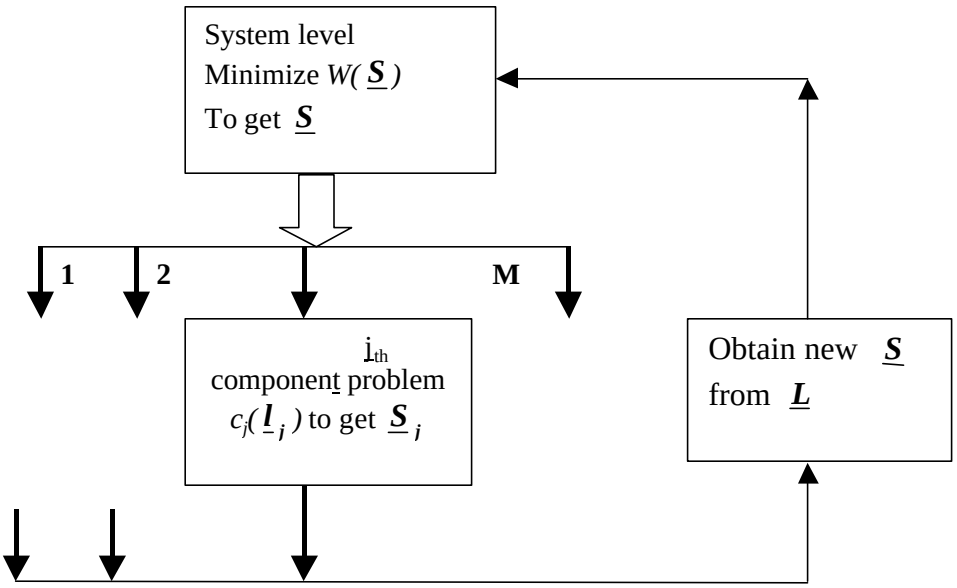

Figure 2-1: Multilevel approach

The basic idea of minimizing the change of stiffness is to reduce load redistribution at the system level due to component level synthesis. Schmit et al. (Schmit & Ramannathan 1978; Schmit & Mehrinfar 1982) coworkers successfully applied this approach into minimum weight design of truss and wing box structures with sandwich and hat-stiffened fiber-component panels.

Sobieszczanski-Sobieski (1985) developed a more general multilevel approach. Compared with Schmit's approach, Sobieszczanski-Sobieski used a cumulative constraint concept which is a number used to measure the degree of constraint violation of all constraints.

In Schmit's approach, the discrepancy between the system level and the component level was measured by c_j which is a quadratic function of the discrepancy. Sobieszczanski-Sobieski (1985) used a cumulative constraint to replace both the equality constraints between component and system level as well as the local constraints. The cumulative constraint is the Kreisselmeier-Steinhauser (KS) function,

$$KS(g_j) = \frac{1}{r} ln\left[\sum_{j=1}^{m} exp(r g_j)\right] \tag{2-4}$$

where g_j is a local constraint, r is user-defined constant, and m is the number of local constraints. Compared to the quadratic penalty function, the KS function has the advantage that it does not have zero derivative at the optimum (which, as we see later, can cause numerical difficulties). This was a conceptual improvement, since in Schmit's approach the system-level design problem does not receive any input from the local problem during its optimization.

In the system level, cumulative constraint of the components was added to the system-level constraints to assure satisfaction of all of the local constraints.

In both Schmit's and Sobieszczanski-Sobieski's approaches, equality constraints are directly or indirectly to assure consistency between the system level and the component level. However, Thareja and Haftka (1986) demonstrated via a portal frame example that numerical difficulties are introduced by using equality constraints. First, the problem was solved using a single-level formulation without equality constraints. Second, equality

constraints were introduced to create a hierarchical structure, but the problem was still solved as a single-level problem. Finally, a two-level approach that took advantage of the hierarchical structure was used. It was found that the two-level formulation solution was sensitive to the optimization parameters but the one-level formulation solution was not. Numerical difficulties were associated with the additional global variables and the presence of equality constraints. These problems are further discussed in the context of a two-level optimization approach to multidisciplinary design in the next section.

Two-level Multidisciplinary Optimization

Multidisciplinary design optimization (MDO) can be described as a methodology for the design of systems where the interaction between several disciplines must be considered, and where the designer is free to significantly affect system performance in more than one discipline. For example, the design of aircraft involves significant interaction among the disciplines of aerodynamics, structural analysis, propulsion, and control.

Typically when beginning a multidisciplinary project, a project leader must decompose the original problem and distribute the relevant parts among the existing organizational groups. The multilevel optimization approach takes the same route. Collaborative optimization (CO) is a popular example of this approach (Kroo 1995). Collaborative optimization is based on the decomposition of the system problem along the lines of the constituent disciplines.

Collaborative optimization seeks to formulate and solve the MDO problem in a way that preserves the autonomy of disciplinary calculations by eliminating those local variables to individual disciplinary subsystems from the system level using equality

constraints similar to those used in the multilevel optimization discussed previously. The values of these constraints are obtained by solving distributed low-level optimization subproblems whose objectives minimize the interdisciplinary inconsistency, subject to satisfying the disciplinary design constraints.

Collaborative optimization was first proposed by Kroo (1995), and improved by Kroo et al. (1995, 1996). The algorithms have been applied by researchers to a number of different design problems since then. Braun et al. (1996a, 1996b) applied this approach to the design of launch vehicles, and Sobieski and Kroo (1996) applied it to aircraft configuration design.

An example of a two-discipline design (Alexandrov & Lewis 2000) is used to describe CO formulation as follows:

The mathematical statement of the standard MDO formulation is

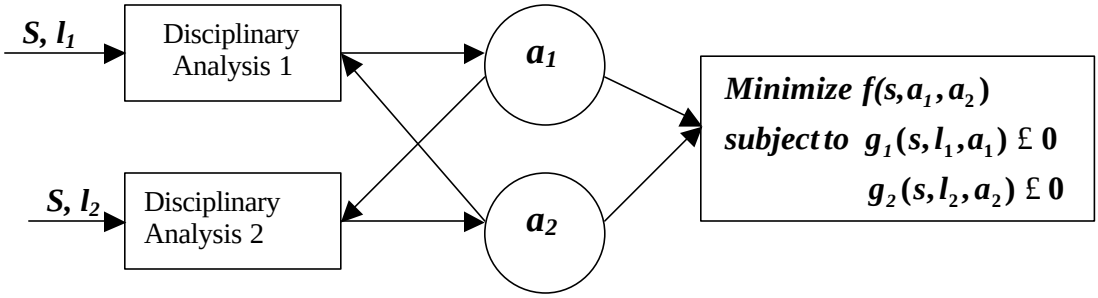

Figure 2-2: Two-level MDO problem

where s is a system variable, l_1 and l_2 are local variables that belong to discipline 1 and discipline 2 respectively; and g_1 and g_2 are discipline scope constraints; a_1 *and* a_2 are computed via the disciplinary analysis.

$$a_1 = A_1(s_1, l_1, l_2) \tag{2-5}$$

Similarly,

$$\boldsymbol{a}_2 = \boldsymbol{A}_2(s_2, \boldsymbol{l}_2, \boldsymbol{t}_1) \tag{2-6}$$

Reformulation in terms of CO can be expressed as follows:

System-level optimization which coordinates two disciplinary design as

$$\begin{aligned} &\underset{s,t_1,t_2}{\boldsymbol{Mimimize}} \quad \boldsymbol{f}(s,\boldsymbol{t}_1,\boldsymbol{t}_2) \\ &\boldsymbol{subject\ to}\ \ \underline{\boldsymbol{C}}(s,\boldsymbol{t}_1,\boldsymbol{t}_2) = 0 \end{aligned} \tag{2-7}$$

where $\boldsymbol{C}$ is called $\boldsymbol{N}$ interdisciplinary consistency constraints. $\underline{\boldsymbol{C}} = \{\boldsymbol{c}_1, \boldsymbol{c}_2\}$ is shown below; $\boldsymbol{t}_1$ and $\boldsymbol{t}_2$ are system-level targets of $\boldsymbol{a}_1$ and $\boldsymbol{a}_2$.

The system-level problem issues design targets $(s, \boldsymbol{t}_1, \boldsymbol{t}_2)$ to the constituent disciplines. In the lower-level problem, the disciplines must design to match these targets as follow:

$$\text{Discipline 1:} \quad \begin{aligned} &\underset{s_1,l_1}{\boldsymbol{minimize}} \quad \boldsymbol{c}_1 = \frac{1}{2}\left[\left\|s_1 - \boldsymbol{s}\right\|^2 + \left\|\boldsymbol{a}_1(s_1, \boldsymbol{l}_1, \boldsymbol{t}_2) - \boldsymbol{t}_1\right\|^2\right] \\ &\boldsymbol{subject\ to} \quad \boldsymbol{g}_1(s_1, \boldsymbol{l}_1, \boldsymbol{a}_1(s_1, \boldsymbol{l}_1, \boldsymbol{t}_2)) \geq 0 \end{aligned} \tag{2-8}$$

where s_1 is the target of s at discipline 1.

$$\text{Discipline 2:} \quad \begin{aligned} &\underset{s_2,l_2}{\boldsymbol{minimize}} \quad \boldsymbol{c}_2 = \frac{1}{2}\left[\left\|s_2 - \boldsymbol{s}\right\|^2 + \left\|\boldsymbol{a}_2(s_2, \boldsymbol{l}_2, \boldsymbol{t}_1) - \boldsymbol{t}_2\right\|^2\right] \\ &\boldsymbol{subject\ to} \quad \boldsymbol{g}_2(s_2, \boldsymbol{l}_2, \boldsymbol{a}_2(s_2, \boldsymbol{l}_2, \boldsymbol{t}_1)) \geq 0 \end{aligned} \tag{2-9}$$

where s_2 is the target of s at discipline 2.

Another two-level MDO approach, Current Subspace Optimization (CSSO) introduced by Sobieszczanski-Sobieski (1988), allocates the design variables uniquely to subspaces that correspond to engineering disciplines or subsystems. Each subspace performs a separate optimization operating on its own unique subset of design variables. The coordination problem is solved by using the Global Sensitivity Equation (GSE)

(Sobieszcazanski-Sobieski 1990) and optimum sensitivity derivatives with respect to parameters.

The CSSO permits the decoupling of a large engineering system into smaller subsystem modules in order to achieve concurrent optimization in each of these subspaces. The CSSO eliminates the need for a full analysis in each subspace, thereby enabling their simultaneous treatment. Subspaces are created on the basis of a non-hierarchic decomposition (by discipline or design goals) and at any given time, each design variable is considered active in one of the subsystems.

The system optimization procedure begins with a system-level analysis. The actual assignment of design variables to a particular subspace is made on the basis of the ability of variable to influence the goals within that subspace based on the sensitivity of the objective function and cumulative constraints in each subspace. After system analysis, we perform a system sensitivity analysis to compute the system-sensitivity derivatives. Each derivative measures the influence of a particular design variable $\boldsymbol{l_j}$ on a particular behavior variable $\boldsymbol{a_i}$.

After allocating design variables, temporarily decoupled optimization is performed concurrently in each subspace. The goal of these subspace optimizations is to reduce the violation of the cumulative constraints with the least increase of the system objective function or greatest decrease of the cumulative constraints which are already satisfied.

After finishing all of the subspace optimizations, an optimum-sensitivity analysis is performed in order to determine the sensitivity of objective function to cross influence coefficients which measure how subspaces affect one another. The derivative information obtained in optimum-sensitivity analysis will be now used in coordination optimization

problem in which the system function is minimized with respect to the coefficients. Completion of coordination optimization yields new coefficients for use in the next subspace optimization.

The advantages of the CSSO are modularity of the subsystems and the ability of to incorporate human intervention and decision making. However, application of this algorithm without move limits may lead to convergence problems (Shankar et al. 1993). Bloebaum et al. (1992) reformulated the approach by using an expert system made up of heuristic rules to adjust the move limits and other parameters that control the process. The algorithm was extended to problems with discrete design variables, and there are several variants of CSSO developed (see Sobieszczazanski-Sobieski & Haftka, 1997 for additional references).

After numerical difficulties in multilevel structural optimization were found out by Thareja and Haftka (1986), similar computational difficulties were also found in numerical tests of CO (Alexandrov & Kodiyalamm 1998, Kodiyalam 1998). Alexandrov and Lewis (2000) showed that the treatment of compatibility via quadratic penalties led to system-level optimization problems that necessarily failed to satisfy the standard Karush-Kuhn-Tucker optimality conditions, either because multipliers did not exist, or because the constraint Jacobian was discontinuous at solutions. In addition, collaborative optimization formulations lead to system-level problems that are nonlinear even when the original problem is linear. These features make it difficult for conventional optimization algorithms to solve the CO system-level problem reliably or efficiently.

The CSSO also used equality constraints, and indeed some numerical difficulties were found in applying it to simple problems (Shankar et al. 1993).

An older approach, which avoids the numerical difficulties associated with equality constraints is to find a simple approximation for lower-level optima as function of upper-level design variables. This approach has been particularly successful when the lower level involves structural design. Weight equations that predict the optimal structural weight of wing and fuselage structures have been popular.

Shanley (1960) proposed to use weight prediction method for minimization of wing weight based on elementary-strength or element-stiffness considerations, augmented by experimental results and statistical data. A weight equation, which relies on a computational procedure where the amount of material are required to resist bending and torsion at a number of selected spanwise locations, is determined numerically. The primary wing box weight is thus found from integration along the span. The weight equation produced this way can then be used by the aircraft designer, obviously the need for including the structural design in the aircraft configuration design.

Torenbeek (1992) presented a method for generating weight equations for wing structures. The method makes use of elementary stress analysis combined with historical data. The wing-group weight is expressed as the sum of the primary weight (top and bottom covers, spars, ribs, and attachments) and the secondary weight comprised of the weight of components in front of the front spar, components behind the rear spar, plus any miscellaneous weight.

Initially, wing weight equations were based on historical data and simple beam models. Later, large number of structural optimizations were performed and used to generate these equations (McCullers 1984). These equations then allow upper-level

configuration design because they predict the optimum structural weight as function of the aircraft configuration variables (McCullers 1997).

Instead of using weight equations that are applicable to all transports, Kaufman et al. (1996) developed weight equations customized to a high speed civil transport (HSCT) design by fitting large number of structural optimizations by a polynomial response surfaces. A similar approach was also used by Balabanov et al. (1999) for a two-level aerodynamic and structural optimization of the HSCT.

The advantages of using response surfaces to fit a large number of disciplinary optima can be summarized as follows: 1) It allows the disciplinary optimizations to be performed by specialists. 2) It provides a simple method for facilitating communication between the specialists on the design team. 3) RS techniques smooth the discontinuities and noise associated with two-level formulations. 4) Performing large number of optimizations allows easy use of parallel computers (Burgee et al. 1996; Eldred & Schimel 1999, Krasteva et al. 1999) and error deletion (Papila & Haftka, 2000; Kim et al. 2000). However, response surfaces become increasingly expensive or inaccurate with increasing dimensionality of the design space. This difficulty typically limits response surfaces to problems under 30 design variables.

Composite Wing Structural Design by Two-level Optimization Using Response Surfaces

Thin-walled box beams are extremely efficient structures. The thin-walled box beam in some forms has become a fundamental structural element in the construction of aircraft, ships, offshore platforms, bridges and the cores of tall buildings. The advantage of the hollow section is that the material is efficiently used both in flexure and torsion. The wing-box structure belongs to a generic and simplified prototype of this kind of structures.

Due to higher ratios of stiffness-to-weight or strength-to-weight, complex composite structures like wing box and fuselages consisting of composite laminates, have attracted much industry attention. In general, composite structures are typically made of laminates where distinct layers are stacked. Each layer is composed of fibers of a given orientation embedded in a matrix of different materials. Fibrous composites are usually manufactured in the form of layers of fixed thickness, and fiber orientation angles are limited to a small set. Designing composite structures involves finding the number of layers and the fiber orientation of each layer inside each laminate that maximize the performance of the structures under requirements such as failure, geometry and cost. Compared with wing box with isotropic material, design of composite wing box structures is more complicated and more computationally expensive. Consequently, designing a composite wing or fuselage structure at one level is not feasible computationally.

A natural decomposition of wing or fuselage structures is to deal with them as an assembly of stiffened panels. Consequently, early approach to design wing box structures was based on weight equations developed by Shanley (1960) and Gerard (1960) During 50's, a common form of multi-cell construction with relative thick covers supported by a series of longitudinal webs was used. Efficiently using these structures with the rearrangement and reduction of structure materials of the cover plates was the objective. This is prototype of panel-level design based on loads from wing-level design. Gerard (1960) used orthotropic plate theory to analyze idealized long-plate structures —longitudinal, transverse, and waffle-grid stiffening system for flat plates, which keep the significant details of the actual structure and yet are sufficiently simplified to permit broad conclusion to be drawn as to the optimum stress and configuration of the minimum weight

plate. A comparison of the optimum plate of each type in terms of common weight and loading parameters can then be effected to establish the ranges of efficient application of each type. So minimum weight is obtained for a given set of loads and geometric parameters by using plate-weight equations or plate-weight tables. These weight equations or weight tables can then be used in the overall wing design.

In Gerard's approach for panel-level design, stiffness constraints for wing-level design are not included. This does not provide any mechanism for wing-level stiffness constraints to affect panel design. In addition, the effect of panel design on load redistribution is not considered.

An approach that provides for including global stiffness constraints on panel-weight equations was developed by Ragon et al. (1997). At the global level, design variables are stringer areas and skin thicknesses. Global constraints included required stress constraints for all elements, global stiffness constraints and weight constraints using ADOP program (Sharma et al. 1993). A weight equation for optimal panel weight was fitted as a RS to a large number of panel structural optima as a function of the loads on the panel and of inplane-stiffness parameters. The PASCO program (Stroud et al. 1981) was used for panel structural optimization. Panel-design variables described ply thicknesses of elements of the stiffened panel and constraints included buckling, strength, and manufacturing constraints as well as constraints on the inplane stiffness A_{11} and A_{66}. Response surface of the optimum-panel weight is a function of the inplane loads N_x, N_y, and N_{xy}, and inplane stiffness A_{11} and A_{66}. This response surface is used in the weight constraints in the global optimizer.

$$\boldsymbol{g} = 1.0 - \frac{\boldsymbol{w}_g}{\boldsymbol{w}_l} \leq 0 \qquad (2\text{-}10)$$

where w_g is panel weight in the overall design, and w_l is the local panel weight (response surface). This constraint requires the overall optimizer to allocate to each panel enough weight to satisfy the local constraints under the specified loads and inplane-stiffness requirements.

While Ragon et al. (1997) obtained good designs, they ran into one problem in the generation of the response surface. For many combinations of loads and inplane-stiffness parameters, no feasible panel design could be found. The work in this dissertation eliminates this problem by using the optimizations to create a response surface of an optimum load instead of an optimum weight. This is described in Chapter 4.

Stacking Sequence Optimization by Genetic Algorithms

Genetic algorithms (GAs) are search techniques based on a simulation of the Darwinian concept of survival of the fittest and natural reproduction genetics operating on a population of designs. These algorithms belong to the class of probabilistic search methods. Compared with traditional search algorithms such as gradient based continuous variable methods or enumerative integer-programming techniques, probabilistic search methods sample the design space based on probabilistic rules, and they are of global scope because they have a nonzero probability of eventually reaching any point of the design space, and also they are not sensitive to the problem nonconvexities and nonlinearities.

Holland (1975) pioneered the implementation and theoretical analysis of genetic algorithms. DeJong (1975) then applied GAs to optimization. Since then, many people applied GAs to many fields. Application includes artificial neutral networks (Fullmer 1991), geophysics (Gallagher 1992), social science (Greene 1987), control (Kristinsson 1992), biology (Lucasuis 1991), and diagnosis (Potter 1990).

Goldberg and Santani (1987) pioneered the application of GAs to structural optimization. Since then, GAs have been applied to numerous structural optimization applications (Furuya & Haftka 1993, Hajela 1990, Hajela 1991, Hajela & Lin 1992; Powell & Skolnick 1993, Shoenauer & Xanthakis 1993, Watabe & Okino 1993).

The design of composite laminates is often formulated as a continuous optimization problem with ply thickness and ply orientation angles used as design variables. Schmit and Farshi (1977) first formulated the design of composite laminates as a continuous optimization problem with ply thickness used as design variables. However for many practical problems, the ply thickness is fixed, and ply orientation angles are limited to a small set such as 0°, ±45°, and 90°. Thus, the design problem becomes a combinatorial problem of choosing the fiber direction from a permissible set for each ply.

Mesquita and Kamat (1987) optimized the stacking sequence of laminates with the number of plies of given orientation used as the design variables by integer programming. Haftka and Walsh (1992) used ply-identity design variable to maximize buckling load using linear integer programming. However, when strength constraints are also considered, the problem becomes nonlinear and has been solved as a sequence of linearized integer programming subproblems (Nagendra et al. 1992).

GAs has been used extensively to solve this combinatorial problem (Le Riche & Haftka 1993, 1995; Kogiso et al., 94a, 94b; Nagendra et al., 93a, 93b). GAs are well suited for stacking sequence optimization, and because of their random nature, they easily produce alternative optimum in repeated runs. This latter property is particularly important in stacking sequence optimization, because widely different stacking sequences can have very similar performance (Shin et al. 1989).

Stacking sequence design of composite panels is a local design problem that is often strongly coupled to the overall design of a structure. In wing structural optimization, the overall wing structural design imposes constraints on individual panel designs. The optimization of the overall wing structure often specifies number of 0°, ±45°, and 90° plies and in-plate loads of each panel. The stacking sequence design is then limited to permutations of given plies, but not to changes in the number of plies of each orientation.

It is possible to solve this problem by using a conventional GA with additional constraints imposed on the design. However, permutation GAs, developed mostly for solving scheduling problems (Michalewicz 1992), handle more efficiently the search for an optimal permutation, because they reduce the dimensionality of the design space. Permutation GAs mostly were developed for the traveling salesman problem, which seeks to minimize travel cost for a given list of towns, and is insensitive to where the sequence starts, so that cyclical permutations do not matter. In stacking sequence design, in contrast, a cyclical permutation will move the outermost ply into the innermost position, and thus greatly influence the bending properties of the laminate.

Aside from the use of permutation GAs, number-of-ply constraints may be handled by repair strategies. Such repair strategies may also be useful for dealing with another constraint common to a laminate design — a limit on the number of contiguous plies of the same orientation (Todoroki & Haftka 1998).

The next chapter describes a permutation GA and repair strategy developed for laminate stacking sequence design.

CHAPTER 3
PERMUTATION GENETIC ALGORITHM FOR STACKING SEQUENCE OPTIMIZATION OF COMPOSITE LAMINATES

Introduction

Stacking sequence design of composite panels is a local design problem that is often strongly coupled to the overall design of a structure. In wing structural optimization, the overall wing structural design imposes constraints on individual panel designs. The optimization of the overall wing structure often specifies the number of 0°, ±45°, and 90° plies and in-plate loads of each panel. The stacking sequence design is then limited to permutations of given plies, but not to changes in the number of plies of each orientation.

It is possible to solve this problem by using a conventional genetic algorithm (GA) with additional constraints imposed on the design. However, permutation GAs, developed mostly for solving scheduling problems (Michalewicz 1992), handle more efficiently the search for an optimal permutation, because they reduce the dimensionality of the design space. Permutation GAs were mostly developed for the traveling salesman problem, which seeks to minimize travel cost for a given list of towns, and is insensitive to where the sequence starts, so that cyclical permutations do not matter. In stacking sequence design, in contrast, a cyclical permutation will move the outermost ply into the innermost position, and thus greatly influence the bending properties of the laminate.

Aside from using permutation GAs, number-of-ply constraints may be handled by repair strategies. Such repair strategies may also be useful for dealing with another

constraint common to a laminate design — a limit on the number of contiguous plies of the same orientation.

This chapter presents a permutation GA that is better suited to stacking sequence design. We compare the permutation algorithm to a standard permutation GA, Partially Mapped GA (Goldberg & Lingle 1985), as well as to a standard genetic algorithm. The new algorithm shares some properties with Bean's Random Keys algorithm (Bean 1994) and therefore the two algorithms are compared. In addition, the use of a repair strategy for the standard GA and the permutation GA based on a Baldwinian repair strategy is introduced (Todoroki & Haftka 1998). We compare the algorithm for maximization of the buckling load of a laminate with specified number of 0°, ±45°, and 90° plies.

Genetic algorithms are random in nature, and therefore comparing the efficiencies of alternative algorithms requires averaging many runs. For this reason, a simply supported unstiffened panel is selected since its closed form solutions are available. We can thus perform the millions of analyses required for a thorough comparison of the efficiency of the various genetic algorithms. We measure efficiency of the algorithms in terms of number of analyses required for high reliability in finding the optimal design. Computation times are not given because they are dominated by GA operations, while they will be dominated by structural analyses in more realistic problems.

The rest of the chapter starts by describing the physical model of the composite laminates and a standard formulation of optimization of a composite laminate. A new permutation GA, which we call a gene-rank crossover GA, suited for stacking sequence optimization is developed, and the standard GA and a permutation GA based on partially mapped crossover are reviewed and implemented. The computational efficiency of the

three GAs are then compared under various load cases. The effect on performance of a contiguity constraint limiting the number of identical adjacent ply orientations to four, is

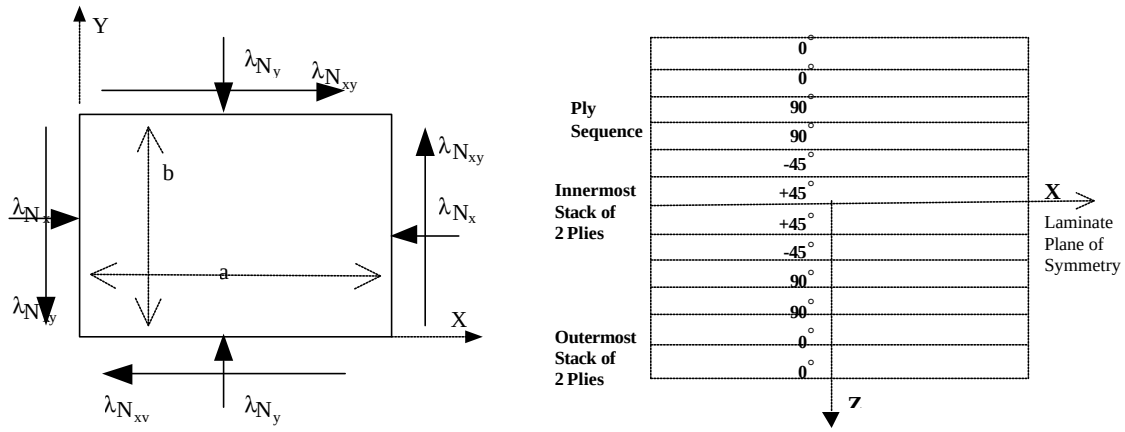

a) Laminate Plate Geometry and Applied Loading **b) Ply Sequence Location**

Figure 3-1: Composite laminate plate geometry and loads

investigated. Two repair strategies, chromosome repair and laminate repair, for permutation violating the contiguity constraint are discussed.

Composite Laminate Analysis and Optimization

Buckling Load Analysis of Composite Laminate

This chapter deals with the optimization of symmetric and balanced stacking sequences of composite wing panels. Usually, a panel is to be designed for given in-plane loads and specified total number of of 0°, ±45°, and 90° plies. The loads and the specified number of plies come from the overall wing-level optimization. Here the panel is designed to maximize the buckling load subject to a constraint on the number of contiguous plies of the same orientation.

An unstiffened, simply supported, laminated panel with dimensions *a* and *b* (Figure 3-1) is subjected to normal loads per unit length N_x and N_y, and a shear load per unit length

N_{xy}. It is made of a symmetric and balanced graphite-epoxy laminate composed of 0°, ±45°, and 90° plies.

Because of symmetry, there is no extensional-flexural coupling. The pre-buckling deformations are hence purely in-plane. The balance condition requires that for every ply with a positive fiber-orientation angle, there is a corresponding ply with the negative fiber-orientation angle. This implies no normal-shear extensional couplings. In addition, the laminate is assumed specially orthotropic (i.e. there will be no bending-torsion coupling). This is a common assumption in the analysis of balanced symmetric laminates for which the bending-torsion coupling terms are usually very small and negligible.

Normal Buckling Load Analysis

Under biaxial loading, the laminate can buckle into *m* and *n* half waves in the *x* and *y* directions, respectively, when the load amplitude (a factor multiplying the applied loads) reaches a value $l_n^{(m,n)}$, which depends on flexural stiffness D_{ij} and loads N_x and N_y.

$$\frac{l_n^{(m,n)}}{p^2} = \frac{\boldsymbol{D}_{11}(\boldsymbol{m}/\boldsymbol{a})^4 + 2(\boldsymbol{D}_{12} + 2\boldsymbol{D}_{66})(\boldsymbol{m}/\boldsymbol{a})^2(\boldsymbol{n}/\boldsymbol{b})^2 + \boldsymbol{D}_{22}(\boldsymbol{n}/\boldsymbol{b})^4}{(\boldsymbol{m}/\boldsymbol{a})^2 \boldsymbol{N}_x + (\boldsymbol{n}/\boldsymbol{b})^2 \boldsymbol{N}_y} \tag{3-1}$$

The pair *(m, n)* that yields the smallest value of $l_n^{(m,n)}$, which is the critical buckling load l_{cb}, varies with the loading conditions, total number of plies considered, material, and the plate aspect ratio.

Shear Buckling Load Analysis

A second mechanism is buckling due to shear loading. Modeling of this buckling mode for a finite plate is computationally expensive. Instead, the plate is assumed to have an infinite length, and analytical solutions available for a plate of infinite length in the x

direction are used as approximations (Whitney 1985). The critical shear buckling load factor λ_s is given in Whitney (1985) as a function of the variable G

$$l_s = \frac{4b_1(D_{11}D_{22}^3)^{1/4}}{b^2 N_{xy}} \quad , \qquad for \ 1 \le \Gamma \le \infty$$
$$= \frac{4b_1\sqrt{D_{22}(D_{12}+2D_{66})}}{b^2 N_{xy}} \quad , \quad for \ 0 \le \Gamma \le 1 \tag{3-2}$$

$$\Gamma = \frac{\sqrt{D_{11}D_{22}}}{D_{12}+2D_{66}} \tag{3-3}$$

and values of β_1 are given in Table 3-1.

Table 3-1: Coefficient β1 for shear buckling load factor (Whitney 1985)

Γ	β_1
0.0	11.71
0.2	11.80
0.5	12.20
1.0	13.17
2.0	10.80
3.0	9.95
5.0	9.25
10.0	8.70
20.0	8.40
40.0	8.25
¥	8.13

Combined Buckling Load Analysis

When normal and shear loads are applied simultaneously to the panel their interaction is approximated by the following interaction equation (Lekhnitskii 1968)

$$\frac{1}{l_c^{(m,n)}} = \frac{1}{l_n^{(m,n)}} + \frac{1}{l_s^2} \tag{3-4}$$

where $\lambda_n^{(m,n)}$ and λ_s are the critical load amplitudes under normal and shear loads, respectively. The combined buckling load factor $\lambda_c^{(m,n)}$ is always more critical than the normal buckling load factor $\lambda_n^{(m,n)}$.

To prevent buckling, $\lambda_c^{(m,n)}$ and λ_s must be greater than one. Shear buckling occurs independently of the sign of the shear load. So buckling load λ is taken to be the minimum of the load factors.

$$l = \min\left\{|l_s|, l_c^{(m,n)}\right\} \tag{3-5}$$

In addition, to reduce problems with matrix cracking, we do not allow more than four contiguous plies with the same orientation. This is referred to as the contiguity constraint.

Statement of Stacking Sequence Optimization

For maximizing the buckling load of composite laminates for given total number of 0°, ±45°, and 90° plies, and ply-contiguity constraints, the optimization problem can be stated as follows:

Given three ply orientation choices (0°, ±45°, and 90°), applied in-plane normal and shear loading N_x, N_y, and N_{xy}, and the total number of 0°, ±45°, and 90° plies.

Optimize a symmetric and balanced stacking sequence in order to maximize the buckling load λ (that is the panel will buckle under loads λN_x, lN_y, and λN_{xy}).

Subject to the constraints that there be no more than four contiguous plies of the same orientation, and number of 0°, ±45°, and 90° plies be equal to given total number of 0°, ±45°, and 90° plies.

Results were obtained for a 24-inch square graphite-epoxy plate with the following properties shown in Table 3-2.

Table 3-2: Material properties of graphite-epoxy T300/5208

E_1	18.5×10^6 psi (128 GPa)
E_2	1.89×10^6 psi (13.0 GPa)
G_{12}	0.93×10^6 psi (6.4 GPa)
ν_{12}	0.3
t_{ply}	0.005 in (0.0127 cm)

Genetic Algorithms

A genetic algorithm is a guided random search technique that works on a population of designs. Each individual in the population represents a design, i.e. a stacking sequence, coded in the form of a bit string. The genetic algorithm begins with the random generation of a population of design alternatives. Designs are processed by means of genetic operators to create a new population, which combines the desirable characteristics of the old population, and then the old population is replaced by the new one. Herein the best design of each generation is always copied into the next generation, which we call an elitist strategy. The process is repeated for a fixed number of generations or for a fixed number of analyses resulting in no improvement in the best design.

A genetic search changes the population of strings by mimicking evolution. The individual strings are mated to create child designs. Each individual has a fitness value that determines its probability of being chosen as parents. Here the fitness is based on a rank in terms of objective function in the population. The fitness assigned to the *i*th best individual of *n* designs is then equal to $[2(n+1-i)/(n^2+n)]$, so that the sum of all fitnesses is equal to 1.

Standard Genetic Algorithm

For the standard GA, a laminate is coded using the standard stacking sequence notation. Because of the symmetry of the laminate and its balance, only one quarter of the

plies is encoded. This is done by adding the requirement that the laminate is composed of pairs of 0° plies, pairs of 90° plies, or a stack of ±45° plies. For example, the laminate $[0_2/\pm 45/90_2/90_2/\pm 45/0_2]$ is encoded as $[0/45/90]$, the latter being the chromosome for the laminate. The rightmost gene corresponds to the stack closest to the laminate midplane. The leftmost position in the chromosome describes the outermost stack of two plies. A two-point crossover is used.

Mutation is applied with a small probability by randomly switching a stack orientation (0°, ±45°, 90°) to one of the other two choices available. Since the total numbers of 0°, ±45°, and 90° two-ply stacks are fixed, the mutation is biased to promote compliance with this constraint. The mutation is biased so that a $0°$ stack will mutate only if the number of $0°$ plies is not equal to the allocated amount. This rule also applies to ±45° and 90° stacks. The mutation operator hence uses the problem information and acts as a partial repair operator. Besides the regular mutation, there is also an interchange mutation operator called stack-swap, which allows two stacks to exchange their genes with a given probability.

The objective function for maximizing the failure of the composite laminate is equal to the failure load λ penalized for violations of the given number of plies and the limit of no more than four contiguous plies of the same orientation. We denote the number of 0°, ±45°, and 90° two-ply stack in the string by n_0, n_{45}, n_{90} respectively, and denote the specified total number as n_{0g}, n_{45g}, n_{90g} respectively. Then the objective function is given as follows:

$$j = \boldsymbol{r}^{Penalty} f \tag{3-6}$$

where Penalty is a parameter (set to 2.0) for violation of specified amounts of 90°, 45°, and 0° plies, and

$$r = r_0 r_{45} r_{90} \tag{3-7}$$

$$r_0 = \begin{cases} \dfrac{n_0 + 1}{n_{0g} + 1} & \text{if } n_0 < n_{0g} \\ 1 & \text{if } n_0 = n_{0g} \\ \dfrac{n_{0g} + 1}{n_0 + 1} & \text{if } n_0 > n_{0g} \end{cases} \tag{3-8}$$

with similar definitions for r_{45} and r_{90}.

This form of the penalty function and penalty parameters were selected according to previous studies with similar constraints (Kogiso et al. 1994a, 1994b; Le Riche & Haftka 93, 95). That is

$$f = 1 \Big/ P_{cont}^{Ncont} \tag{3-9}$$

P_{cont} is penalty parameter (set to 1.05 here) for violation of the four-ply limit on contiguous plies of the same orientation, n_{cont} is total number of same-orientation contiguous plies in excess of four. Note that the contiguity constraint is applied only to 0° and 90° plies. The ±45° plies alternate between 45° and -45° directions, and so do not have any contiguity problem, no matter how many 45° stacks are contiguous.

Using a penalty function to incorporate the limits on the number of plies slows down the progress of the optimization. This justifies using permutation based GAs, which do not need these constraints.

Permutation problems seek the optimal arrangement of a list of items, in our case, the given 0°, ±45°, and 90° stacks. Natural coding with the orientation angles 0°, 45°, and ±90° is not well suited for representing permutations since it will tend to generate

duplicate or missing allele values. A permutation encoding is represented by a list of distinct integer values, such as 1, 2, 3, …, coding the orderings of 0°, ±45°, and 90° stacks referenced to a baseline laminate. We selected the baseline laminate to have all the specified 90° stacks on the outside, followed by the ±45° stacks and then the 0° stacks. So the baseline laminate looks like $[90_2^\circ / 90_2^\circ / \cdots / \pm 45^\circ / \pm 45^\circ / \cdots / 0_2^\circ / 0_2^\circ]_s$ and it is coded as $[1/2/\ldots/n_0+1/\ldots/n_0+n_{45}+1/\ldots/n_0+n_{45}+n_{90}]$. A baseline laminate $[90_2/\pm45_2/0_2]_s$, for example, is coded into the permutation [1/2/3], while the laminate $[90_2/0_2/\pm45_2]_s$ is coded [1/3/2] by reference to the baseline laminate.

Permutation coding has the advantage, compared to the traditional coding, that the specified amounts of 0°, 45°, and 90° stacks are always met. However, traditional crossover and mutation do not work well for permutation coding because they tend to produce infeasible children from feasible parents. Specific permutation crossovers have been developed for the travelling salesman problem (TSP). In this work we use the partially mapped crossover, developed by Goldberg and Lingle (1985). We also developed a crossover suited for the design of composite laminates that we call a Gene-Rank crossover. Mutation for permutation coding is performed by randomly selecting two genes, and then swapping them with a given probability.

Permutation Genetic Algorithms

Gene-Rank Crossover

In a composite laminate, the outermost plies, hence leftmost genes, affect flexural stiffnesses more than the inner plies. This is in contrast with TSP, where the chromosome may be viewed as a ring, where the absolute position of a gene does not matter. A

chromosome for coding a stacking sequence in contrast may be viewed as a directed linear segment.

Gene-rank crossover is based on imitating the process used to average the rankings that two judges give a group of contestants with plies playing the role of contestants. Each laminate can then be viewed as a ranking of the set of plies, and gene-rank crossover averages the two rankings. For example, consider the simple case with three contestants, A, B, and C. The first judge ranked them as: A—1, B—2, C—3, denoted in shorthand as [A B C]. The second judge ranked them as: A—2, B—3,C—1, or [C, A, B]. We associate weights W_1 and W_2 with the two judges, representing their relative influence (with $W_1 + W_2 = 1$). In the implementation of the crossover, W_1 is a uniformly distributed random number in [0., 1.] selected anew for each pair of parents for each generation. The final ranking is then obtained as the weighted rank of each individual

A: (1) (W_1)+(2) (W_2)
B: (2) (W_1)+(3) (W_2)
C: (3) (W_1)+(1) (W_2)

For example, with W_1 =0.4, W_2 =0.6, we get [1.6, 2.6, 1.8] for the weighted averages, corresponding to a composite ranking of [A, C, B].

Consider next, for example, the stacking sequence of the baseline laminate $[90_2/90_2/90_2/\pm45/\pm45/0_2]_S$, with its permutation being defined by the chromosome [1/2/3/4/5/6]. If two permutations of the laminate are:

Permutation 1 (Parent 1)	[2/5/4/3/6/1]
Laminate	$[90_2/\pm45/\pm45/90_2/0_2/90_2]_s$
Permutation 2 (Parent 2)	[1/2/4/5/3/6]
Laminate	$[90_2/90_2/\pm45/\pm45/90_2/0_2]_s$

For W_1= 0.4634 and W_2=0.5366, the average rank of each gene of the child design is shown in the table below. For example, the average rank of gene 1 is equal to $6W_1+W_2$ since gene 1 is ranked the sixth and the first in the two permutations, respectively.

Table 3-3: Weighted gene-rank values of child averaging gene-rank values of two parents

Gene	Rank-Value in Permutation 1	Rank-Value in Permutation 2	Weighted Rank-Value
1	6	1	3.32
2	1	2	1.53
3	4	5	4.54
4	3	3	3.00
5	2	4	3.07
6	5	6	5.54

Sorting genes by their average weighted ranks (Table 3-3), the permutation of the child is

Permutation (Child) [2/4/5/1/3/6]

Laminate $[90_2/\pm45/\pm45/90_2/90_2/0_2]_s$

Besides the uniformly distributed random weight, W_1, we also experimented with a random variable biased to be close to one or zero, so that one of the parent laminates dominates. However, we did not find a distinct advantage to that variant. The Gene-Rank GA has some similarities with Bean's Random Keys algorithm (Bean 1994). The Random Keys algorithm uses a chromosome with numbers in [0, 1.], with their order determining the permutation. For example, the chromosome [.46/ .91/ .33/ .75/ .51] corresponds to the permutation [3/1/5/4/2]. The advantage of this form of coding is that standard crossover and mutation can be used. This coding tends to preserve rank more than the partially

mapped crossover discussed next, but it is not as conscious of rank as the Gene-Rank algorithm. For example, consider two parents that are both identical with the baseline laminate, so that in permutation coding they will both be coded as [1/2/3/4]. Any Gene-Rank crossover will produce a child design identical to the parents. On the other hand, with the Random Keys algorithm, one parent may be coded as [.1/.2/.3/.4], and the other parent may be coded as [.5/.6/.7./.8]. Some of the child designs obtained by crossover are very different. For example, with a cut in the middle of the chromosome, one child design is [.5/.6./.3/.4], which corresponds to a permutation of [3/4/1/2].

Partially Mapped Crossover

The partially mapped crossover, developed by Goldberg and Lingle (1985) for the TSP, employs the following four steps:

1. Define two break points randomly.
2. Use the middle sub-string between the two cut points from the second parent.
3. Take genes of the two outer sub-strings from the first parent when they do not conflict with the genes taken from the second parent.
4. Define the map relationship of genes in conflict, and fill genes in conflict by a map relationship.

The mechanism of the crossover is illustrated through an example of a laminate with a nominal stacking sequence of 8 stacks corresponding to 32 plies. The stacking sequence of the baseline laminate is $[90_2/90_2/\pm45/\pm45/\pm45/\pm45/0_2/0_2]_s$, its gene code is defined as [1/2/3/4/5/6/7/8]. Two permutations of the laminate are listed as follows:

Permutation 1 (Parent 1)	[3/6/4/2/7/5/8/1]
Laminate	$[\pm45/\pm45/\pm45/\pm45/90_2/0_2/0_2/90_2]_s$
Permutation 2 (Parent 2)	[3/7/5/1/6/8/2/4]
Laminate	$[\pm45/0_2/\pm45/90_2/\pm45/0_2/90_2/\pm45]_s$

The random cut points are 2 and 5, so the segment between two-cut points of the child design is

Child permutation	[*/7/5/1/6/*/*/*]

where the asterisk denotes presently unknown. Then we fill positions of the genes, which are not in conflict with these genes,

Child permutation [3/7/5/2/1/6/*/8/*]

Two genes from Parent 1 in Positions 6 and 8 of the permutation conflict with genes in the middle sub-string, which come from Parent 2. The conflicting gene in position 6 is 5, and the corresponding gene in Parent 2 was in same position as gene 4 from Parent 1. (Since the gene will not conflict with any genes from same parent, we need to go back to Parent 2 to find the corresponding gene of Parent 2). We check whether the mapped gene 4 conflicts with genes previously filled in the child. We find that it does not conflict with any. So the conflicting gene 5 from parent 1 in position 6 in the child's permutation is replaced by gene 4. Similarly, we find that conflicting gene 1 from parent 1 in position 8 of the child's permutation mapped gene 2 from parent 2. We fill genes 4 and 2 into position's 5 and 8 of the child's permutation to obtain

Child permutation [3/7/5/1/6/4/8/2]

Laminate $[\pm 45/0_2/\pm 45/90_2/\pm 45/\pm 45/0_2/90_2]_s$

Comparison of Efficiency of Three GAs

The efficiency of the three GAs is discussed here in terms of the computational cost—the average of number of analyses required for obtaining a given level of reliability in finding the global optimum. The reliability is calculated here by performing 100 optimization runs each for 4000 analyses and checking how many of the 100 runs reached the optimum at any given point. For example, if 63 runs reached the global optimum after 500 analyses, then the reliability of the algorithm is estimated to be 0.63 after 500

analyses. Of course, this is only an estimate, but it is easy to check that the standard deviation of a value *r* of the reliability estimated from *n* runs is

$$s_r = \sqrt{\frac{r(1-r)}{n}} \tag{3-10}$$

So that for 100 runs and r=0.63, we obtain a standard deviation of about 0.048.

Table 3-4: Optimum number of stacks of the three orientations for five load cases using sequential quadratic programming (λ_s and λ_c are the shear buckling load and combined buckling load factors, respectively)

Loading (lb/in)				Non-Rounded Optimization Results					
Case	N_x	N_y	N_{xy}	n_0	n_{45}	n_{90}	n_{total}	λ_s	λ_c
1	-20000	-2000	1000	9.18	18.32	9.18	36.65	26.56	1.0
2	-15000	-2000	1000	8.41	16.82	8.41	33.63	21.24	1.0
3	-10000	-2000	1000	7.49	14.98	7.49	30.00	15.09	1.0
4	-5000	-2000	1000	6.28	12.52	6.28	25.10	8.87	1.0
5	0	-2000	1000	4.31	8.62	4.31	17.24	2.87	1.0

Table 3-5: Comparison of computational efficiency of the three GAs

Loading	Given Number of Stacks (Rounded From Table 3-4)			Failure Load	Number of Analyses Required For 80% Reliability		
Case	n_{0g}	n_{45g}	n_{90g}	λ	SGA	GR	PMX
1	9	18	9	0.948	10432	1184	1328
2	8	17	8	0.948	8600	856	1224
3	7	15	7	0.909	5216	776	1024
4	6	12	6	0.870	3304	608	824
5	4	8	4	0.778	1672	408	560

SGA: Standard GA GR: Gene-Rank Crossover
PMX: Partially Mapped Crossover
Refer appendix for selection of the genetic parameters.

Because reaching the global optimum is often very time consuming, the requirement is often relaxed, and replaced by a *practical global optimum*, which is defined to be

within a specified fraction of the optimum. In the present work, a design was considered to be a practical optimum if the failure load was within 0.5% of the global optimum.

In general, the loads and number of plies used in the panel optimization come from the overall wing design. Here, in order to generate test cases, we selected some representative load cases, and used continuous optimization to find reasonable required number of plies. For the continuous optimization, we used nine ply thicknesses as continuous design variables t_i, $i=1,¼9$ and sequential quadratic programming (SQP) as implemented in the DOT program (Vanderplaats et al. 1995). The stacking sequence was set as $\mathbf{[90^\circ_{t9}/\pm 45^\circ_{t8}/0^\circ_{t7}/90^\circ_{t6}/\pm 45^\circ_{t5}/0^\circ_{t4}/90^\circ_{t3}/\pm 45^\circ_{t2}/0^\circ_{t1}]_s}$ The results are given in Table 3-5 in terms of number of plies of a given orientation (for ply thickness of 0.005 in) rather than the detailed stacking sequence. Next, the number of plies was rounded into integers, and the rounded numbers were used as the specified set for the genetic algorithms.

The results for the three algorithms were obtained with a population size of 8 and with the probabilities of mutation and crossover set to 1. The appendix discusses choice of three parameters. For the mutation operation, one gene is changed to one of two other alleles available in each child design for the standard GA, and for the permutation GAs, two genes are swapped for each child design. The number of multiple runs is 100, and the number of generations is 500. Table 3-5 gives results for the three GAs in terms of number of analyses required for 80% reliability.

From Table 3-5, we can also see that, as expected, thicker laminates are computationally more expensive to optimize. All the laminates in Table 3-5 are quasi-isotropic or close to quasi-isotropic. The small number of 0° and 90° plies in such

laminates makes the contiguity constraint easy to satisfy. To explore the performance for more general and thicker laminates, three new cases, defined in Table 3-6, were selected.

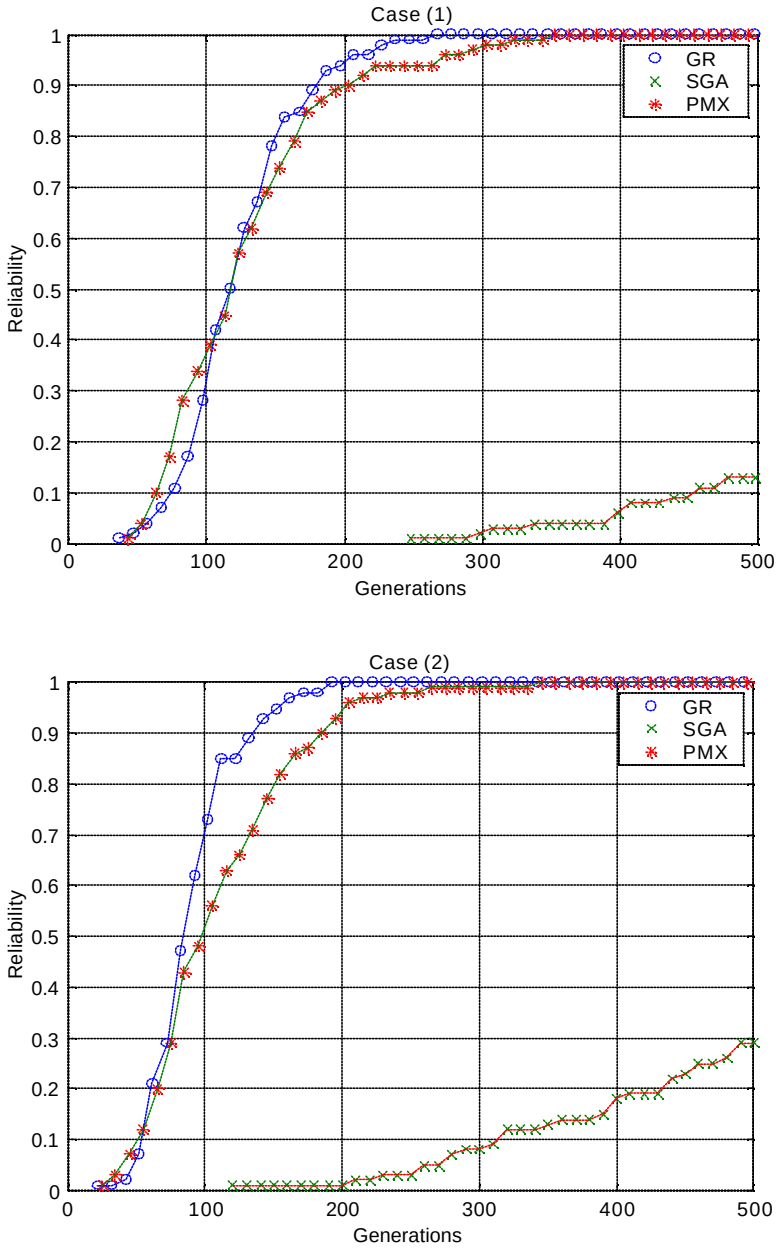

Figure 3-2: Reliability versus number of generations for five loading cases: Case (1) and Case (2)

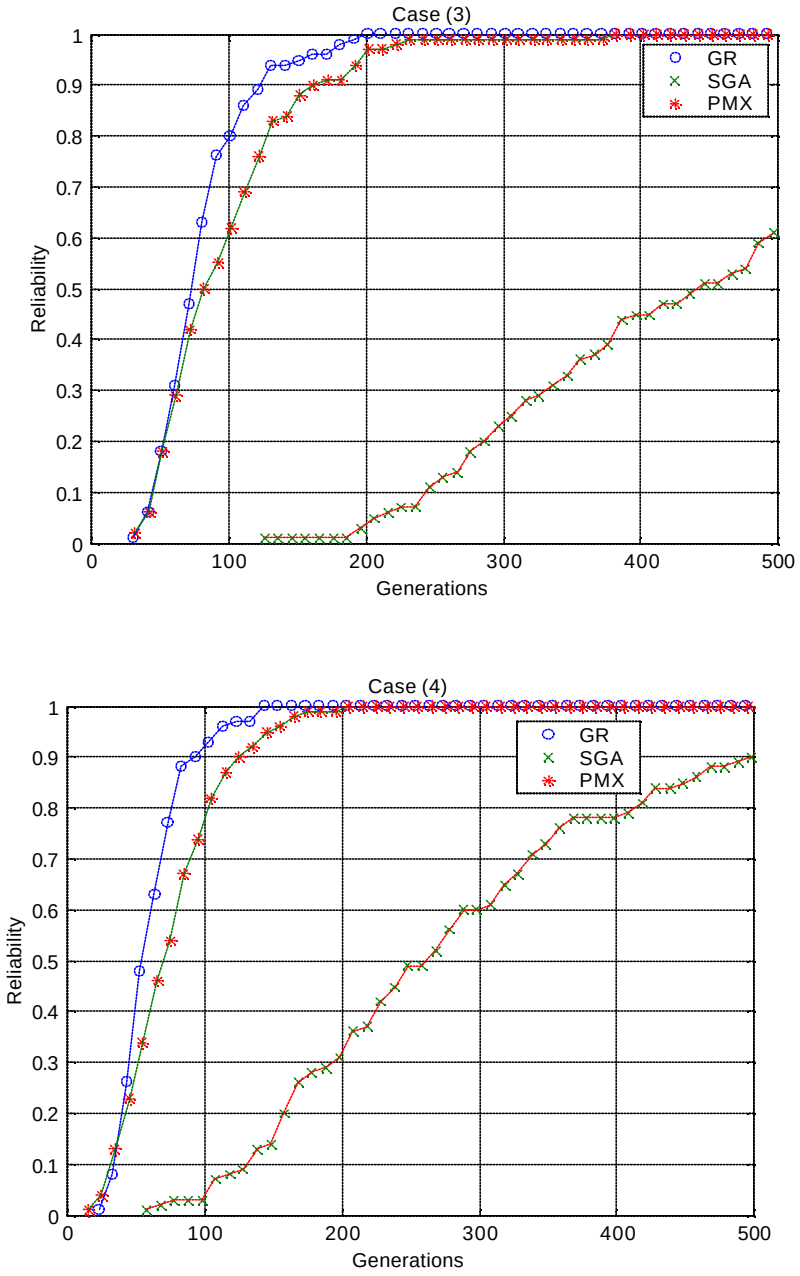

Figure 3-2: Reliability versus number of generations for five loading cases: Case (3) and Case (4)

From Table 3-5 we see that for the first three load cases, the reliability of the standard GA did not reach 80% for 4000 analyses. The reliability is shown versus number of generations in Figure 3-2. From the figure, it is clear that the two permutation GAs

perform much better than the standard GA. The Gene-Rank Crossover generally has the highest reliability except occasionally for low number of generations.

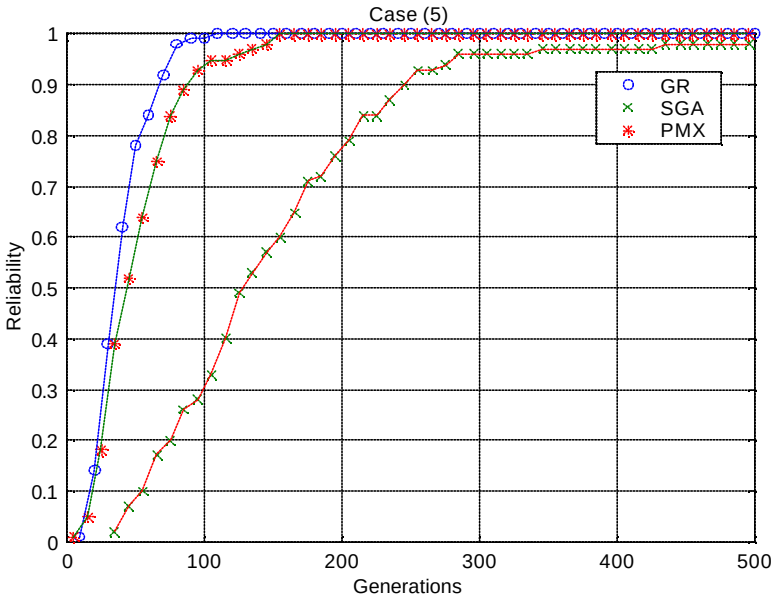

Figure 3-2: Reliability versus number of generations for five loading cases: Case (5)

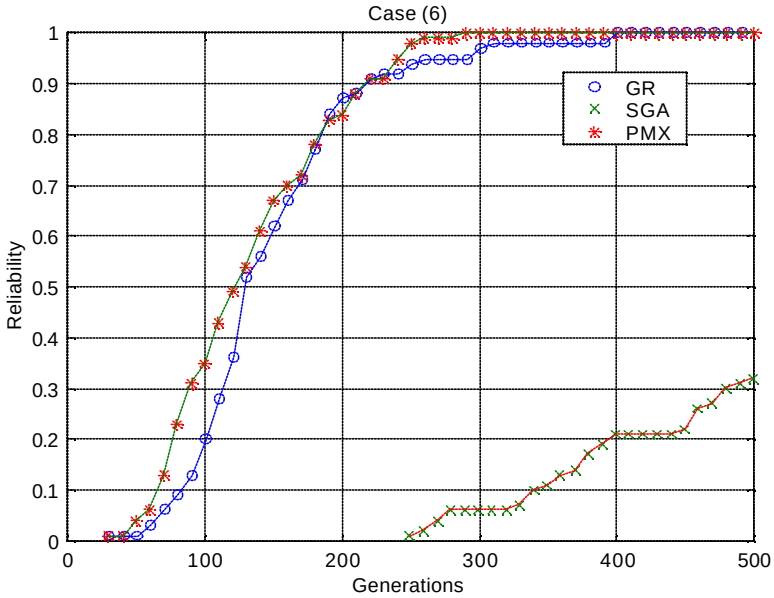

Figure 3-3: Reliability versus number of generations for the three thick laminates: Case (6)

Table 3-6: Three tick test laminates

Case No.	N_x (lb/in)	N_y (lb/in)	N_{xy} (lb/in)	n_0	n_{45}	n_{90}	n_{total}
6	0	-16000	8000	8	16	8	32
7	15980	-14764	10160	9	8	13	30
8	-16657	1963	828	13	7	15	35

Table 3-7: Comparison of computational efficiency of the three GAs for three thick laminates

Case No.	Number of Analyses Required For 80% Reliability					
	SGA		GR		PMX	
	With	Without	With	Without	With	Without
6	7984	5112	1328	480	1480	848
7	23544	2176	11840	360	5784	336
8	26320	5024	2216	296	2504	840

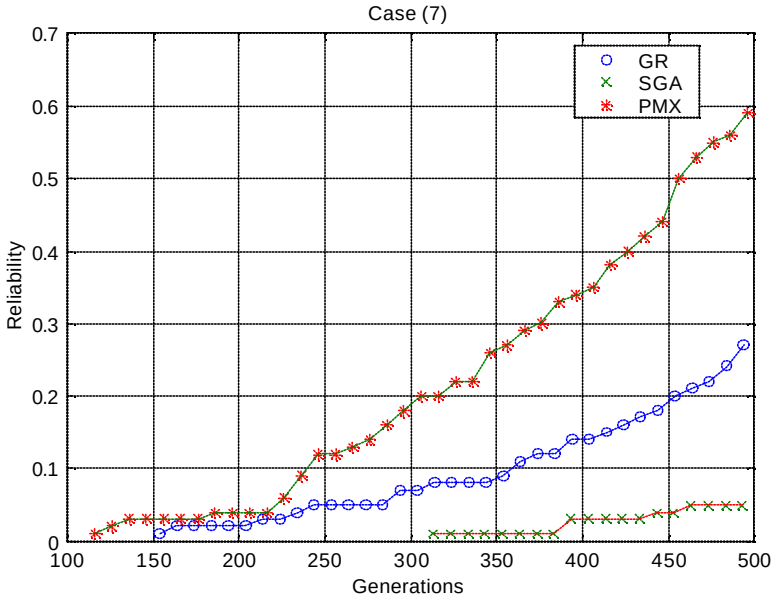

Figure 3-3: Reliability versus number of generations for the three thick laminates: Case (7)

The results summarized in Table 3-7 show that for the three thicker laminates, the contiguity constraint dominate the search for the optimum. Comparing the three thick

laminates above with contiguity constraints and without contiguity constraint, we can easily see that case 7 has the most difficult constraints. This is explained by examining the optimum laminates shown in Table 3-8. For case 6 and case 8, the outermost plies in the optimum design are ±45°, so that the contiguity constraint affects only the less important inner plies, while for case 7 it affects the critical outer plies. Figure 3-4 shows the reliability versus number of generations of the three thick laminates. We also inspected the various solutions and found that for the cases we optimized here, the optimum design was unique, so that the number of analyses needed for 80% reliability is a good indicator of the efficiency of the algorithm.

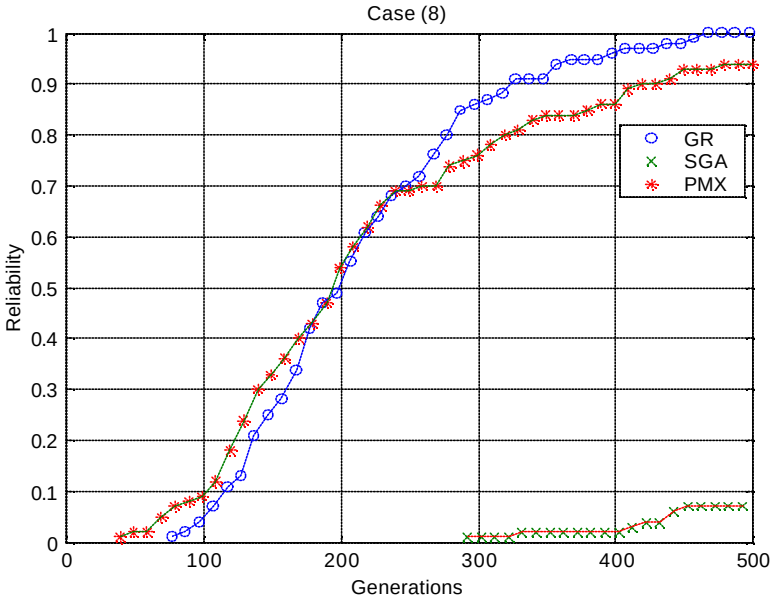

Figure 3-3: Reliability versus number of generations for the three thick laminates: Case (8)

Baldwinian Repair for Number of Plies and Continuity Constraint

The previous results demonstrate the high cost of dealing with constraints via penalty function. An alternate approach is to repair laminates that violate constraints. Todoroki & Haftka (1998) introduced a Baldwinian repair strategy, which they called

recessive repair, for dealing with contiguity constraints for standard GA. Here the strategy is extended to the permutation GAs. Additionally, a similar repair approach is used for enforcing the required number of plies of given orientations for the standard GA.

The key concept of Baldwinian repair is to repair the stacking sequence without repairing the chromosome. Repairing the chromosome is known as Lamarckian repair. The advantages of Baldwinian repair have been noted before, for example, by Hinton & Nowlan (1987). There may be also an advantage to repairing a small percentage of the chromosomes (Orvosh & Davis 1994).

Table 3-8: Optimum lay-up for the three thick laminates

Case 6	Without Contiguity	$[(\pm 45)_{16}/(90_2)_8/(0_2)_8]_s$
	With Contiguity	$[(\pm 45)_{16}/(90_2)_2/0_2/90_2/0_2/(90_2)_2/(0_2)_2/(90_2)/(0_2)_2/(90_2)/(0_2)_2/(90_2)]_s$
Case 7	Without Contiguity	$[(90_2)_8/(\pm 45)/90_2/(\pm 45)_2/(90_2)/(\pm 45)_2/(90_2)_2/(\pm 45)/90_2/(\pm 45)/(0_2)_9/(\pm 45)]_s$
	With Contiguity	$[(90_2)/(\pm 45)/(90_2)_2/(\pm 45)/(90_2)/(90_2/\pm 45)_3/(90_2)_2/(\pm 45)/(0_2)/(90_2)_2/(0_2)_2/(90_2)/(0_2)_2/(\pm 45)/(0_2)_2/(\pm 45)/(0_2)/(90_2)/(0_2)]_s$
Case 8	Without Contiguity	$[(\pm 45)_7/(90_2)_{15}/(0_2)_{13}]_s$
	With Contiguity	$[(\pm 45)_4/(90_2/\pm 45)_2/(90_2)_2/(\pm 45)/(90_2)/(0_2/90_2)_4/(0_2)/(90_2/0_2)_2/(0_2)/(90_2)/(0_2)_2/(90_2/0_2)_3]_s$

The process is explained first for enforcing the required number of plies of given orientation for the standard GA. The decoding of a chromosome proceeds from the outermost plies to the innermost ones, one two-ply stack at a time. As long as the number of

decoded stacks of any given orientation does not exceed the prescribed number of stacks, the decoding proceeds normally. However, once the number of stacks of any given orientation reaches the prescribed number, subsequent genes that indicate that orientation will be translated to the next available orientation (in a circular 0/45/90 order). For example, consider a laminate with n_0=2, n_{45}=0, and n_{90}=1. When a chromosome [0/90/90] is decoded, the first two genes are decoded normally, but when the third gene is encountered, it cannot be decoded into a 90-stack because the number of decoded 90-genes already reached the target of n_{90}=1, so it is decoded as a zero ply. Similarly, when a chromosome [0/0/0] is decoded, the first two genes are decoded normally. The third gene cannot be decoded into a 0-stack, because the number of required 0-stacks is two. The decoding procedure then tries to see if there are available stacks for a 45-stack, and when it finds that none are available, it puts a 90-stack in the innermost position. It should be noted that the circular order chosen for the orientation used in repair may introduce some bias, and a random selection of the orientation may be a good alternative.

The repair of the stacking sequence without changing the chromosome allows a sequence of mutations needed to achieve a good design to complete successfully even if the intermediate steps are infeasible designs. For example, consider the evolution of a design defined by [0/0/90] chromosome when the optimum is defined by [0/90/0] chromosome (that is stacking sequences of $[0_4/90_2]_s$ to $[0_2/90_2/0_2]_s$, respectively). Without repair we have to depend on hitting the single permutation that will exchange the second and third genes. With the repair strategy described above, we can also go through the intermediate step of [0/90/90], which is decoded into $[0_2/90_2/0_2]_s$, or through the intermediate step of [0/0/0], which is decoded into $[0_4/90_2]_s$. Then another mutation can transform either

intermediate step into the optimum. The last gene in both alternatives acts like a recessive gene, in that it is unexpressed due to the decoding scheme, but it will become expressed following the mutation of another gene.

The repair of violations of contiguity constraints follows the similar approach of repairing only the laminate, and of trying to apply the repair to the innermost plies, which have the least effect on the buckling load. Details may be found in (Todoroki & Haftka, 1998).

For the permutation GA, the constraints of number of plies are incorporated into gene coding, and only contiguity constraints may be violated. To repair contiguity violations, it is desirable to interchange the closest couple of genes with different orientation angles since this minimizes the change in bending properties. The following example illustrates the repair operator.

For the laminate

$[0_2/0_2/90_2/90_2/90_2/\pm 45]_s$

Three contiguous 90 stacks violate the contiguity constraint. Two candidate couples of stacks can be swapped: the rightmost 90° with the ±45°, or the leftmost 90° with its neighouring 0° stack. The first option is selected because the inner plies influence laminate stiffness less than the outer plies.

$$[0_2/0_2/90_2/90_2/\underline{\pm \mathbf{45/90_2}}]_s$$

In order to demonstrate the advantage of recessive repair, it is compared to direct repair of the chromosome in Table 3-9.

From Table 3-9, we can see that the Baldwinian repair (laminate only) is more efficient than repairing the chromosome (Lamarckian repair). The advantage is most

pronounced for the repair strategy helps the standard GA achieve similar efficiencies to that of the permutation GAs, except for the most difficult case (7). Comparing Table 3-9 to Table 3-7, we see that the combined use of permutation and repair is to reduce the cost of the standard GA by one to two orders of magnitude**.**

Table 3-9: Computational cost of laminate repair and chromosome repair

Case No.	Number of Analyses Required for 80% Reliability					
	GR		PMX		SGA	
	Chromosome Repair	Laminate Repair	Chromosome Repair	Laminate Repair	Chromosome Repair	Laminate Repair
1	1048	456	944	792	368	672
2	952	400	808	792	400	536
3	832	352	784	658	384	368
4	680	304	560	496	280	224
5	304	184	272	272	128	80
6	744	416	688	552	416	400
7	480	288	416	336	3936	3512
8	728	352	744	696	56	48

Summary and Concluding Remarks

In this chapter, maximization of the buckling load of composite laminates via stacking sequence optimization for a given number of 0°, ±45°, and 90° plies and for a given in-plane loading was investigated using genetic algorithms. A new permutation GA, which we called a gene-rank crossover GA, was developed and implemented along with two other GAs, a standard GA and a permutation GA based on partially mapped crossover. Computational efficiency of these GAs were compared under eight load cases in terms of

the number of analyses required to reach a certain reliability. The effect on performance of a contiguity constraint, which limits the number of identical adjacent ply orientations to four, was investigated and two repair strategies for dealing with violation of this constraint were implemented.

Stacking sequence design for given number of plies is a combinatorial problem consisting of seeking an optimal permutation. It was demonstrated that the two genetic algorithms based on permutation are much more efficient and more reliable for solving this problem than standard genetic algorithms. Furthermore, a genetic algorithm developed for stacking sequence design showed an advantage over an algorithm developed originally for the traveling salesman problem. Repair developed for overcoming violation of constraints can significantly reduce the computational cost for both the standard GA and the permutation GAs, and with repair the difference between the standard GA and permutation GA is smaller.

The permutation GAs and the repair strategy developed can be easily tailored for application to more complicated structures with more constraints by coding these constraints into gene coding or through repair.

The scope of this chapter research work is panel-level optimization for maximum buckling load of composite laminates. The permutation GA and its corresponding chromosome-repair technique were used in a large number of stacking sequence optimization runs for a range of loads and number of plies. Based on these optima, a cubic polynomial response surface was fitted as a function of in-plane loads and number of 0°, ±45°, and 90° plies. The response surface was then used in a wing box optimization that is described chapter four.

CHAPTER 4
TWO-LEVEL COMPOSITE WING STRUCTURAL OPTIMIZATION USING RESPONSE SURFACES

Introduction

The objective of this chapter is to demonstrate use of a two-level optimization technique for wing panels when the design involves discrete or combinatorial optimization. A wing structure is composed of a large number of panels that must be designed simultaneously to obtain an optimum structural design. Composite stiffened panels often have complex geometries and failure modes. The design of each panel requires a substantial number of variables to describe geometry, ply composition, and stacking sequence. Designing all the panels simultaneously constitutes a complex optimization problem that requires detailed structural modeling of the entire wing, and appears to be beyond present computational capabilities.

This chapter demonstrates use of response surface for maximal panel buckling loads, which involves for coordinating wing-level and panel-level optimization. The methodology is demonstrated for design of a simple wing structure, where the panel design is performed by a genetic algorithm.

First, we described a two-level optimization procedure and summarized formulation of panel and wing optimization and coordination of two-level optimization. Second, we briefly reviewed response surface methodology and discussed normalized response surface of normalized buckling load. Then, we presented results of 6-variable,

18-variable and 54-variable cases of wing box structure. Finally, we summarized concluding remarks of the two-level optimization.

Two-level Optimization Approach

Two-Level Optimization Procedure

In this work, the wing is assumed to consist of *n* unstiffened composite panels. Ply orientations are limited to *0°*, *90°*, and *±45°*. It is also assumed that wing depth is much greater than skin thickness, so that the stresses in the skin are influenced by the number of plies of each orientation rather than their arrangement in the stacking sequence. Consequently, the design process will have the overall wing design determine the amount of plies of each orientation, while the panel design will determine the stacking sequence. The two design processes must be coordinated in order to assure the optimality of the process and insure that the wing design optimization takes into account the effect of its decisions on the panel design.

Here, the two design processes are coordinated through an equation that predicts the buckling load multiplier that a panel can attain with the best stacking sequence. This optimal load equation is a function of the number of plies of each orientation and the loads on the panel. The equation is obtained as a response surface fitted to a large number of panel stacking sequence optimizations for various combinations of numbers of plies and loads.Internal loads and number of 0°, ±45°, and 90° plies which completely determines panel stiffness parameters are used as input parameters for subsystem (panel) optimization. That is, the response surface for optimal buckling load depends on loads $\boldsymbol{N_x}$, $\boldsymbol{N_y}$, $\boldsymbol{N_{xy}}$, and $\boldsymbol{n_0}$, $\boldsymbol{n_{45}}$, $\boldsymbol{n_{90}}$ to output approximate buckling loads. These approximated

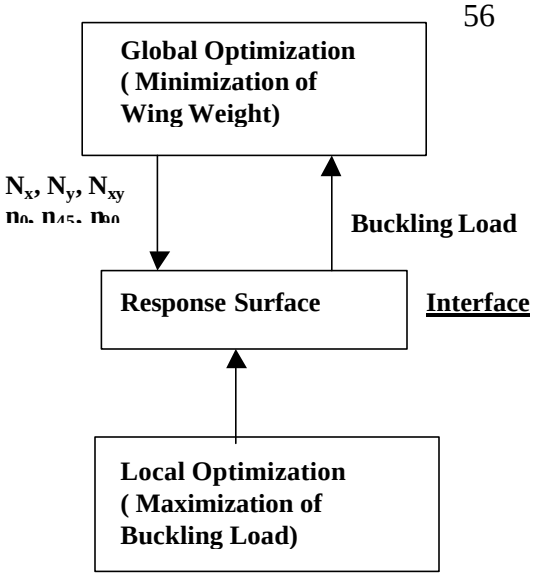

Figure 4-1: Response surface interface of two-level optimization

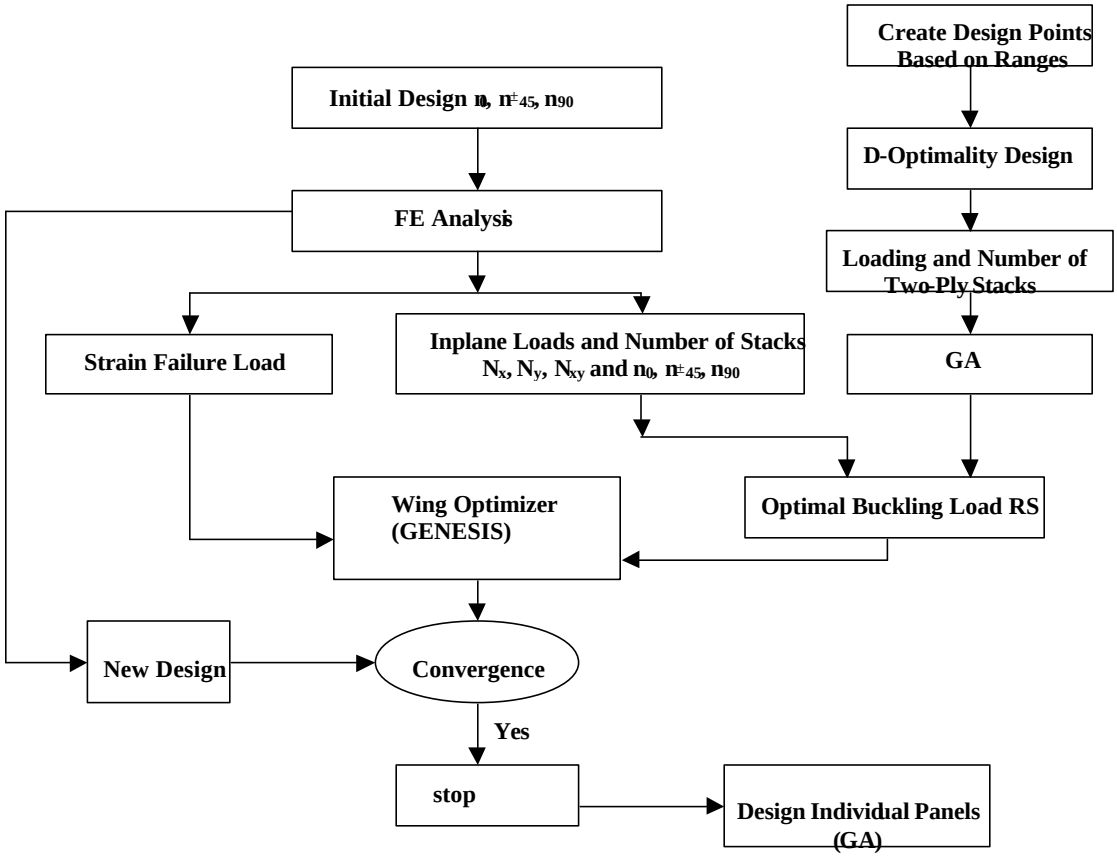

Figure 4-2: Flowchart of two-level optimization procedure

buckling loads are used as constraints in the upper-level (wing) optimization. The process is shown schematically in figure 4-1.

The two-level optimization process is described by the flow chart in Figure 4-2. The process starts with the creation of the response surface shown on the right side of the flow chart. First, a set of design points in specified ranges of loads and number of plies is created. Then a subset of these points is selected by a design of experiments procedure known as D-optimal design. A genetic optimization (GA) of the stacking sequence is carried out at all points at that set, and a response surface for the optimal buckling load is fitted to the results.

The wing-level optimization is carried out by the GENESIS (Vanderplaats et al. 1997) program using the response surface optimization results. Following a finite element analysis of a candidate design, strain constraints are calculated directly by GENESIS, and the buckling load constraint is calculated from the response surface by using the panel loads obtained from the finite element analysis. GENESIS iterates to find the optimum design, using, as *continuous* design variables, the number of plies in each direction for each panel.

Finally, when the wing-level optimization converges, the ply-number design variables have to be rounded to the nearest integer, then each panel is redesigned by the GA. Rounding and errors in the response surface usually cause some panels to be infeasible. For these panels, the last part of the process requires some adjustment in the number of plies to satisfy buckling constraints.

Panel-Level Optimization and Response Surface

In the panel level optimization, the number of $0_2^\circ, \pm 45_2^\circ$, and 90_2° stacks, n_0, n_{45}, and $n_{90,}$ and the inplane loads on the panel, N_x, N_y, and N_{xy} are specified. Thus, the design problem becomes a combinatorial problem of choosing the optimal stacking sequence for given amounts of plies in each direction so as to maximize the buckling load factor l_b (that is, the loads that the optimized panel can carry are $l_b N_x$, $l_b N_y$, and $l_b N_{xy}$). This naturally forms a permutation problem. The stacking sequence is optimized subject to a limit of four contiguous plies of the same orientation (applied to reduce the chance of matrix cracking). A permutation genetic algorithm (GA) developed by the authors (Chapter 3) is used for the stacking sequence design. Buckling analysis is described in Chapter 3.

The panel-level optimization is repeated for a large number of load and ply number combinations and the optimum buckling loads l_b^* are fitted by a cubic response surface as a function of n_0, n_{45}, n_{90}, N_x, N_y, and N_{xy}.

Wing-Level Optimization

The objective function for the wing-level optimization is structure weight. Design variables are the thicknesses of upper and lower skin panels. The ply orientations are limited to $0°$, $90°$, and $\pm 45°$, and each panel has three design variables describing the number of plies of each orientation (with the balance condition, the number of $+45°$ and $-45°$ plies is the same). Strain and buckling constraints are applied.

The numbers of stacks per panel, n_0, n_{45}, and n_{90} are treated as continuous design variables. Each stack consists of two plies: 0_2^0, 90_2^0, and $\pm 45^0$. Minimizing wing weight is equivalent to minimize the total number of plies. GENESIS is used to perform the overall optimization subject to strain and buckling constraints in all panels.

Wing level optimization is formulated as follows:

$$\text{Minimize} \qquad \sum_{i=1}^{n} \left(n_0^i + n_{45}^i + n_{90}^i \right) \tag{4-1}$$

where i is the panel number.

By changing $n_0^i, n_{45}^i, n_{90}^i \qquad i=1, ¼, n$

Subject to: Laminates are symmetric and balanced

$$\text{(Strain)} \qquad l_{ce}^i \geq 1.0, \; i = 1, \cdots, n \tag{4-2}$$

$$\text{(Buckling)} \qquad l_b^{*i} \left(n_0^i, n_{45}^i, n_{90}^i, N_x^i, N_y^i, N_{xy}^i \right) \geq 1.0, \; i = 1, \cdots, n \tag{4-3}$$

where l_{ce}^i indicates the load factor (failure load over applied load) for strain constraints, as calculated by GENESIS. The buckling load factor l_b^{*i} is calculated using the response surface approximation fitted to the optimum buckling load factor of the panels.

Table 4-1: Allowable strains and safety factor

ε_{1a}	0.008
ε_{2a}	0.029
γ_{12}	0.015
Safety Factor	1.5

Example Problem Description

The wing structure considered here is an unswept, untapered, wing box with four spars and three ribs with a total of 18 panels. The wing box is clamped at the root and subjected at the tip to the applied load distribution shown in Figure 4-3.

All the panels are symmetric and balanced laminates made of graphite-epoxy T300/5208, with material properties given in Table 3-2. The allowable strains and safety factor used are given in Table 4-1. Each panel is assumed to be simply supported.

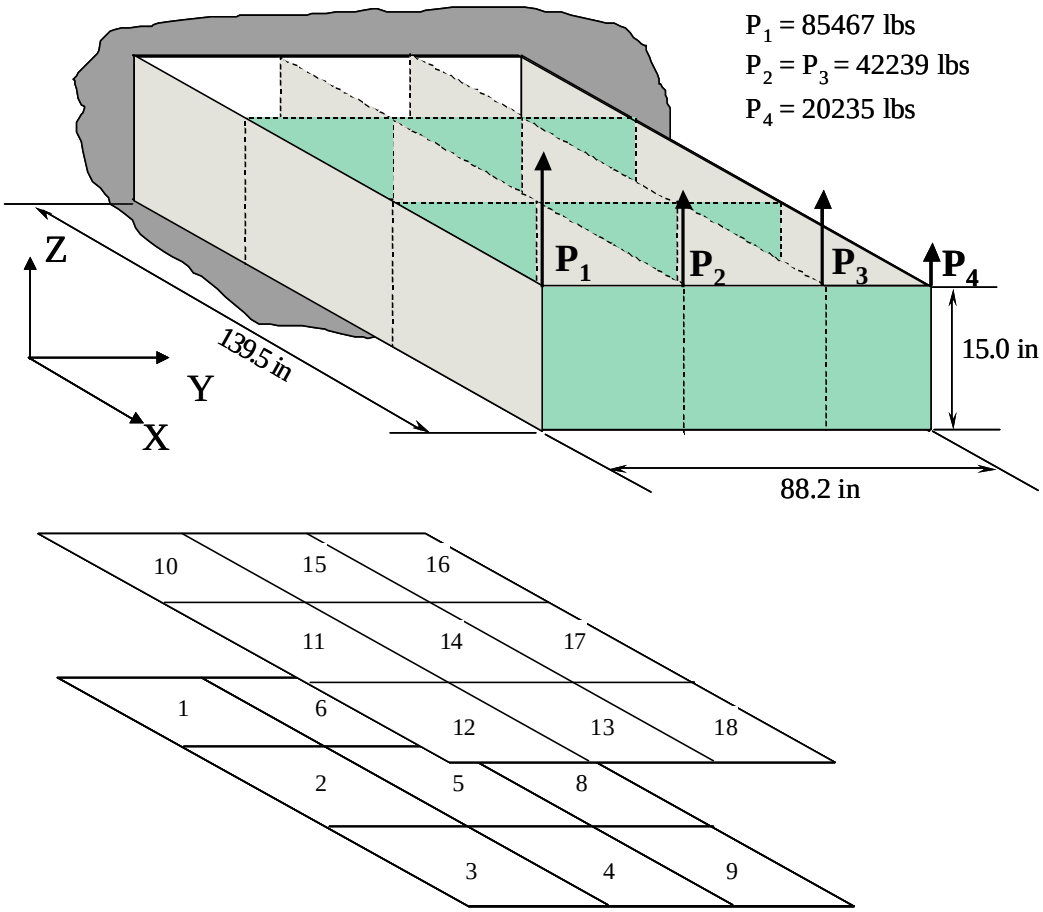

Figure 4-3: Wing box structure

Response Surface Approximation of Optimal Buckling Loads

Response Surface Approximation

Response surfaces are used to obtain an approximate relationship between the response of a system and its control variables. The response function is denoted as *Y* and it

is assumed that it can be approximated as a function of the control variable vector X and a vector of n_b parameters b; that is,

$$\boldsymbol{Y} = \overline{\boldsymbol{Y}}(\boldsymbol{X}, b) + e \tag{4-4}$$

where $\overline{Y}$ represents the approximation, and ε is the error. Least square fit is generally used to estimate the values of the unknown linear regression coefficients b.

Selecting points in the design space where numerical experiments are to be performed is possibly the most important part of obtaining a good approximation to a response function. Several standard designs are available. One example is the central composite design. Standard designs are easy to use, but they may only be applied to a regularly shaped design domain. For more general domains, D-optimal design is widely used. The D-optimality criterion minimizes variance associated with the estimation of the unknown coefficients in the response model. In the present work, the JMP software (SAS 1995) was used to select a D-optimal set of points.

Normalized Buckling Load Response Surface

Because the buckling load is proportional to the cube of the thickness, its magnitude varies greatly from thin laminates to thick ones. This large variation can reduce accuracy of the response surface. To overcome this problem, a buckling load is divided by the cube of the number of stacks and normalized to be order of one (O(1)) as shown below.

$$\overline{l} = \frac{10000\, l_b^*}{(\boldsymbol{n}_0 + \boldsymbol{n}_{45} + \boldsymbol{n}_{90})^3} \tag{4-5}$$

The number of stacks and loads were also normalized.

$$\begin{aligned} r_0 &= \frac{n_0}{n_0 + n_{45} + n_{90}} \\ r_{45} &= \frac{n_{45}}{n_0 + n_{45} + n_{90}} \\ r_{90} &= 1.0 - r_0 - r_{45} \end{aligned} \tag{4-6}$$

$$\begin{aligned} \overline{N}_x &= \frac{2N_x - N_{x\max} - N_{x\min}}{N_{x\max} - N_{x\min}} \\ \overline{N}_y &= \frac{2N_y - N_{y\max} - N_{y\min}}{N_{y\max} - N_{y\min}} \\ \overline{N}_{xy} &= \frac{2N_{xy} - N_{xy\max} - N_{xy\min}}{N_{xy\max} - N_{xy\min}} \end{aligned} \tag{4-7}$$

In the above expressions, “max” and “min” denote the ranges of variables and load components.

Because $r_0+r_{45}+r_0=1$, the normalized buckling load can be expressed as a function of five control parameters.

$$\overline{l} = \overline{l}(r_0, r_{45}, \overline{N}_x, \overline{N}_y, \overline{N}_{xy}) \tag{4-8}$$

Results of Response Surfaces of Optimal Buckling Loads

For the wing shown in Figure 4-3, all panels have the same dimensions. Lower skin panels are subjected mainly to shear load N_{xy} and tensile loads N_x, N_y. Upper skin panels are mostly subjected to compressive loads N_x, N_y, and shear load N_{xy}. Therefore, buckling constraints are applied only for upper skin panels. Since the load ranges are very different, in order to construct high accuracy response surfaces, three critical buckling load response surfaces are fitted, one for root panels, one for intermediate panels, and one for tip panels.

Load ranges for root panels are

$$\begin{aligned} &-15000\ lb/in \le N_x \le -20000\ lb/in \\ &-1000\ lb/in \le N_y \le -4000\ lb/in \\ &0 \le N_{xy} \le 3000\ lb/in \end{aligned} \tag{4-9}$$

Load ranges for intermediate panels are

$$\begin{aligned} &-10000\ lb/in \le N_x \le -15000\ lb/in \\ &-1000\ lb/in \le N_y \le -4000\ lb/in \\ &0 \le N_{xy} \le 3000\ lb/in \end{aligned} \tag{4-10}$$

Load ranges for tip panels are

$$\begin{aligned} &-2000\ lb/in \le N_x \le -5000\ lb/in \\ &-1000\ lb/in \le N_y \le -2000\ lb/in \\ &0 \le N_{xy} \le 3000\ lb/in \end{aligned} \tag{4-11}$$

For all panels, the following ranges of number of $0°$, $\pm 45°$, and $90°$ stacks are used.

$$\begin{aligned} &5 \le n_0 \le 20 \\ &5 \le n_{45} \le 35 \\ &5 \le n_{90} \le 20 \end{aligned} \tag{4-12}$$

Table 4-2: Statistics of three optimal buckling load response surfaces

Statistics	Root Panels	Middle Panels	Tip Panels
R	0.9969	0.9976	0.9956
R_a	0.9955	0.9966	0.9936
Root Mean Square Error $\bar{l}$	0.0020	0.0027	0.0122
Mean of Response $\bar{l}$	0.1312	0.1705	0.4706
RMS Error/ Mean (%)	1.51%	1.56%	2.02%
Average Absolute Error of l_b^*	0.0111	0.0147	0.0613
Average Value l_b^*	1.2411	1.7108	4.7981
Absolute Error of l_b^* /Average Value	0.89%	0.86%	1.28%

More than 30,000 points were randomly generated for each of the three domains defined in (4-9), (4-10), (4-11), and (4-12), and then 180 D-optimal design points were selected from each domain. Stacking sequence GA optimizations were performed at each point. A cubic response surface was fitted to the normalized optimal buckling load $\bar{l}$ in

terms of r_0, r_{45}, and $\overline{N}_x$ $\overline{N}_y$ $\overline{N}_{xy}$. The statistics of the three response surfaces are given in Table 4-2, where R and R_a are the coefficients of multiple determination and its adjusted value, respectively.

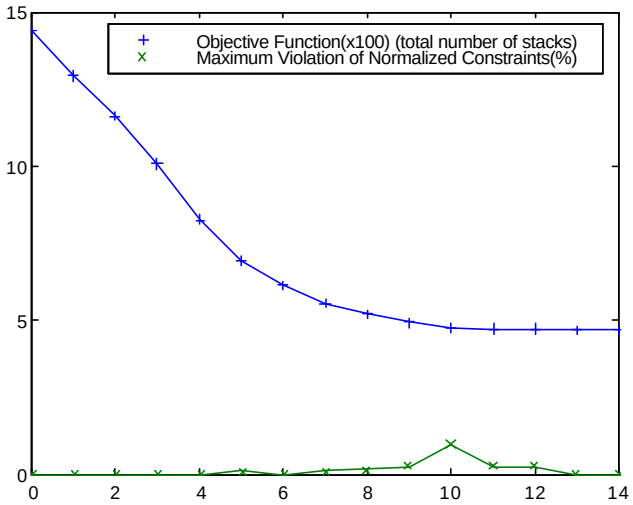

Figure 4-3: History of the objective function and maximum violation of normalized constraints for six-variable case.

The results indicate that the response surfaces have average errors below 2.1% for the normalized optimal buckling load, and average errors below 1.3% for optimal buckling load.

Results of Composite Wing Box Structure Design

The performance of the two-level optimization procedure is demonstrated through six-variable, 18-variable, and 54-variable design problems.

Six-variable Design Problem

For this case, all upper-skin panels are the same and all lower-skin panels are the same, so that the design variables are n_0, n_{45}, and n_{90} for the lower skin and the upper skin. Table 4-3 shows the final design, including the number of *0°*, *±45°*, and *90°* stacks for lower skin panels and upper skin panels, the total number of stacks for all the panels, and the type of active constraints at the optimum. Figure 4-4 shows the history of the objective function and the maximum violation of normalized constraints during the wing-level optimization.

Table 4-3: GENESIS and rounded optimal design with six variables

	Active Constraints	$n_0/n_{45}/n_{90}$ (GENESIS)	$n_0/n_{45}/n_{90}$ (Rounded)	Failure Load Factor λ
Lower Skin Panels	Strain (Panel #7)	8.69/1.76/0.04	9/2/0	1.04127
Upper Skin Panels	Buckling (Panel #16)	15.33/12.44/13.92	15/12/14	0.9664
Objective Function (Total Number of Stacks)		469.70	468	

Table 4-4: Rounded and adjusted upper panel design with six variables

Panel #	GENESIS Design	Rounded Design	λ (Rounded Design)	Adjusted Design	λ (Adjusted Design)
Objective Function	469.70	468		477	
	$n_0/n_{45}/n_{90}$	$n_0/n_{45}/n_{90}$		$n_0/n_{45}/n_{90}$	
16	15.33/12.44 /13.92	CHAPTER 21 5/12/14	0.9664	16/12/14	1.0326
Stacking Sequence (Panel #16)	Rounded Design	$[(\pm45)_{12}/90_4/0_4/(90_4/0_2)_2/90_2/0_2/(0_2/90_2)_3/(90_2/0_4)_3/90_2/0_2]_s$			
	Adjusted Design	$[(\pm45)_{12}/(90_4/0_2)_2/(90_2/0_4)_2/90_2/0_2/90_4/0_2/(0_2/90_2)_2/(0_4/90_2)_3]_s$			

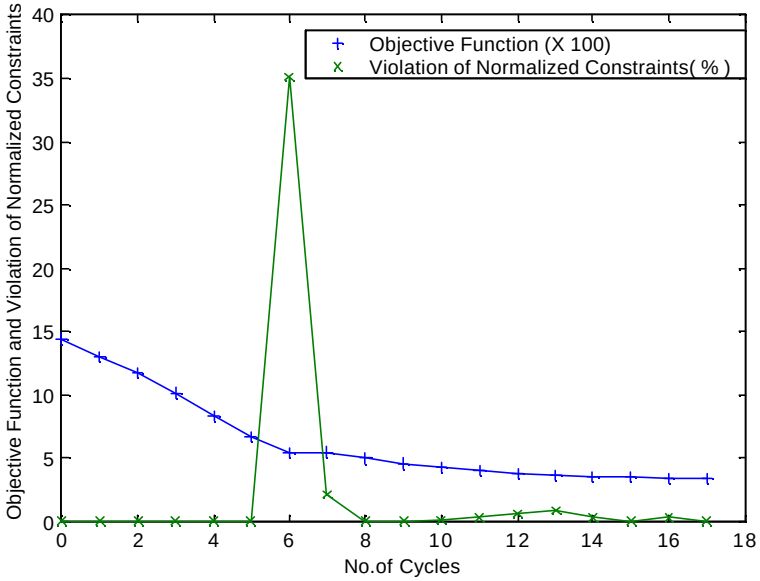

Figure 4-5: History of the objective function and maximum violation of normalized constraints for 18-variable case.

At the optimum, upper root panel 16 is active in buckling, and one strain constraint is active at lower root panel 7. Table 4-3 shows that upper skin panels are thicker than lower skin panels because of the buckling constraints. After the wing level optimization was completed, the continuous design variables obtained by GENESIS were rounded to the nearest integer, and each panel was re-optimized by permutation genetic algorithm. The buckling constraint was violated after rounding as can be expected, because the objective function was reduced to 468 from the optimal 469.7. Table 4-4 shows the buckling load and stacking sequence after manual adjustment. This adjustment increased the total number of stacks to 477.

18-variable Design Problem

For the 18-variable design, each wing skin is divided into three regions: root panels, intermediate panels, and tip panels. Each region has three stack design variables.

Table 4-5: GENESIS and rounded optimal design with 18 variables

Lower Skin Panels	$n_0/n_{45}/n_{90}$ (GENESIS)	$n_0/n_{45}/n_{90}$ (Rounded))	Failure Load λ
(Panel #7)	9.78/0/0	10/0/0	1.0064
Panel #8	5.42/0.29/0	5/0/0	0.8601
Panel #4	0.87/2.04/0	1/2/0	1.0767
Upper Skin Panels	$n_0/n_{45}/n_{90}$ (GENESIS)	$n_0/n_{45}/n_{90}$ (Rounded))	Failure Load λ
(Panel #16)	14.20/13.29/14.13	14/13/14	0.9557
Panel #14	4.60/21.33/7.06	5/21/7	1.0161
Panel #18	3.70/16.80/2.84	4/17/3	1.0583
Objective Function (Total Number of stacks)	349.22	348	

Table 4-5 shows the continuous optimum obtained by GENESIS and the rounded design, and also reveals that after rounding one strain constraint and one buckling constraint are violated. The manually adjusted designs are shown in Tables 4-6 and 4-7. This time most of the lower skin is made of unidirectional material, which is not feasible. In actual design, a limit on the maximum percentage of zero plies must be added.

Table 4-6: Rounded and adjusted lower skin panels with 18 variables

	GENESIS Design	Rounded Design	λ (Rounded Design)	Adjusted Design	λ (Adjusted Design)
	$n_0/n_{45}/n_{90}$	$n_0/n_{45}/n_{90}$		$n_0/n_{45}/n_{90}$	
Panel #7	9.78/0/0	10/0/0	1.0064	10/0/0	1.0183
Panel #8	5.42/0.29/0	5/0/0	0.8601	7/0/0	1.0919
Panel #4	0.87/2.04/0	1/2/0	1.0767	3/1/0	1.0884

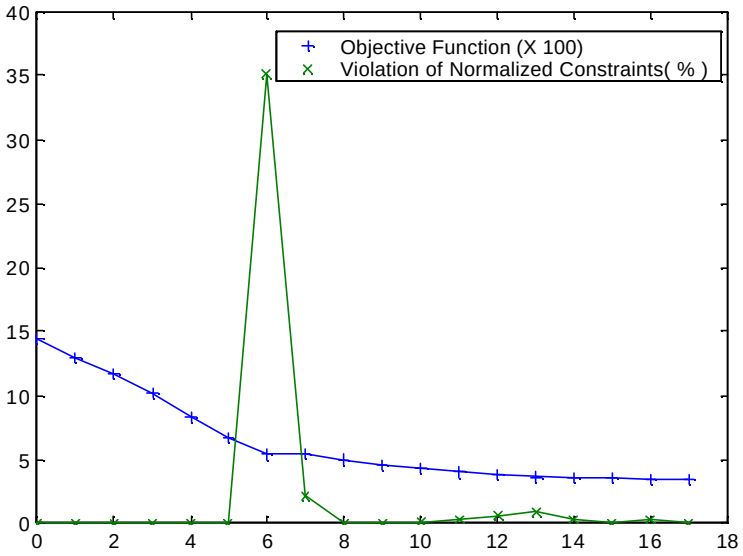

Figure 4-6: History of the objective function and maximum violation of normalized constraints for 54-variable case.

Table 4-7: Rounded and adjusted upper skin panels with 18 variables

Panel #	Unrounded Design	Rounded Design	λ (Rounded Design)	Adjusted Design	λ (Adjusted Design)
	$n_0/n_{45}/n_{90}$	$n_0/n_{45}/n_{90}$		$n_0/n_{45}/n_{90}$	
16	14.02/13.29/14.13	14/13/14	0.9557	15/13/14	1.0361
14	4.60/21.33/7.06	5/21/7	1.0161	5/21/7	1.0186
18	3.70/16.80/2.84	4/17/3	1.0583	4/17/3	1.0241
Stacking Sequence of Rounded Design	Panel #16	$[(\pm45)_{13}/0_4/(90_2/0_2)_2/0_2//90_2/(90_2/0_2)_2/90_4/0_4/(90_4/0_2)_3/0_2/90_2/0_2]_s$			
	Panel #14	$[(\pm45)_{15}/90_2/(\pm45)_4/90_2/(90_2/\pm45)_2/(90_2/0_4)_2/90_2/0_2]_s$			
	Panel #18	$[(\pm45)_{17}/0_4/(90_2/0_2)_2/90_2]_s$			
Stacking Sequence of Adjusted Design	Panel #16	$[(\pm45)_{13}/(90_2/0_4)_4/90_2/(90_2/0_2)_2/90_2/0_4/(90_4/0_2)_2/90_2/0_2]_s$			
	Panel #14	$[(\pm45)_{15}/90_4/(\pm45)_3/90_2/\pm45/90_4/0_2/(0_2/90_2/0_2)_2]_s$			
	Panel #18	$[(\pm45)_{17}/0_4/90_2/(0_2/90_2)_2]_s$			

The total number of stacks for the continuous design was 349.22. It was reduced to 348 for the rounded design, and increased to 360 after adjustment necessary to satisfy the constraints.

Table 4-8: GENESIS and rounded optimal design for 54 variables

Lower Skin Panels	$n_0/n_{45}/n_{90}$ (GENESIS)	$n_0/n_{45}/n_{90}$ (Rounded)	Failure Load λ
1	6.09/0.66/0.17	6/1/0	1.0444
2	3.37/0/0.12	3/0/0	0.9388
3	0.77/0/0	1/0/0	1.2893
4	0.61/1.72/0.0001	1/2/0	1.2399
5	4.73/2.28/0.54	5/2/1	1.0376
6	6.9/0.68/0	7/1/0	1.0111
7	11.16/0.69/1.10	11/1/1	1.0013
8	6.09/0.75/0.70	6/1/1	1.0037
9	1.18/1.59/0	1/2/0	1.0335
Upper Skin Panels	$n_0/n_{45}/n_{90}$ (GENESIS)	$n_0/n_{45}/n_{90}$ (Rounded)	Constraints (Buckling)
10	11.67/11.61/11.83	12/12/12	1.0824
11	6.62/16.37/6.53	7/16/7	1.1200
12	4.15/12.07/5.40	4/12/5	1.1535
13	5.03/12.01/5.40	5/13/5	1.0307
14	5.84/17.32/8.96	6/17/9	0.9747
15	14.67/13.85/11.67	15/14/12	1.0833
16	12.06/18/13.3	12/18/13	1.0524
17	5.91/20.52/6.92	6/21/7	1.0211
18	4.82/14.58/5.46	5/15/5	1.0310

54-variable Design Problem

For the 54-variable design case, each of the panels was permitted to have its own three design variables. Table 4-8 shows the GENESIS and rounded designs, and indicates that one strain constraint and one buckling load constraint are violated. Tables 4-9 and 4-10 compare the strain failure loads and the buckling loads of the rounded design and manually adjusted design for the lower and upper panels, respectively. Table 4-11 shows the stacking sequences of the manually adjusted design. The total number of stacks for the continuous design, increased from 335.44 to 340 for the rounded design, and reduced to 338 after manual adjustment to satisfy all the strain and buckling constraints. The objective function was reduced from 477 to 360 to 338 by increasing the number of design variables

Table 4-9: Comparison of rounded and adjusted designs for lower skin panels, 54 variables

Panel #	GENESIS Design	Rounded Design	λ (Rounded Design)	Adjusted Design	λ (Adjusted Design)
	$n_0/n_{45}/n_{90}$	$n_0/n_{45}/n_{90}$		$n_0/n_{45}/n_{90}$	
1	6.09/0.66/0.17	6/1/0	1.0444	6/1/0	1.0332
2	3.37/0/0.12	3/0/0	0.9388	4/0/0	1.0789
3	0.77/0/0	1/0/0	1.2893	1/0/0	1.0949
4	0.61/1.72/0.0001	1/2/0	1.2399	1/2/0	1.1171
5	4.73/2.28/0.54	5/2/1	1.0376	4/2/1	1.0600
6	6.9/0.68/0	7/1/0	1.0111	7/1/0	1.0423
7	11.16/0.69/1.10	11/1/1	1.0013	11/1/1	0.9928
8	6.09/0.75/0.70	6/1/1	1.0037	7/1/1	1.0507
9	1.18/1.59/0	1/2/0	1.0335	2/2/0	1.2442

Table 4-10: Comparison of rounded and adjusted designs for upper skin panels, 54 variables

Panel #	GENESIS Design	Rounded Design	λ (Rounded Design)	Adjusted Design	λ (Adjusted Design)
	$n_0/n_{45}/n_{90}$	$n_0/n_{45}/n_{90}$		$n_0/n_{45}/n_{90}$	
10	11.67/11.60/11.8	12/12/12	1.0824	11/12/12	1.02384
11	6.62/16.37/6.53	7/16/7	1.1200	6/16/7	1.0895
12	4.15/12.07/4.82	4/12/5	1.1535	3/12/5	1.0921
13	5.03/12.61/5.40	5/13/5	1.0307	5/13/5	1.0782
14	5.84/17.32/8.96	6/17/9	0.9747	7/17/9	1.0003
15	14.67/13.85/11.7	15/14/12	1.0833	15/14/12	1.0236
16	12.06/18.01/13.0	12/18/13	1.0524	11/18/13	0.9915
17	5.91/20.52/6.92	6/21/7	1.0211	6/21/7	1.0134
18	4.82/14.58/5.46	5/15/5	1.0310	5/15/5	1.0051

Table 4-11: Stacking sequences of wing-level panels for the adjusted design

Panel Number	Real Number			Integer Number			Stacking Sequence	Buckling Load
	n_0	n_{45}	n_{90}	n_0	n_{45}	N_{90}		
10	11.67	11.60	11.83	11	12	12	$[(\pm45)_{12}/90_4/0_2/(90_2/0_2)_5/(0_2/90_4)_2/0_4/90_2/0_2]_s$	1.02384
11	6.62	16.37	6.53	6	16	7	$[(\pm45)_{15}/0_2/\pm45/0_4/(90_4/0_2)_3/90_2]_s$	1.0895
12	4.15	12.07	4.82	3	12	5	$[(\pm45)_{12}/(0_2/90_4)_2/0_2/90_2]_s$	1.0921
13	5.03	12.61	5.40	5	13	5	$[(\pm45)_{12}/0_2/\pm45/0_4/(90_4/0_2)_2/90_2]_s$	1.0782
14	5.84	17.32	8.96	7	17	9	$[(\pm45)_{16}/0_2/\pm45/0_2/(0_2/90_4)_4/0_2/90_2]_s$	1.0003
15	14.67	13.85	11.67	15	14	12	$[(\pm45)_{11}/90_2/(\pm45)_2/90_2/\pm45/90_2/(90_2/0_2)_3/(0_2/90_2/0_2)_6]_s$	1.0236
16	12.06	18.01	13.30	11	18	13	$[(\pm45)_{16}/(90_2/\pm45)/(90_4/0_2)_3/(90_2/0_2)_2/(0_2/90_2/0_2)_3]_s$	0.9915
17	5.91	20.52	6.92	6	21	7	$[(\pm45)_{20}/0_2/\pm45/0_4/(90_4/0_2)_3/90_2]_s$	1.0134
18	4.82	14.58	5.46	5	15	5	$[(\pm45)_{15}/0_4/(90_2/0_2)_2/90_4/0_2/90_2]_s$	1.0051

Concluding Remarks

A two-level wing design optimization was developed and demonstrated using a simple wing example. The procedure is based on continuous optimization at the wing level using a finite element model, and genetic optimization at the panel level. A response surface of optimal panel buckling load is used for communication between the two levels.

It was shown that a cubic response surface can fit accurately the buckling load of the optimal panel stacking sequence as a function of the loading on the panel and the given number of plies in each orientation. It was also shown that the response surface could be used effectively to allow the wing-level optimization to find a near optimal wing design.

The use of continuous variables at the wing level allowed for inexpensive optimization and use of the commercial GENESIS software program. Some constraint violations occurred when the number of plies was rounded off and the stacking sequence was optimized to find the actual design. However, it was possible to manually adjust thicknesses to correct violations with very small increases in total weight.

CHAPTER 5
COMPOSITE WING STRUCTURAL DESIGN OPTIMIZATION WITH CONTINUITY CONSTRAINTS

Introduction

Because of efficiency for structure weight compared to traditional structures consisting of isotropic materials, industry now is paying much more attention to the use of composite structures. Complex composite structures, such as aircraft wing or fuselage structures or car chassis structures, commonly consist of multiple laminates. Composite laminates consist of layers of one or more materials stacked at different orientation angles. The layer thickness for each material is usually fixed and fiber orientation angles are often limited to a discrete set such as 0°, ±45°, and 90°.

In the design of complex structures, it is customary to divide the structures into panels or regions that may be designed independently or semi-independently (Schmit & Mehrinfar 1982; Ragon et al. 1997; Liu et al. 2000). This is done not only for computational convenience, but also because the loads vary from one part of the structure to another, so that structural efficiency dictates variation in structural properties. With this design approach, adjacent laminates may have different total thicknesses, and some plies may terminate at the laminate boundaries. These discontinuities can cause stress concentrations and increase manufacturing difficulty and cost.

While some discontinuities are inevitable if structural efficiency is to be maintained, it is desirable to minimize these discontinuities. It is therefore desirable to add continuity constraints for adjacent laminates in the design process, or include a measure of

continuity in evaluating competing designs. It may be expected that optimization including continuity constraints may lead to designs with fewer and smaller discontinuities.

Kristinsdottir et al. (2001) recently developed the concept of blending rule to measure ply continuity in adjacent composite panels. Two ways of specifying the blending rules in optimal design formulation are set forth and compared. Comparing results with blending measure and results without blending measure, design with blending is heavier than design without blending but design with blending is easier to manufacture.

The first step in incorporating continuity in the design process is to develop measures of continuity between adjacent panels. The objective of this chapter is to develop such measures. Two continuity measures are defined in terms of material composition and stacking sequence. The continuity measures are applied to a simple wing design problem, and trade-off studies between weight and continuity are performed.

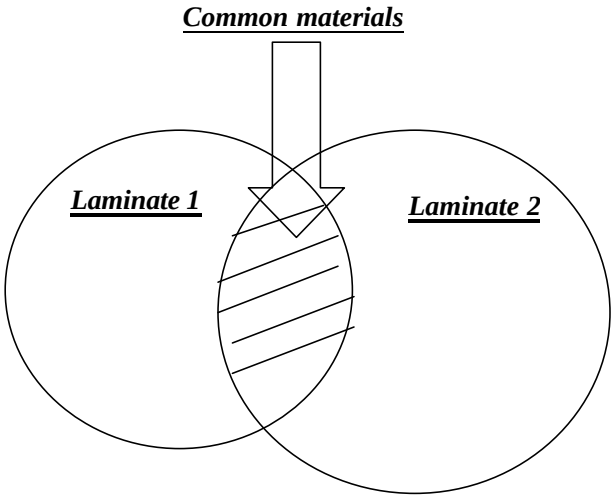

Figure 5-1: Common layers of two laminates

Material and stacking sequence continuity measures for symmetric laminates

Algorithms for designing complex composite structures often design panels at two levels (see chapter 4). At the global level the material composition of each laminate is determined. For example, at that level it may be decided based on overall stiffness considerations that a laminate is made of 20% 0° tape plies, 30% ±45° tape plies, and 50% 90° cloth plies. At the local level, the stacking sequence of the plies is decided. Consequently, it may be useful to develop two measures of continuity: one measure of material composition continuity for the global design, and another measure of stacking sequence continuity for the local level design.

Material Composition Continuity

We assume that there are $\boldsymbol{N}$ possible layer types. These layer types may differ in material properties, thickness, or fiber orientation angles. Layer type $\boldsymbol{l_i}$ has material $\boldsymbol{m_i}$, fiber orientation angle a_i, and thickness $\boldsymbol{t_i}$. Of course, it is possible that all the materials and thicknesses are the same, in which case we just have a problem of continuity of ply orientations.

Given two composite laminates, our first measure of continuity, composition continuity C_m, is the fraction of common layers of the two laminates to the total thickness of one of the two laminates, used as a reference. This is depicted schematically in Figure 5-1.

We will describe a laminate using the notation $[l_1/l_3/l_2/l_4/\ldots l_2]_s$, where l_i denotes a layer of type i. For example, two laminates are given as follows:

$$\textit{Laminate 1} \quad [\boldsymbol{l}_{i1}/\boldsymbol{l}_{i2}/\cdots/\boldsymbol{l}_{in}]_s$$
$$\textit{Laminate 2} \quad [\boldsymbol{l}_{j1}/\boldsymbol{l}_{j2}/\cdots/\boldsymbol{l}_{jm}]_s$$

where n and m are the total number of lamina in the first and second laminate, respectively. We denote by $h_1(l_i)$ the thickness of layers with type l_i in Laminate 1, and by $h_2(l_i)$ the thickness of layers with type l_i in Laminate 2.

The thickness of common layers $h_c(l_i)$ of type l_i is then

$$h_c(l_i) = Minimum\{h_1(l_i),\ h_2(l_i)\} \tag{5-1}$$

Then, a one-sided composition continuity measure, referred to the first panel is defined as

$$C^c_{1->2} = \frac{sum\{\min\{n_i, m_i\}\}}{H_2} \tag{5-2}$$

Similarly, the same measure, referred to the second panel is

$$C^c_{2->1} = \frac{sum\{\min\{n_i, m_i\}\}}{H_2} \tag{5-3}$$

where H_1 is the total thickness of Laminate 1, and H_2 is the total thickness of Laminate 2.

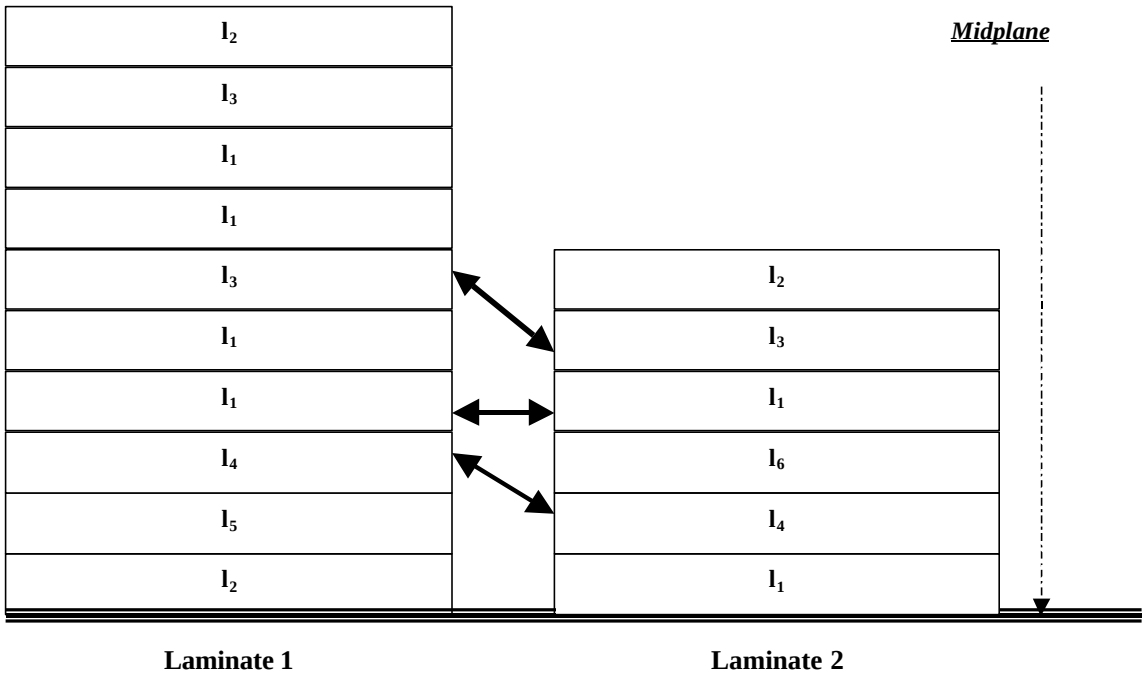

Figure 5-2: Count of the number of continuous layers of two laminates

In contrast to the one-sided composition continuity measure, a two-sided composition continuity measure is defined as the fraction of common layers to the thicker laminate:

$$C_c = \frac{sum\{\min\{n_i, m_i\}\}}{\max imum\{H_1, H_2\}} \tag{5-4}$$

Stacking sequence continuity

Stacking sequence continuity is a measure of the number of layers that can be continuous between two adjacent laminates. That is, a ply in one laminate can continue to the next laminate if both layers are of the same type l_i and if they are separated in the thickness direction by a small number of terminated layers. In the present work, we assume that this separation must not exceed one layer. For example, given the two laminates

Laminate 1: $_s[l_2/\ l_5/\ l_4/\ l_1/\ l_1/\ l_3/\ l_1/\ l_1/\ l_3/\ l_2]$
Laminate 2: $_s[l_1/\ l_4/\ l_6/\ l_1/\ l_3/\ l_2]$

Figure 5-2 shows how we count the number of continuous plies by assuming that the symmetric laminates share their midplane. Note that the outermost plies of Laminate 1 and Laminate 2, of type l_2, are assumed to be terminated because they are separated by three truncated plies.

From Figure 5-2, we observe that there are three continuous layers, and these layer with thicknesses h_1, h_3 and h_4. (h_i is the layer thickness with layer type l_i). So the total thickness of the continuous layers h_{cont} is

$$h_{cont} = h_1 + h_3 + h_4 \tag{5-5}$$

and the one-sided stacking sequence continuity indices are calculated as

$$C^s_{1->2} = \frac{h_{cont}}{H_1} \tag{5-6}$$

$$C^s_{2->1} = \frac{h_{cont}}{H_2} \tag{5-7}$$

The two-sided stacking sequence continuity measure is calculated as

$$C_s = \frac{h_{cont}}{\max imum\{H_1, H_2\}} \tag{5-8}$$

Examples

In order to demonstrate the continuity measures, two cases are selected. The fiber orientation angle set is {0°, 45°, 90°}, the material property set is {m_1, m_2}, and the ply thickness set is {0.01,0.02, 0.03} (in). The notation $(a_i \mid m_j \mid t_k)$ represents fiber orientation angle a_i, material property m_j, and ply thickness t_k, $a_i \in \{0^\circ, 45^\circ, 90^\circ\}$, $m_j \in \{m_1, m_2\}$, $t_k \in \{0.01, 0.02, 0.03\}$. The total number of layer types is 18, see Table 5-1.

Table 5-1: Definition of layer type and its layer code for examples

Layer code	Layer type	Layer code	Layer type	Layer code	Layer type
l_1	(0°/m_1/0.01)	l_7	(45°/m_1/0.01)	l_{13}	(90°/m_1/0.01)
l_2	(0°/m_1/0.02)	l_8	(45°/m_1/0.02)	l_{14}	(90°/m_1/0.03)
l_3	(0°/m_1/0.03)	l_9	(45°/m_1/0.03)	l_{15}	(90°/m_1/0.03)
l_4	(0°/m_2/0.01)	l_{10}	(45°/m_2/0.01)	l_{16}	(90°/m_2/0.01)
l_5	(0°/m_2/0.02)	l_{11}	(45°/m_2/0.02)	l_{17}	(90°/m_2/0.02)
l_6	(0°/m_2/0.03)	l_{12}	(45°/m_2/0.03)	l_{18}	(90°/m_2/0.03)

Material composition continuity and stacking sequence continuity indices are listed in Table 5-2. Detailed stacking sequences of two laminates are shown in Figure 5-3.

Case 1

Laminate 1 $_s[l_{12}\backslash l_{15}\backslash l_{17}\backslash l_{15}\backslash l_{16}]$
Laminate 2 $_s[l_4\backslash l_2\backslash l_{15}\backslash l_6]$
Case 2

Laminate 1 $_s[l_{17}\backslash l_{10}\backslash l_{13}\backslash l_4\backslash l_{16}\backslash l_{11}\backslash l_{14}\backslash l_{10}\backslash l_{17}\backslash l_4\backslash l_4\backslash l_{13}\backslash l_{18}\backslash l_2]$

Laminate 2 $_s[l_{18}\backslash l_2\backslash l_2\backslash l_{18}\backslash l_5\backslash l_{11}\backslash l_8\backslash l_{16}\backslash l_{10}\backslash l_{13}\backslash l_{13}]$

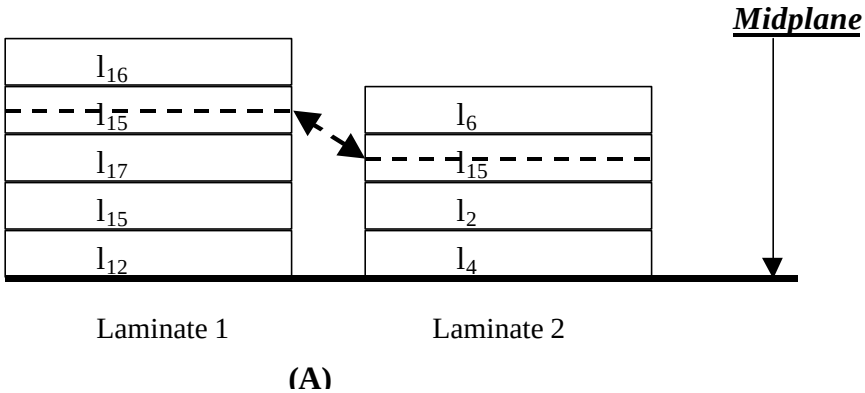

(A)

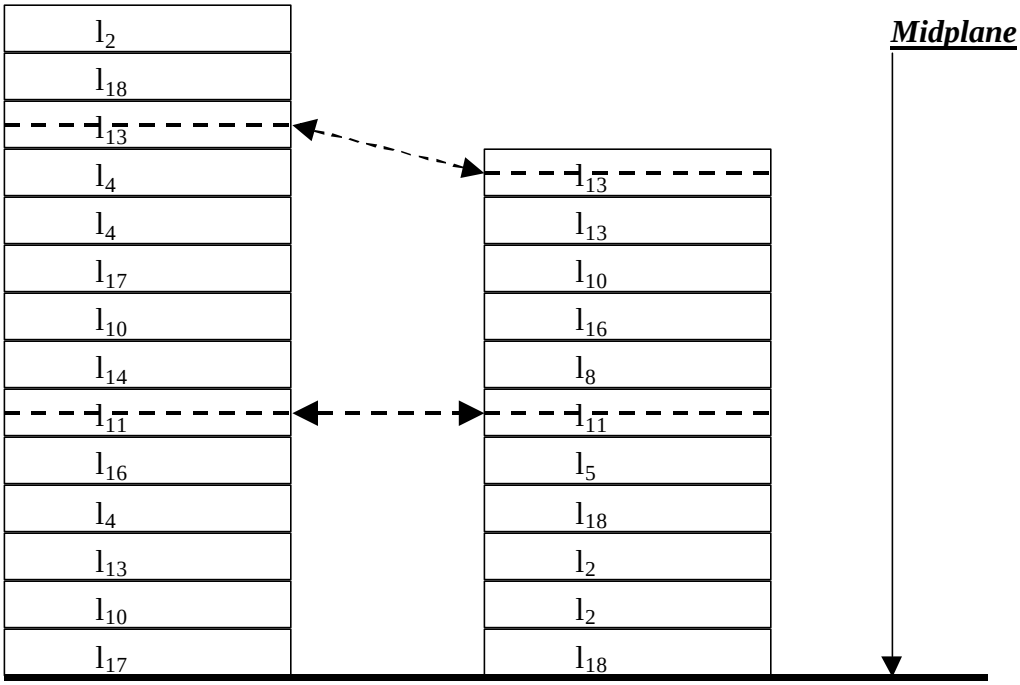

(B)

Figure 5-3: Details of stacking sequence continuity: (A) Case 1; (B) Case 2

Table 5-2: Composition and stacking sequence continuity indices for two laminate examples

Case No.	Number of Layers/ Thickness (Laminate 1)	Number of Layers/ Thickness (Laminate 2)	Common Materials (Thickness)	Number of continuous layers/Thickness of continuous layers
1	5/0.12	4/0.09	0.03	1/0.03
2	14/0.21	11/0.20	0.11	2/0.03
Type of continuity	One-sided composition	Two-sided composition	One-sided stacking sequence	Two-sided stacking sequence
1	$C_{1->2}$=25% $C_{2->1}$=33.33%	25%	$C_{1->2}$=33.33% $C_{2->1}$=25%	25%
2	$C_{1->2}$=52.4% $C_{2->1}$=55%	52.4%	$C_{1->2}$=15% $C_{2->1}$=14.3%	14.3%

Minimization of composite wing weight with continuity constraints

The composite wing structure considered here is an unswept and untapered wing box with four spars and three ribs, with a total of 18 skin panels, shown in Figure 4-3. The wing box is clamped at the root and subject to the tip load distribution shown in Figure 4-3. All the panels are symmetric and balanced laminates made of graphite-epoxy T300/5208 whose material properties are shown in Table 3-2. Ply thickness is fixed at 0.005 in, and the fiber orientation angle is selected from a small set {0º, ±45º,90º}. So continuity of laminates is calculated only considering fiber orientation angles.

The optimization of the composite wing is performed using a two-level optimization procedure using response surfaces for communication between the two levels (Chapter 4). The upper skin panels are substantially thicker than the lower skin panels due to buckling constraints. After an overall wing design is obtained that defines the number of 0°, ±45° and 90° plies for each panel, a genetic algorithm is used to obtain the stacking sequence of each panel.

The formulation of the minimization of the wing weight with continuity constraints is expressed as follows:

$$\text{Minimize} \quad \sum_{i=1}^{18} (n_0^i + n_{45}^i + n_{90}^i) \tag{5-9}$$

where i is the panel number, by changing n_0^i, n_{45}^i, n_{90}^i, $i=1,¼, n$, subject to:

Laminates are symmetric and balanced

Strain failure load constraints: $l_{ce}^i \geq 1$ (5-10)

Buckling load constraints: $l_b^{*i}(n_0^i, n_{45}^i, n_{90}^i, N_x^i, N_y^i, N_{xy}^i) \geq 1$ (5-11)

Continuity constraints: $C_{i->j}^c \geq x\%$ (5-12)

The design variables are the number of 0°, ±45° and 90° stacks (n_0, n_{45}, and n_{90}) in each panel. The objective function is the total weight of 18 composite panels that is proportional to the sum of the number of 0°, ±45° and 90° stacks in all the panels.

The strain failure load is calculated by a finite element (FE) analysis using GENESIS (Vanderplaats 1997). Buckling loads are approximated through response surfaces fitted to the results of multiple panel optimizations that maximize the buckling load by changing the stacking sequence of the panels. Continuity constraints for multiple panels $C_{i->j}^c$ are calculated for given amounts of 0°, ±45°, and 90° stacks of two laminates. Additional details about the continuity constraints are given in following sections for the wing box problem. Because the two-sided continuity constraints are non-smooth, only one-sided continuity constraints are considered.

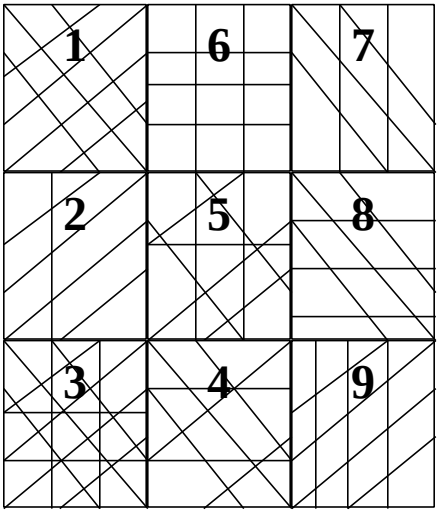

Figure 5-4: Lower skin panels

One-sided Continuity Constraints for Multiple Composite Panels

Continuity constraints are applied to each pair of adjacent panels in the wing. For the nine lower skin panels, the total number of continuity constraints is 24, and the same numbers of constraints are used for the nine upper skin panels. For example, Panel 1 has two neighbors: Panels 2 and Panel 6. So the two continuity constraints for Panel 1 are:

$$C_{1->2} = \frac{sum\{\min\{n_i^{Panel\,1}, m_i^{Panle\,2}\}\}}{H_1} \quad (5\text{-}13)$$

$$C_{1->6} = \frac{sum\{\min\{n_i^{Panel\,1}, m_i^{Panel\,6}\}\}}{H_1} \quad (5\text{-}14)$$

Similarly,

Panel 2: $C_{2->1}$, $C_{2->5}$ and $C_{2->3}$

Panel 3:$C_{3->2}$ and $C_{3->4}$

Panel 4: $C_{4->3}$, $C_{4->5}$ and $C_{4->9}$

Panel 5: $C_{5->2}$, $C_{5->4}$, $C_{5->6}$ and $C_{5->8}$

Panel 6: $C_{6->1}$, $C_{6->5}$ and $C_{6->7}$

Panel 7: $C_{7->6}$ and $C_{7->8}$

Panel 8: $C_{8->5}$, $C_{8->7}$ and $C_{8->9}$

Panel 9: $C_{9->4}$ and $C_{9->8}$

Table 5-3: Minimum weight of composite wing versus required average (over all panels) continuity

Continuity Requirement X	Weight	Average continuity
50%	323.64	78.87%
55%	324.70	79.77%
60%	326.40	80.94%
65%	330.68	83.22%
70%	336.23	85.95%
75%	342.83	87.36%
80%	358.23	89.27%
85%	378.32	91.80%
90%	405.81	95.27%
95%	432.08	97.77%
98%	454.19	99.00%
99%	462.43	99.40%

Similarly for the 9 upper skin panels,

Panel 10: $C_{10->11}$ and $C_{10->15}$

Panel 11: $C_{11->10}$, $C_{11->12}$ and $C_{11->14}$

Panel 12: $C_{12->11}$, $C_{12->13}$

Panel 13: $C_{13->12}$, $C_{13->14}$ and $C_{13->18}$

Panel 14: $C_{14->11}$,$C_{14->13}$,$C_{14->15}$ and $C_{14->17}$

Panel 15: $C_{15->10}$,$C_{15->14}$ and $C_{15->16}$

Panel 16: $C_{16->15}$ and $C_{16->17}$

Panel 17: $C_{17->16}$, $C_{17->14}$ and $C_{17->18}$

Panel 18: $C_{18->17}$ and $C_{18->13}$

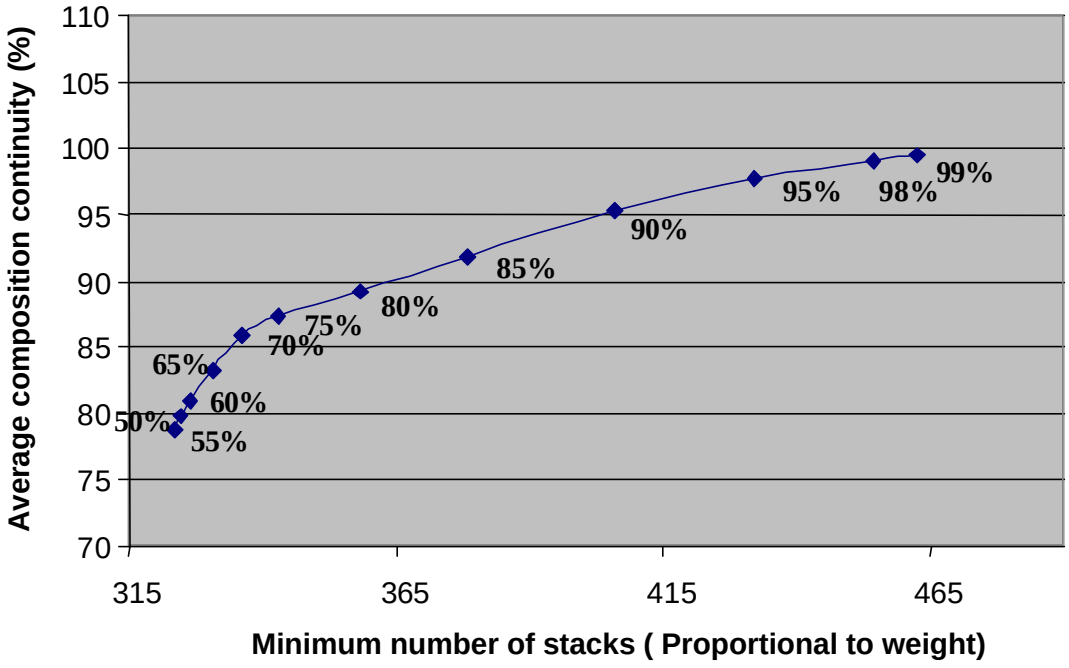

Figure 5-5: Average (abscissa) and required (numbers on graph) material continuity vs. minimum number of stacks.

Weight-continuity tradeoffs

The design variables of this problem are the numbers of 0°, ±45° and 90° stacks for each of the 18 wing panels. So the number of design variables is 54. If we constrain all nine lower skin panels to have the same laminate and all nine upper skin panels to have same laminate, we obtain a six-design variable problem. For this six-variable problem, there are no discontinuities between adjacent laminates, so that the continuity indices are

100%. The weight of the wing provides one extreme to the tradeoff between weight and continuity for X=100% in Eq. (5-9). The weight of the wing with 54 design variables and no continuity constraints provides another extreme to this tradeoff. As will be shown below, this design can be obtained without continuity constraints, or also with X=50%.

Table 5-3 shows the average composition continuity and minimum weight for different continuity requirement value *X*. The average continuity is taken over all the panels in the wing. The information is illustrated graphically in Figure 5-5.

From Table 5-3 and Figure 5-5, we observe that increasing the required continuity up to 70% requires only about 4% increase in weight, increasing it from 70% to 80% requires about an additional 7% increase in weight, and increasing it from 80% to 90% an additional 13%. Thus it appears that substantial increases in continuity are available at little additional weight, but beyond a certain point it becomes very expensive.

Stacking Sequence Design

After the global level optimization, continuous global optima need to be rounded to integer optima and GAs are employed to obtain the stacking sequence design of individual panel. Stacking sequence continuity constraints may be included in panel level design. In the present work, these constraints are not included, and instead we simply observe what level of stacking sequence continuity is achieved without these constraints. The procedure is to first round the continuous optima of numbers of 0°, ±45°, and ±90° stacks and obtain the stacking sequence from the GA. The rounding of ply stack numbers will normally cause internal panel load redistribution and cause some of the buckling and strain constraints to be violated. So, manual adjustment of integer optima is necessary, see Chapter 4.

Table 5-4: GENESIS, rounded and adjusted optima for composition continuity requirement of 50%

Panel No.	Genesis optima	Rounded optima	Adjusted optima
Lower skin	$n_0/n_{45}/n_{90}$	$n_0/n_{45}/n_{90}$	$n_0/n_{45}/n_{90}$
1	4.61/0.00/0.00	5/0/0	5/0/0
2	2.93/0.00/0.04	3/0/0	3/0/0
3	1.47/0.00/0.01	1/0/0	1/0/0
4	2.11/0.00/0.00	2/0/0	2/0/0
5	4.10/0.00/0.00	4/0/0	4/0/0
6	6.97/0.00/0.00	7/0/0	7/0/0
7	12.97/0.00/0.00	13/0/0	13/0/0
8	8.04/0.18/0.001	8/0/0	8/0/0
9	3.93/0.28/0.00	4/0/0	4/0/0
Upper skin panels	$n_0/n_{45}/n_{90}$	$n_0/n_{45}/n_{90}$	$n_0/n_{45}/n_{90}$
10	0.52/18.79/9.42	1/19/9	3/19/9
11	0.35/26.72/0.77	0/27/1	2/23/1
12	0.03/18.74/0.42	0/19/0	2/17/0
13	16.83/20.20/0.75	0/20/0	0/19/1
14	0.01/26.21/6.55	0/26/7	0/25/7
15	19.42/15.18/8.81	19//15/9	19/15/19
16	12.35/17.15/12.8	12/17/13	12/17/13
17	0.79/31.93/3.26	1/32/3	1/33/3
18	15.07/23.30/0.00	2/23/0	2/24/0
Optima	323.64	323	324
Average Composition Continuity	78.87%	78.10%	77.79%

Table 5-5: Stacking sequence and average continuity of nine upper skin panels for composition continuity requirement X=50%

Panel No.	Stacking Sequence
10	$_s[0_2/\pm45/0_2/90_4/(\pm45)_2/90_2/(90_2/\pm45)_2/\pm45/(\pm45/90_2)_2/(\pm45)_7/(\pm45/90_2)_2/(\pm45)_3]$
11	$_s[0_2/\pm45/0_2/(\pm45)_{14}/90_2/(\pm45)_9]$
12	$_s[0_2/(\pm45)_{18}]$
13	$_s[90_2/(\pm45)_{19}]$
14	$_s[90_2/(\pm45/90_4)_2/(\pm45)_2/90_2/(\pm45)_4/90_2/(\pm45)_{17}]$
15	$_s[0_2/90_2/0_4/90_2/0_4/\pm45/(0_4/90_2)_4/(0_4/\pm45)_2/0_4/\pm45/0_4/(\pm45)_9/90_2/(\pm45)_3]$
16	$_s[90_2/0_2/(90_4/0_2)_5/(90_2/0_4)_2/\pm45/0_4/(\pm45)_{16}]$
17	$_s[0_2/(\pm45)_3/90_2/(\pm45)_{13}/90_2/(\pm45)_{16}/90_2/\pm45]$
18	$_s[0_2/\pm45/0_2/(\pm45)_{23}]$
Average Stacking Sequence Continuity	56.52%

For each panel, the average material and stacking sequence continuity measures are computed. The average is taken over all neighboring panels. Two design cases are selected here for comparison purposes. One is the material continuity requirement at 50%. The other is the material continuity requirement at 85%. Table 5-4 shows GENESIS optima (continuous optima), rounded optima and manual design. Table 5-5 lists the detail stacking sequence of 9 upper skin panels at material continuity 50% and gives the average stacking continuity for 9 upper skin panels.

Table 5-6, 5-7 show results of GENESIS optima, rounded optima, adjusted optima and corresponding to stacking sequence, average stacking sequence continuity at material continuity requirement 85%. Here, the stacking sequence continuity mentioned is two-sided stacking sequence continuity.

Table 5-6: GENESIS, rounded and adjusted optima for composition continuity requirement X=85%

Panel No.	Genesis optima	Rounded optima	Adjusted optima
Lower skin panels	$n_0/n_{45}/n_{90}$	$n_0/n_{45}/n_{90}$	$n_0/n_{45}/n_{90}$
1	7.56/0.00/0.00	8/0/0	8/0/0
2	6.41/0.07/0.00	6/0/0	6/0/0
3	5.43/0.07/0.00	5/0/0	5/0/0
4	6.41/0.07/0.00	6/0/0	6/0/0
5	7.55/0.07/0.00	8/0/0	8/0/0
6	8.91/0.07/0.00	9/0/0	9/0/0
7	10.49/0.06/0.00	10/0/0	11/0/0
8	8.90/0.07/0.00	9/0/0	9/0/0
9	7.55/0.07/0.00	8/0/0	8/0/0
Upper skin panels	$n_0/n_{45}/n_{90}$	$n_0/n_{45}/n_{90}$	$n_0/n_{45}/n_{90}$
10	12.44/6.36/10.25	12/13/10	11/13/11
11	10.40/6.37/7.00	10/13/7	10/13/7
12	10.44/4.21/6.82	10/8/7	10/8/7
13	10.40/4.21/11.30	10/8/11	10/8/11
14	10.37/6.36/12.28	10/13/12	10/13/12
15	16.60/6.33/12.28	7/13/12	17/13/12
16	11.57/7.50/15.96	12/15/16	12/15/16
17	6.48/7.51/14.70	6/15/15	6/15/15
18	6.51/5.99/12.35	7/12/12	7/12/12
Optima	378.32	375	376
Average Composition Continuity	91.80%	91.23%	90.89%

Table 5-7: Stacking sequence and average continuity of nine upper skin panels for composition continuity requirement X=85%

Panel No.	Stacking Sequence
10	$_s[0_2/90_2/(0_4/90_2)_3/0_2/90_2/(0_2/90_4)_3/(\pm45)_{13}]$
11	$_s[90_2/(0_2/90_4)_2/0_2/90_2/0_4/90_2/(0_4/\pm45)_2/0_2/(\pm45)_{11}]$
12	$_s[90_2/(0_2/90_4)_2/0_2/(90_2/0_4)_2/\pm45/0_4/\pm45/0_2/(\pm45)_6]$
13	$_s[90_2/(0_2/90_4)_4/(0_2/90_2)_2/0_4/\pm45/0_4/(\pm45)_7]$
14	$_s[90_2/0_2/(90_4/0_2)_5/90_2/0_4/\pm45/0_4/(\pm45)_{12}]$
15	$_s[0_2/90_2/(0_4/90_2)_8/\pm45/90_2/((\pm45)_2/90_2)_2/(\pm45)_8]$
16	$_s[0_2/90_4/0_2/(0_2/90_2)_2/0_4/90_4/0_2/(0_2/90_4)_5/(\pm45)_{15}]$
17	$_s[90_2/(0_2/90_4)_6/\pm45/90_4/(\pm45)_{14}]$
18	$_s[90_2/(0_2/90_4)_5/0_2/90_2/0_2/(\pm45)_{12}]$
Average Stacking Sequence Continuity	72.11%

From the above tables, we can see that, for both cases, we can adjust the stacking sequences to satisfy the constraints with only a little change in composition continuity compared with the continuous optima.

Comparing the two cases, we observe that the minimum number of 324 stacks for a composition continuity requirement of 50% rises to 376 stacks for a composition continuity requirement of 85%. The weight increases 16%, the average composition continuity increases 13.1% from 77.8% to 90.9% and the average stacking continuity increases 15.6% from 56.5% to 72.1%. It is to be expected that if stacking sequence continuity constraints were included, additional improvements can be made. So in future work, stacking sequence continuity constraints will also be included in the wing and panel level optimization.

Concluding Remarks and Future Work

In this chapter, two measures of composition continuity and stacking sequence continuity are introduced. Composition continuity constraints are included in the global

wing level optimization of a simple composite wing example. The results demonstrate that substantial improvements in continuity can be first obtained with little weight penalty. However, beyond a certain point, additional increases in continuity measures require large increases in weight. The results may be helpful for a designer for finding the best compromise between weight and continuity requirements. In future work, stacking sequence continuity requirement will be included in global wing and local panel design.

CHAPTER 6
SINGLE-LEVEL COMPOSITE WING OPTIMIZATION BASED ON FLEXURAL LAMINATION PARAMETERS

Introduction

In Chapter 4, we discussed a decomposition scheme whereby a response surface fitted to many combinatorial optimizations of wing-panel stacking sequences are as an interface between the local panel optimization and the overall wing design. The response surface provides an approximation of the maximum buckling load that can be achieved by rearranging the plies of a panel when the number of plies of each orientation is determined by the wing-level optimization. The objective of the present chapter is to compare this approach with a single-level optimization based on the use of lamination parameters.

Lamination parameters (Tsai et al. 1968) provide a compact representation of the stiffness properties of composite laminates. They allow efficient approximate optimization of laminates for desired stiffness properties. Miki (1986) developed a graphical procedure for the design optimization. Miki and Sugiyama (1991, 1993), and Fukunaga and Sekine (1992, 1994) graphically solved stacking sequence design problems for stiffness and strength maximization of symmetric laminates using lamination parameters. This simple graphical approach also allows us to see that for many problems the optimal design lies on the boundary of the lamination parameter space, corresponding to angle ply designs (Grenestedt & Gudmandson 1993).

In composite laminate design, Nagendra et al. (1996) demonstrated the use of lamination parameters as intervening variables in developing Taylor-series approximation,

while Todoroki and Haftka (1998) demonstrated a similar approach using response surface approximations.

While lamination parameters allow continuous optimization of laminates with small number of design variables, they do not allow constraints associated with the discrete nature of thicknesses and ply angles. Moreover, they do not accommodate ply contiguity constraints, which do not allow too many plies with the same fiber orientation angle to be stacked together. Yamazaki (1996) used a continuous solution based on lamination parameter and then used a genetic algorithm to find the closest discrete solution.

The objective of this chapter is to use a single-level continuous optimization procedure for wing design based on lamination parameters to compare to a two-level optimization procedure (Chapter 4) that employs genetic algorithms. While the two-level procedure satisfies contiguity and discreteness constraints, it may produce sub-optimal designs due to the use of approximations and the two-level decomposition. The single-level continuous solution developed here provides a lower bound on the wing weight, and thus can be used to judge how well the two-level procedure works. In the two-level procedure, the lower-level optimization employs a genetic algorithm to design composite panels with a given number of plies of each orientation for maximization of buckling loads. Therefore, we start by comparing the solution of this panel design problem using lamination parameters to designs obtained with genetic algorithms. Then we compare the decomposition approach (Chapter 4) to a single-level optimization for minimization of wing weight using lamination parameters as design variables.

Maximization of Buckling Loads of Composite Laminates With Given Number of Plies of Each Orientation

In this work, we first develop a continuous optimization procedure based on the flexural lamination parameters W_1^*, W_3^* for maximization of the buckling load of composite laminates with a given number of plies in the 0º, ±45º, and 90º directions. First, the flexural lamination parameters W_1^*, W_3^* and their domain of variation are introduced. Second, we will show that the lamination parameters are confined to a hexagonal domain for given number of plies in the 0º, ±45º, and 90º directions. Then the continuous variable optimization based on W_1^*, W_3^* is formulated. Finally, we will compare this approach with the genetic algorithm (GA) (discussed in Chapter 3) for maximization of buckling loads of a few laminates.

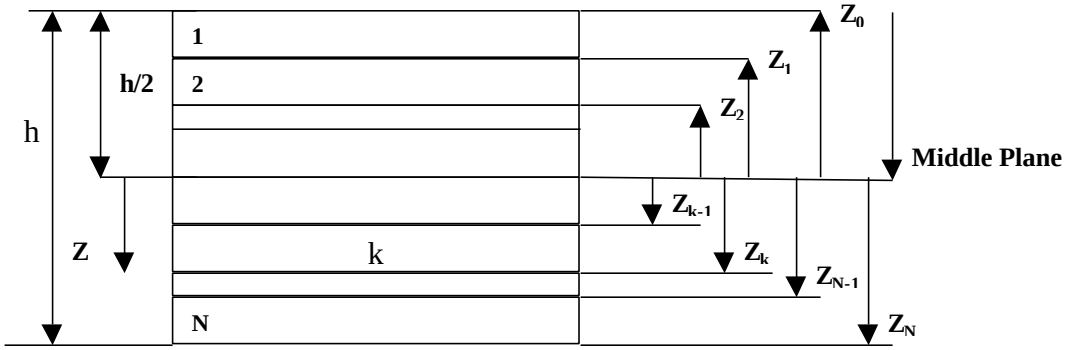

Figure 6-1: Ply geometry in a laminate

Bending Lamination Parameters

We consider a symmetric and balanced laminate with a stacking sequence of the form:

$[(\pm q_i)_{Ni}/¼/(\pm q_2)_{N2}/(\pm q_n)_{Nn}/(\pm q_1)_{N1}]_s$ as shown in Fig. 6-1.

The flexural lamination parameters W_1^* and W_3^* are defined as

$$W_1^* = \frac{24}{h^3}\int_0^{h/2} \cos 2q \; Z^2 dZ = \sum_1^{N/2}\left[\left(\frac{2Z_i}{h}\right)^3 - \left(\frac{2Z_{i-1}}{h}\right)^3\right]\cos(2q_i) \tag{6-1}$$

$$W_3^* = \frac{24}{h^3}\int_0^{h/2} \cos 4q \; Z^2 dZ = \sum_1^{N/2}\left[\left(\frac{2Z_i}{h}\right)^3 - \left(\frac{2Z_{i-1}}{h}\right)^3\right]\cos(4q_i) \tag{6-2}$$

where N is total number of layers of the laminate, h is the total thickness of the laminate, Z_i is measured from middle plane of the laminate (see Fig. 6-1), and q_i is the fiber orientation angle. Miki (1986), Miki and Sugiyama (1991) showed that W_1^* and W_3^* must satisfy

$$W_3^* \geq 2W_1^{*2} - 1 \tag{6-3}$$

Therefore, any balanced symmetric laminates with multiple orientation angles can be represented as a point in a region bounded by

$$W_3^* = 2W_1^{*2} - 1 \tag{6-4}$$

as shown in Figure 6-2, where the maximum and minimum values of W_1^*, W_3^* are 1 and –1, respectively.

For a balanced and symmetric laminate, the flexural stiffness matrix D_{ij}^* is given by

$$\begin{Bmatrix} D_{11}^* \\ D_{22}^* \\ D_{12}^* \\ D_{66}^* \end{Bmatrix} = \frac{h^3}{12}\begin{bmatrix} U_1 & W_1^* & W_3^* \\ U_1 & -W_1^* & W_3^* \\ U_4 & 0 & -W_3^* \\ U_5 & 0 & -W_3^* \end{bmatrix}\begin{Bmatrix} 1 \\ U_2 \\ U_3 \end{Bmatrix} \tag{6-5}$$

where U_1, U_2, U_3, U_4 and U_5 are material property invariants (see Appendix B).

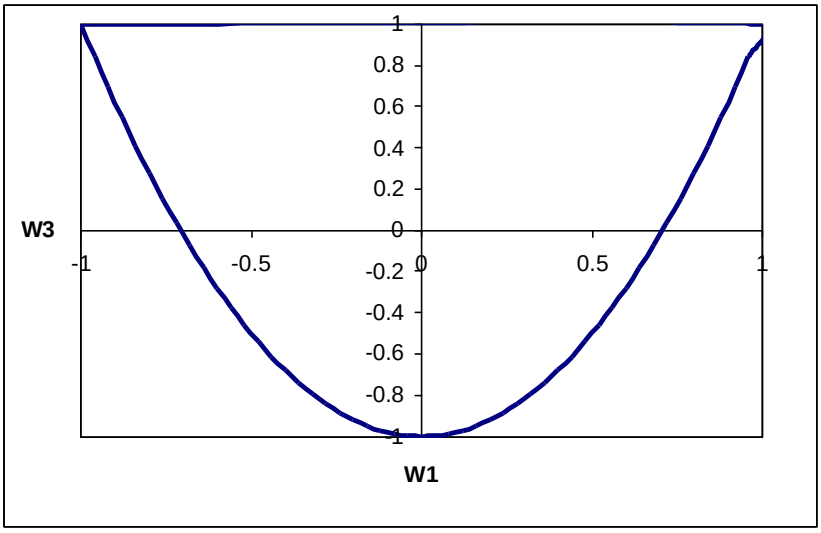

Figure 6-2: Bending lamination parameter domain

If only bending considerations affect the design, we can use W^*_1 and W^*_3 as design variables, and search for the best combination in the parabolic domain shown in Fig. 6-2. Here, we are concerned instead with the design of panels where the amount of plies of each orientation is specified by the overall wing design. In that case, the region where W^*_1 and W^*_3 can vary is restricted to a hexagon, as discussed next.

Domain of Flexural Lamination Parameters for Specified Amount of Plies

We denote the total thicknesses of 0°, ±45°, and 90° plies by $\boldsymbol{h_0}$, $\boldsymbol{h_{45}}$ and $\boldsymbol{h_{90}}$, respectively. The corresponding volume fractions of 0°, ±45° and 90° stacks in the laminate are

$$\boldsymbol{v_i} = \frac{\boldsymbol{h_i}}{\boldsymbol{h}}, \qquad \text{i=0, 45, 90} \tag{6-6}$$

Further, we consider the special cases of laminates whose 0° layers are stacked together, ±45° layers are stacked together and 90° layers are stacked together. There are six laminates, as shown in Fig. 6-4, with n_0, n_{45} and n_{90} being the number of stacks in the

three possible directions. The following integrals, related to equations (6-1, 6-2), are important to study the domain of variation of W_1^*, W_3^* for laminates only with a specified number of 0°, ±45°, and 90° plies.

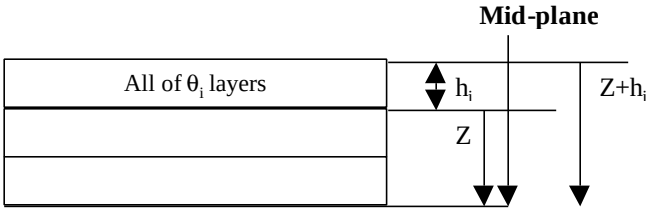

Figure 6-3: Laminates with all plies of the same orientation stacked together

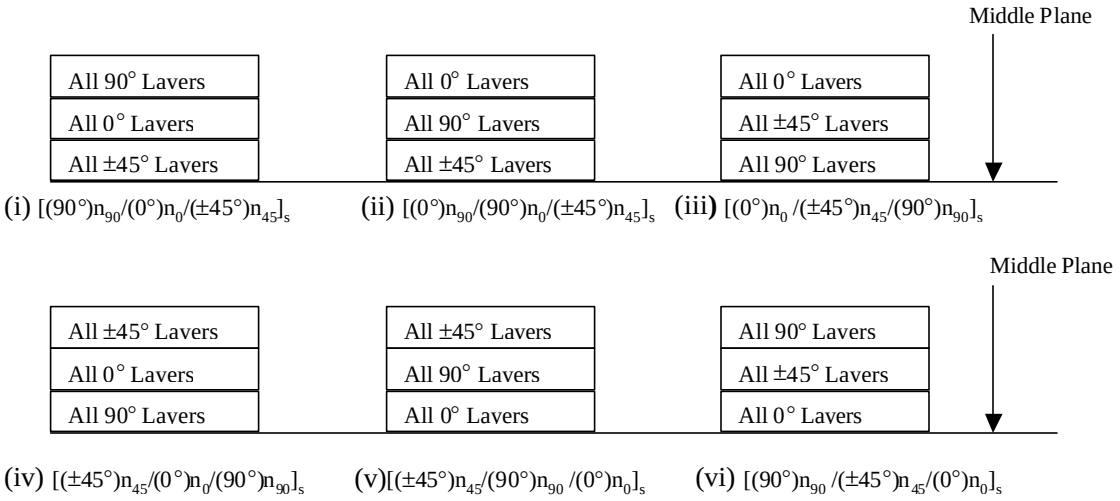

Figure 6-4: Six laminates corresponding to the six vertices of a hexagonal domain

The following integral is very important to study variation of W_1^* and W_3^*. For details, see Appendix C.

$$a_i = 2\int_{Z}^{Z+h_i/2} Z^{*2} dZ^* = \frac{2}{3}(3Z_i^2 h_i/2 + 3Z_i h_i^2/4 + h_i^3/8), \quad i = 0, 45, 90 \qquad (6\text{-}7)$$

where α_i is a bending index which is useful for defining maximum and minimum values of W_1^* and W_3^*; Z is the coordinate measured from the middle plane of laminates shown in Figure 6-3.

The laminates shown in Figure 6-4 are important because they represent the limits of variation of W_1^* and W_3^*. The $[(0°)n_0/(\pm45°)n_{45}/(90°)n_{90}]_s$ laminate will have the highest possible W^*_1. The $[(90°)n_{90}/(\pm45°)n_{45}/(0°)n_0]_s$ laminate will have the lowest possible W^*_1. The laminates $[(\pm45°)n_{45}/(0°)n_0/(90°)n_{90}]_s$ and $[(\pm45°)n_{45}/(90°)n_{90}/(0°)n_0]_s$ will have the lowest possible W^*_3, with the line between them giving the range of possible W^*_1 corresponding to this lowest value of W^*_3. Finally, the laminates $[(0°)n_0/(90°)n_{90}/(\pm45°)n_{45}]_s$ and $[(90°)n_{90}/(0°)n_0/(\pm45°)n_{45}]_s$ will have the highest possible W^*_3, with the line between them giving the range of variation of W^*_1 corresponding to this highest value of W^*_3. We need to find the boundaries of the domain, connecting the six points corresponding to these six extreme laminates in order to define the range of variation of the lamination parameters.

Appendix C shows that the domain of variation of W_1^* W_3^* is inside the hexagon connecting these six points (Figure 6-5). Equations (6-8) to (6-10) are the inequality constraints that define the hexagon.

$$4a^*_{0\min} - 1 \leq 2W_1^* + W_3^* \leq 4a^*_{0\max} - 1 \tag{6-8}$$

$$4a^*_{90\min} - 1 \leq -2W_1^* + W_3^* \leq 4a^*_{90\max} - 1 \tag{6-9}$$

$$W^*_{3\min} \leq W_3^* \leq W^*_{3\max} \tag{6-10}$$

where $a^*_{0\min}$, $a^*_{0\max}$, $a^*_{45\min}$, $a^*_{45\max}$, $a^*_{90\min}$, $a^*_{90\max}$ $W^*_{3\min}$, $W^*_{3\max}$ are given below.

$$a^*_{0\min} = \nu_0^3 \tag{6-11}$$

$$a^{*}_{0\max} = 12\frac{Z^{2}_{0\max}}{h^{2}}v_0 + 6\frac{Z_{0\max}}{h}v_0^{2} + v_0^{3} \tag{6-12}$$

$$Z_{0\max} = h_{45} + h_{90} \tag{6-13}$$

$$a^{*}_{90\min} = v_{90}^{3} \tag{6-14}$$

$$a^{*}_{90\max} = 12\frac{Z^{2}_{90\max}}{h^{2}}v_{90} + 6\frac{Z_{90\max}}{h}v_{90}^{2} + v_{90}^{3} \tag{6-15}$$

$$Z_{90\max} = h_{45} + h_0 \tag{6-16}$$

$$a^{*}_{45\min} = v_{45}^{3} \tag{6-17}$$

$$a^{*}_{45\max} = 12\frac{Z^{2}_{45\max}}{h^{2}}v_{45} + 6\frac{Z_{45\max}}{h}v_{45}^{2} + v_{45}^{3} \tag{6-18}$$

$$Z_{45\max} = h_0 + h_{90} \tag{6-19}$$

$$W^{*}_{3\min} = 1 - 2a^{*}_{45\max} \tag{6-20}$$

$$W^{*}_{3\max} = 1 - 2a^{*}_{45\min} \tag{6-21}$$

Maximization of Buckling Loads Using Continuous Optimization

The continuous optimization for maximization of buckling loads using W_1^{*}, W_3^{*} as design variables, cannot include contiguity constraints and is formulated as follows:

Maximize bucking load $l(W_1^{*}, W_3^{*})$, by changing W_1^{*} and W_3^{*} subject to

$$g_1 = W_3^{*} - W^{*}_{3\max} \le 0 \tag{6-22}$$

$$g_2 = W^{*}_{3\min} - W_3^{*} \le 0 \tag{6-23}$$

$$g_3 = 4a^{*}_{0\min} - 1 - 2W_1^{*} - W_3^{*} \le 0 \tag{6-24}$$

$$g_4 = 2W_1^{*} + W_3^{*} - 4a^{*}_{0\max} + 1 \le 0 \tag{6-25}$$

$$g_5 = 4a^{*}_{90\min} - 1 + 2W_1^{*} - W_3^{*} \le 0 \tag{6-26}$$

$$g_6 = -2W_1^{*} + W_3^{*} - 4a^{*}_{90\max} + 1 \le 0 \tag{6-27}$$

where equations. (6-22)-(6-27) limit the lamination parameters to the hexagonal domain defined by the amounts of 0°, ±45° and 90° stacks.

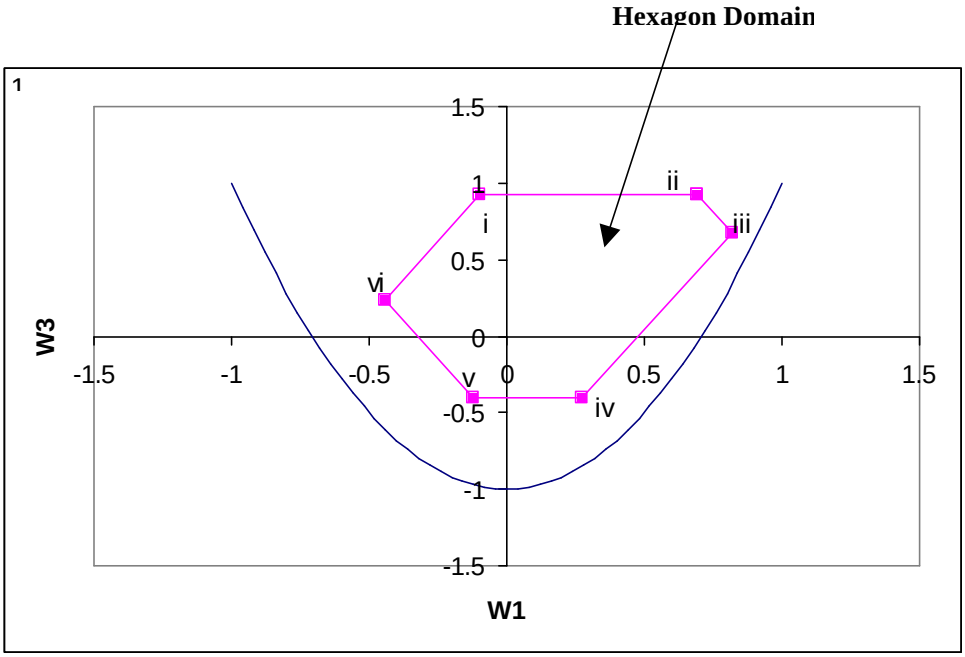

Figure 6-5: Hexagonal domain of variation of flexural lamination parameters when the number of plies of each orientation is specified

Comparison of Laminate Designs

In order to compare the continuous variable based optimization with the exact solution via GA for maximization of buckling loads, several laminates with given amounts of 0°, ±45°, and 90° stacks and loads are used.

The continuous optimization used here is sequential quadratic programming (SQP). The genetic algorithm used here is the permutation GA (Chapter 3).

The rectangular composite laminates are made of graphite-epoxy T300/5208 with material properties given in the Table 3-2. The length and width of the laminates are $a=24$ in; $b=2$ in shown in Figure 3-1, unless an aspect ratio different from one is specified.

The first set of test cases, listed in Table 6-1, consists of medium or thick laminates (40 to 80 plies) with given loads for a square plate. n_0, n_{45} and n_{90} are the number of stacks of 0°, ±45° and 90°. N_x, N_y and N_{xy} are the corresponding loads.

Table 6-2 compares optimal buckling loads for the five test cases of Table 6-1. The optimal buckling loads given by the two approaches are very close, but W_1^* , W_3^* show larger differences. These results indicate that, for such thick or medium square laminates, the continuous optimization using flexural lamination parameters can give excellent estimates of the buckling load that can be carried by the laminate when its stacking sequence is optimized exactly using combinatorial optimization.

Table 6-1: Definition of medium and thick laminates and applied loads

Case #	Loads (lb/in)			Number of Stacks		
	N_x	N_y	N_{xy}	n_0	n_{45}	n_{90}
1	-2000.0	-2000.0	1000.0	5	10	15
2	-3000.0	-2000.0	1000.0	5	5	10
3	-3000.0	-3000.0	2000.0	15	10	5
4	-4000.0	-2000.0	1000.0	10	5	10
5	-5000.0	-4000.0	1500.0	5	5	5

The difference between the continuous approximation and the exact combinatorial solution may be expected to increase as the laminate becomes thinner because the effects of discreteness and contiguity constraints are more pronounced. In addition, high or low aspect ratios may also be expected to increase the difference because they favor designs with extreme values of the lamination parameters, where all the plies of the same orientation are contiguous, which may violate contiguity constraints. Therefore, we

consider next a laminate with various aspect ratios. Table 6-3 presents results for laminates with n_0=5 n_{45}=5, n_{90}=5; loads are N_x=2000 lb/in, N_y=500 lb/in, N_{xy}=100lb/in and length of laminates is a=24 in.

Table 6-2: Comparison of optimal buckling loads by continuous optimization based on W_1^*, W_3^* and by GA for square laminates defined in Table 6-1

Case #	Continuous			GA		
	W_1^*	W_3^*	λ	W_1^*	W_3^*	λ
1	-0.2870	-0.4074	2.7845	-0.2393	-0.3563	2.7528
2	-0.3906	-0.1563	0.6145	-0.1956	-0.1563	0.6121
3	-0.0463	-0.4074	1.8117	0.2393	-0.3563	1.7755
4	-0.2223	0.0240	0.9724	-0.1651	0.0240	0.9719
5	-0.2222	-0.4074	0.1433	-0.1084	-0.4074	0.1421

From Table 6-3, we can observe that, as expected, the optimal buckling loads from the continuous variable based approach are better or at least the same as the GA with various aspect ratios for most cases. For cases 1 to 3, buckling loads from the continuous variable based approach are higher than those from the GA because of violation of contiguity constraints in the continuous variable based approach. For these cases, all of the 90°layers are pushed to the top of the laminates. Therefore, the W_1^* selected by the continuous variable based approach is more positive than that of the GA. For example, the optimal stacking sequence of Case 1 is $[90_4/\pm45/90_4/\pm45/90/\pm45_2/0_4/\pm45/0_4/\pm45/0_2]_s$, with the ±45° inserted layer between the 90° layers to avoid violation of the continuity constraints. The continuous optimum violates these contiguity constraints by putting all the 90° plies together. When aspect ratios are bigger that 1, optima will not favor any single-

degree layers. Violation of contiguity will not easily happen. For example, the optimal stacking sequence of case 5 is $[0_4/\pm45/90_4/0_2/(\pm45_2)_3/0_2/90_2/\pm45/90_2/0_2/90_2]_s$ and layers of 0°, ±45° and 90° are arranged in a mixed way.

Table 6-3: Comparison of maximized buckling loads for various aspect ratios for $n_0=5$, $n_{45}=5$, $n_{90}=5$; loads are N_x=2000 lb/in, N_y=500 lb/in, N_{xy}=100lb/in, a=24 in

	Aspect Ratio b/a	Continuous			GA		
		W_1^*	W_3^*	λ	W_1^*	W_3^*	λ
1	0.1	-0.6667	0.4815	78.5600	-0.5476	0.4210	73.9497
2	0.2	-0.2222	-0.4074	13.7724	-0.1511	-0.3719	13.4899
3	0.5	-0.1614	-0.4074	2.2508	-0.1511	-0.3719	2.2335
4	0.6	-0.2870	-0.2778	1.5840	-0.2631	-0.1479	1.5456
5	1	-0.1084	-0.4074	0.5620	-0.1084	-0.4074	0.5620
6	5	0.2187	0.3961	0.1366	0.2187	0.3961	0.1366
7	7	-0.0907	0.3108	0.0729	-0.0907	0.3108	0.0729
8	10	-0.3751	0.2753	0.0288	-0.3751	0.2753	0.0288

Since discreteness and contiguity constraints are more difficult to satisfy for thin laminates made only with 0° and 90° plies, Table 6-4 lists test cases for such thin, 4-stack laminates with given loads and various aspect ratios. For these 4-stack laminates, the optimal stacking sequence is unique and easily found. For cases 1 to 3, the optimal stacking

sequence is $[90_2/90_2/0_2/90_2]_S$; for cases 4 to 6, the optimal stacking sequence is $[0_2/0_2/90_2/0_2]_s$; and for cases 7 to 9, the optimal stacking sequence is $[\pm 45/0_2/\pm 45/0_2]_s$.

The results of Table 6-4, show large differences in maximal buckling loads (Case 3, Case 4, and Case 6). The results show that, for some ply and load combinations, satisfying the contiguity and discreteness constraints leads to substantial reduction in the maximal buckling load, so that the continuous solution is very different from the discrete one.

Overall, continuous variable optimization works well for the maximization of the buckling load of composite laminates even though it does not consider discreteness of design variables and contiguity constraints. The approach based on W_1^*, W_3^* predicts well the buckling load that can be reached by stacking sequence optimization using GA except for very thin laminates or laminates with very low aspect ratios.

Minimization of Weight of Composite Wing

In this section, we use the composite wing box structure shown in Figure 4-3 to compare a single-level optimization based on flexural lamination parameters with a two-level optimization using response surface (Chapter 4). First, we will develop a single-level optimization method based on lamination parameters for minimization of wing weight. Then, we will compare the results between the single-level optimization and the two-level optimization for three test cases.

Minimization of Weight of Composite Wing by Continuous Variable Algorithm Based on Design Variables of Flexural Lamination Parameters

In the single-level optimization based on flexural lamination parameters, buckling loads can be calculated directly from the total amounts of 0°, ±45°, 90° stacks and W_1^*, W_3^*. By introducing W_1^*, W_3^* as additional design variables, the optimization can also be carried out at a single level, but it cannot accommodate contiguity and discreteness constraints at the panel level.

Table 6-4: Comparison of maximized buckling loads of continuous variable approach based on W_1^*, W_3^* with GA for 4-stack laminates

	Aspect Ratios b/a	Amounts of Stacks	Loads	Continuous			GA		
		$n_0/n_{45}/n_{90}$	$N_x/N_y/N_{xy}$ (lb/in)	W_1^*	W_3^*	λ	W_1^*	W_3^*	λ
1	0.2	1/0/3	-20/-6.67/5	-0.969	1.0	21.026	-0.781	1.0	20.157
2	1.0	1/0/3	-20/-13.3/5	0.000	1.0	0.549	-0.781	1.0	0.551
3	2.0	1/0/3	-20/-20/5	0.156	1.0	0.322	-0.781	1.0	0.166
4	0.2	3/0/1	-20/-6.67/5	-0.156	1.0	17.254	0.781	1.0	9.157
5	1.0	3/01	-20/-13.3/5	0.000	1.0	0.549	0.781	1.0	0.529
6	2.0	3/0/1	-20/-20/5	0.425	1.0	0.337	0.781	1.0	0.268
7	0.2	2/2/0	-20/-6.67/5	0.125	-0.750	16.727	0.313	-0.375	14.256
8	1.0	2/2/0	-20/-13.3/5	0.125	-0.750	0.841	0.313	-0.375	0.774
9	2.0	2/2/0	-20/-20/5	0.274	-0.453	0.368	0.313	-0.375	0.368

The formulation of wing-level optimization is

$$\text{Minimize} \quad \sum_{i=1}^{18} (n_0^i + n_{45}^i + n_{90}^i) \tag{6-28}$$

where i is the panel number.

By changing $n_0^i, n_{45}^i, n_{90}^i, W_1^*, W_3^*$ i=1, …18

Subject to: Laminates are symmetric and balanced

(Strain) $l_{ce}^i \geq 1.0, \; i = 1, 18$ (6-29)

(Buckling without Contiguity) $l_c^i((n_0^i + n_{45}^i + n_{90}^i), W_1^{i*}, W_3^{i*}) \geq 1.0, \; i = 1, 18$ (6-30)

(Hexagonal constraints)

$$4a_{0\min}^* - 1 \leq 2W_1^* + W_3^* \leq 4a_{0\max}^* - 1 \tag{6-31}$$

$$4a_{90\min}^* - 1 \leq -2W_1^* + W_3^* \leq 4a_{90\max}^* - 1 \tag{6-32}$$

$$W_{3\min}^* \leq W_3^* \leq W_{3\max}^* \tag{6-33}$$

where l_{ce}^i is the strain failure load, l_c^i is the buckling load, and Equations (6-28) to (6-33) are the hexagonal domain constraints of W_1^*, W_3^*.

The rounding and manual adjustment is the same as for optimization based on response surfaces described in Chapter 4. The optimum obtained in the above procedure is a continuous optimum. The continuous optimum, that is, the continuous number of 0°, ±45°, and 90° stacks, needs to be rounded into an integer solution in order to find the optimal stacking sequence. After rounding, FE analysis is used to calculate strain failure loads and to extract internal loads in order to calculate the buckling load for the best stacking sequence obtained by permutation GA. In general, the buckling load or strain failure load constraint in some panels may be violated due to rounding and internal load redistribution caused by rounding. Therefore, manual adjustment of the number of 0°, ±45°, and 90° stacks in some panels is necessary. After manual adjustment, FE analysis and permutation GA are all employed to check whether there is any failure for either strain or buckling load

constraints. This manual adjustment will stop until the closest adjusted optimum is found which satisfies all buckling load and strain failure load constraints.

Comparison of Single-level and Two-level Approaches for Composite Wing Design

The results of the single-level wing optimization using lamination parameters are compared to the results of the two-level approach using response surfaces (Chapter 4). Three test examples, a six-variable case, an 18-variable case and a 54-variable case, are demonstrated for minimization of weight of the composite wing box structure. Buckling load constraints are only enforced for 9 upper-skin panels and are ignored for 9 lower-skin panels. The three cases are tested by the two-level optimization in Chapter 4. Here, the same three cases are used to compare the single-level optimization with the two-level optimization.

Six-variable Case

For simplicity, first we require that all of the upper-skin panels share a single laminate. So do all of the lower-skin panels. For the two-level RS approach, each panel has three design variables, the number of 0°, ±45° and 90° stacks. Therefore, the total number of design variables for the two-level optimization approach is six. For the continuous optimization using W_1^*, W_3^*, since buckling load constraints are only considered for upper-skin panels, the lamination parameters are used only for these upper-skin panels, and the total number of design variables is eight.

Table 6-5 compares active constraint types, continuous optima, rounded designs and active failure loads for the rounded designs obtained by the two approaches. Both approaches reach the same optimal weight and active constraints, but the optimal design is very different. After rounding, the two-level (RS) design failed because the buckling load

in panel 16 is less than 1.0. This reflects the approximation inherent in the response surface and the effect of rounding. The single-level optimum failed because the strain failure load is less than 1.0 in panel 7. The fact that the single-level approach could not find a lighter design than the two-level approach strengthens our confidence that the two-level approach provides optimal or near optimal designs.

Table 6-5: Comparison of wing design results between two-level RS approach, and single-level method with lamination parameters. Upper skin is one laminate and lower skin is one laminate

Two-level (GA with RS)	Active Constraints	$n_0/n_{45}/n_{90}$ (GENESIS)	$n_0/n_{45}/n_{90}$ (Rounded)	Failure Load Factor λ
Lower-Skin Panels	Strain (Panel #7)	8.69/1.76/ 0.04	9/2/0	1.0413
Upper-Skin Panels	Buckling (Panel #16)	15.33/12.44 /13.92	15/12/14	0.9664
Objective Function (Total Number of Stacks)		469.70	468	
Single-level (Continuous)	Active Constraints	$n_0/n_{45}/n_{90}$ (GENESIS)	$n_0/n_{45}/n_{90}$ (Rounded)	Failure Load Factor λ
Lower-Skin Panels	Strain (Panel #7)	9.18/0.94 /0.00	9/1/0	0.9856
Upper-Skin Panels	Buckling (Panel #16)	18.22/12.63 /10.81	18/13/11	1.0065
Objective Function (Total Number of Stacks)		466.13	468	

Table 6-6 compares the rounded and manually adjusted designs and the corresponding optimal stacking sequences for both approaches. Both approaches reach the same weight but different corresponding optimal stacking sequences. From Table 6-6, we can also see that the adjusted design for the two-level approach is closer to of the original design than the single-level approach based on W_1^*, W_3^*. The reason for this difference is the need to satisfy the contiguity constraints.

Table 6-6: Adjusted designs for two-level RS approach, and single-level method with lamination parameters. Upper skin is one laminate and lower skin is one laminate

Two-level (GA with RS)	GENESIS Design $n_0/n_{45}/n_{90}$	Rounded Design $n_0/n_{45}/n_{90}$	λ (Rounded Design)	Adjusted Design $n_0/n_{45}/n_{90}$	λ (Adjusted Design)
Panel # 7	8.69/1.76 /0.04	9/2/0	1.0413	9/2/0	1.0440
Panel #16	15.33/12.44 /13.92	15/12/14	0.9664	16/12/14	1.0326
Stacking Sequence (Panel #16)	Rounded Design	$[(\pm45)_{12}/90_4/0_4/(90_4/0_2)_2/90_2/0_2/(0_2/90_2)_3/(90_2/0_4)_3/90_2/0_2]_s$			
	Adjusted Design	$[(\pm45)_{12}/(90_4/0_2)_2/(90_2/0_4)_2/90_2/0_2/90_4/0_2/(0_2/90_2)_2/(0_4/90_2)_3]_s$			
Objective Function	469.70	468		477	
Single-level (Continuous)	GENESIS Design $n_0/n_{45}/n_{90}$	Rounded Design $n_0/n_{45}/n_{90}$	λ (Rounded Design)	Adjusted Design $n_0/n_{45}/n_{90}$	λ (Adjusted Design)
Panel # 7	9.18/0.94/ 0.00	9/1/0	0.9856	9/2/0	1.0469
Panel #16	18.22/12.63 /10.51	18/13/11	1.0065	18/13/11	1.0287
Stacking Sequence (Panel #16)	Rounded Design	$[(\pm45)_2/90_2/(\pm45)_6/90_2/(\pm45)_4/(90_2/0_2)_2/0_2/90_2/0_4/\pm45/0_4/(90_2/0_4)_5/90_2/0_2]_s$			
	Adjusted Design	$[(\pm45)_3/90_2/(\pm45)_5/90_2/(\pm45)_4/(90_2/0_2)_2/(0_2/90_2/0_2)_2/0_2/\pm45/(0_4/90_2)_5/0_2]_s$			
Objective Function	467.08	468		477	

18-variable Case

In order to make the design problem more realistic, we require that the three root panels (Panel No. 10, 15, 16) shown in Fig. 4-3 have one single laminate, the three middle panels (Panel No. 11,14, 17) shown in Fig.4-3 have one single laminate and the three tip panels have one single laminate for upper-skin panels (Panel No. 12, 13,18) as shown in Fig. 4-3. The same approach is used for the nine lower-skin panels. Each laminate has three design variables, which are the number of 0°, ±45°, 90° stacks, and the single-level

approach has additional flexural lamination parameters as design variables. For the two-level response surface approach, the total number of design variables is 18 for the six different laminates. For the single-level continuous optimization, there are also six flexural lamination variables for the three upper-skin laminates. Therefore, the total number of design variables for the single-level optimization is 24.

Table 6-7 compares the continuous optima, rounded optima and their failure loads for both approaches. From Table 6-7, we can see that both approaches reach very close continuous optima and that both rounded optima violate the strain failure load and buckling load constraints.

Table 6-8 shows the results of rounded optima and adjusted optima of lower-skin panels for the two approaches. From Table 6-8, we can see that the adjusted optimum (57 stacks) of the continuous approach is six stacks lighter than the optimum (63 stacks) of the two-level optimization approach

Table 6-9 shows rounded optima, adjusted optima and their stacking sequences of the two approaches for 9 upper-skin panels. The two approaches for 9 upper skin panels reach the same optimal weight but different optimal stacking sequences. The adjusted optimal weight (354 stacks) from the continuous approach based on W_1^*, W_3^* is slightly better than the optimum (360 stacks) of the response surface approach since the adjusted optimal weight of the continuous approach is six stacks less than that of a response surface approach.

Table 6-7: Comparison of the results of GENESIS and rounded optimal design between the two-level RS approach and the single-level method with lamination parameters. The upper skin has three laminates and the lower skin has three laminates

	Two-level (GA with RS)			Single-level (Continuous)		
Lower- Skin Panels	$n_0/n_{45}/n_{90}$ (GENESIS)	$n_0/n_{45}/n_{90}$ (Rounded)	Failure Load λ	$n_0/n_{45}/n_{90}$ (GENESIS)	$n_0/n_{45}/n_{90}$ (Rounded)	Failure Load λ
Panel #7	9.78/0/0	10/0/0	1.0064	9.79/0.00/ 0.00	10/0/0	1.0113
Panel #8	5.42/0.29/0	5/0/0	0.8601	5.41/0.23/ 0.00	5/0/0	0.8782
Panel #4	0.87/2.04/0	1/2/0	1.0767	0.85/2.14 /0.00	1/2/0	1.0760
Upper-Skin Panels	$n_0/n_{45}/n_{90}$ (GENESIS)	$n_0/n_{45}/n_{90}$ (Rounded)	Failure Load λ	$n_0/n_{45}/n_{90}$ (GENESIS)	$n_0/n_{45}/n_{90}$ (Rounded)	Failure Load λ
Panel #16	14.20/13.29 /14.13	14/13/14	0.9557	14.90/12.90 /13.66	15/13/14	1.0346
Panel #14	4.60/21.33/ 7.06	5/21/7	1.0161	4.43/20.92 /7.43	4/21/7	0.9475
Panel #18	3.70/16.80/ 2.84	4/17/3	1.0583	3.13/18.27 /2.40	3/18/2	0.9152
Objective Function (Total Number of Stacks)	349.22	348		349.39	345	

54-variable Case

Finally, we study a more realistic case where all of the upper-skin and lower-skin panels are independent. Each panel has three design variables. For the two-level approach, the total number of panels is 18. Therefore, the total number of design variables is 54. For the continuous approach, nine pairs of lamination parameters W_1^*, W_3^* are added for the nine upper-skin panels since buckling load constraints are only considered in the upper-

skin panels. Therefore, the total number of design variables for the continuous approach is 72.

Table 6-8: Comparison of results of rounded and adjusted lower-skin panels between two-level RS approach and single-level method with lamination parameters. The lower skin has three laminates

Two-level (GA with RS)	GENESIS Design $n_0/n_{45}/n_{90}$	Rounded Design $n_0/n_{45}/n_{90}$	λ (Rounded Design)	Adjusted Design $n_0/n_{45}/n_{90}$	λ (Adjusted Design)
Panel #7	9.78/0/0	10/0/0	1.0064	10/0/0	1.0183
Panel #8	5.42/0.29/0	5/0/0	0.8601	7/0/0	1.0919
Panel #4	0.87/2.04/0	1/2/0	1.0767	3/1/0	1.0884
Single-level (Continuous)	GENESIS Design $n_0/n_{45}/n_{90}$	Rounded Design $n_0/n_{45}/n_{90}$	λ (Rounded Design)	Adjusted Design $n_0/n_{45}/n_{90}$	λ (Adjusted Design)
Panel #7	9.79/0.00/0.00	10/0/0	1.0113	10/0/0	1.0164
Panel #8	5.41/0.23/0.00	5/0/0	0.8782	6/0/0	0.9932
Panel #4	0.85/2.14/0.00	1/2/0	1.0760	1/2/0	1.0837

Table 6-11 lists the continuous and rounded optima and their failure loads for both approaches. From Table 6-11, we can see that rounded optima of lower-skin panels for both approaches are very close but for upper-skin panels, the rounded optima are quite different.

Table 6-9: Comparison of results of rounded and adjusted upper panels between two-level RS and single-level method with lamination parameters. The upper skin has three laminates

Two-level (GA with RS)	Unrounded Design $n_0/n_{45}/n_{90}$	Rounded Design $n_0/n_{45}/n_{90}$	λ (Rounded Design)	Adjusted Design $n_0/n_{45}/n_{90}$	λ (Adjusted Design)
Panel # 16	14.02/13.29/ 14.13	14/13/14	0.9557	15/13/14	1.0361
Panel # 14	4.60/21.33/ 7.06	5/21/7	1.0161	5/21/7	1.0186
Panel # 18	3.70/16.80/ 2.84	4/17/3	1.0583	4/17/3	1.0241
Stacking Sequence of Rounded Design	Panel #16	$[(\pm45)_{13}/0_4/(90_2/0_2)_2/0_2//90_2/(90_2/0_2)_2/90_4/0_4/(90_4/0_2)_3/0_2/90_2/0_2]_s$			
	Panel #14	$[(\pm45)_{15}/90_2/(\pm45)_4/90_2/(90_2/\pm45)_2/(90_2/0_4)_2/90_2/0_2]_s$			
	Panel #18	$[(\pm45)_{17}/0_4/(90_2/0_2)_2/90_2]_s$			
Stacking Sequence of Adjusted Design	Panel #16	$[(\pm45)_{13}/(90_2/0_4)_4/90_2/(90_2/0_2)_2/90_4/0_4/(90_4/0_2)_2/90_2/0_2]_s$			
	Panel #14	$[(\pm45)_{15}/90_4/(\pm45)_5/90_2/\pm45/90_4/0_2/(0_2/90_2/0_2)_2]_s$			
	Panel # 18	$[(\pm45)_{17}/0_4/90_2/(0_2/90_2)_2]_s$			
Single-level (Continuous)	Unrounded Design $n_0/n_{45}/n_{90}$	Rounded Design $n_0/n_{45}/n_{90}$	λ (Rounded Design)	Adjusted Design $n_0/n_{45}/n_{90}$	λ (Adjusted Design)
Panel # 16	14.90/12.90/ 13.66	15/13/14	1.0246	15/13/14	1.0330
Panel # 14	4.43/20.92/ 7.43	4/21/7	0.9169	5/21/7	1.0267
Panel # 18	3.14/18.27 /2.40	3/18/2	0.9153	4/18/2	1.0334
Stacking Sequence of Rounded Design	Panel #16	$[(\pm45)_{13}/(90_2/0_4)_4/(90_2/0_2)_2/0_2/90_2/0_2/(90_4/0_2)_3/90_2]_s$			
	Panel #14	$[(\pm45)_{12}/(90_2/\pm45)_2/(\pm45)_6/90_2/\pm45/(90_4/0_2)_2/90_2/0_2]_s$			
	Panel #18	$[(\pm45)_{18}/90_2/0_4/90_2/0_2]_s$			
Stacking Sequence of Adjusted Design	Panel #16	$[(\pm45)_{13}/90_2/0_4/90_2/0_2/(90_2/0_4)_3/90_2/0_2/90_2/(90_2/0_2)_2/0_2/(90_4/0_2)_2/90_2]_s$			
	Panel #14	$[(\pm45)_{15}/90_2/(\pm45)_5/90_4/\pm45/90_2/(90_2/0_4)_2/90_2/0_2]_s$			
	Panel #18	$[(\pm45)_{18}/(0_4/90_2)_2]_s$			

Table 6-10: Summary of rounded and adjusted optima of the two approaches. The upper skin has three laminates and the lower skin has three laminates

Two-level (GA with RS)			Single-level (Continuous)		
GENESIS	Rounded	Adjusted	GENESIS	Rounded	Adjusted
349.22	348	360	349.39	345	354

Table 6-11: Comparison of the results of GENESIS and rounded optimal design between two-level RS approach and the single-level method with lamination parameters. The upper skin has nine panels and the lower skin has nine panels

	Two-level (GA with RS)			Single-level (Continuous)		
Lower-Skin Panels	$n_0/n_{45}/n_{90}$ (GENESIS)	$n_0/n_{45}/n_{90}$ (Rounded)	λ (Rounded) (Strain)	$n_0/n_{45}/n_{90}$ (GENESIS)	$n_0/n_{45}/n_{90}$ (Rounded)	λ (Rounded) (Strain)
1	6.09/0.66/0.17	6/1/0	1.0444	5.35/0/0	5/0/0	0.9473
2	3.37/0/0.12	3/0/0	0.9388	3.15/0/0	3/0/0	0.9498
3	0.77/0/0	1/0/0	1.2893	0.74/0/0	1/0/0	1.1851
4	0.61/1.72/0	1/2/0	1.2399	0.97/0/0	1/0/0	1.1490
5	4.73/2.28/0.54	5/2/1	1.0376	2.83/0/0.42	3/0/0	1.0455
6	6.9/0.68/0	7/1/0	1.0111	5.32/0/0	5/0/0	0.9753
7	11.16/0.69/1.10	11/1/1	1.0013	13.82/0/0	14/0/2	1.0008
8	6.09/0.75/0.70	6/1/1	1.0037	8.56/0/0	9/0/2	1.0389
9	1.18/1.59/0	1/2/0	1.0335	2.73/0.64/0	3/1/0	1.2618
Upper-Skin Panels	$n_0/n_{45}/n_{90}$ (GENESIS)	$n_0/n_{45}/n_{90}$ (Rounded)	λ (Rounded) (Buckling)	$n_0/n_{45}/n_{90}$ (GENESIS)	$n_0/n_{45}/n_{90}$ (Rounded)	λ (Rounded) (Buckling)
10	11.67/11.61/11.83	12/12/12	1.0824	8.40/10.70/11.97	8/11/12	1.0099
11	6.62/16.37/6.53	7/16/7	1.1200	3.86/14.21/6.49	4/15/6	0.9800
12	4.15/12.07/5.40	4/12/5	1.1535	1.34/11.44/4.88	1/11/5	0.9374
13	5.03/12.01/5.40	5/13/5	1.0307	3.50/12.15/5.74	4/12/6	1.0341
14	5.84/17.32/8.96	6/17/9	0.9747	7.21/17.63/8.36	7/18/8	0.9860
15	14.67/13.85/11.67	15/14/12	1.0833	17.49/13.91/9.93	17/14/10	0.9613
16	12.06/18/13.3	12/18/13	1.0524	12.04/18.57/12.97	12/19/13	1.0184
17	5.91/20.52/6.92	6/21/7	1.0211	6.95/22.15/6.45	7/22/6	0.9536
18	4.82/14.58/5.46	5/15/5	1.0310	6.30/15.62/4.12	6/16/4	1.0254
	335.44	340		319.46	319	

Table 6-12: Comparison of rounded and adjusted designs for lower-skin panels between the two-level RS approach and the single-level method with lamination parameters. The lower skin has nine panels.

Two-level (GA with RS)	GENESIS Design $n_0/n_{45}/n_{90}$	Rounded Design $n_0/n_{45}/n_{90}$	λ (Strain) (Rounded Design)	Adjusted Design $n_0/n_{45}/n_{90}$	λ (Strain) (Adjusted Design)
Panel # 1	6.09/0.66/0.17	6/1/0	1.0444	6/1/0	1.0332
Panel # 2	3.37/0/0.12	3/0/0	0.9388	4/0/0	1.0789
Panel # 3	0.77/0/0	1/0/0	1.2893	1/0/0	1.0949
Panel # 4	0.61/1.72/0	1/2/0	1.2399	1/2/0	1.1171
Panel # 5	4.73/2.28/0.54	5/2/1	1.0376	4/2/1	1.0600
Panel # 6	6.9/0.68/0	7/1/0	1.0111	7/1/0	1.0423
Panel # 7	11.16/0.69/1.1	11/1/1	1.0013	11/1/1	0.9928
Panel # 8	6.09/0.75/0.7	6/1/1	1.0037	7/1/1	1.0507
Panel # 9	1.18/1.59/0	1/2/0	1.0335	2/2/0	1.2442
Single-level (Continuous)	GENESIS Design $n_0/n_{45}/n_{90}$	Rounded Design $n_0/n_{45}/n_{90}$	λ (Strain) (Rounded Design)	Adjusted Design $n_0/n_{45}/n_{90}$	λ (Strain) (Adjusted Design)
Panel # 1	5.35/0/0	5/0/0	0.9473	6/0/0	1.0174
Panel # 2	3.15/0/0	3/0/0	0.9498	4/0/0	1.0839
Panel # 3	0.74/0/0	1/0/0	1.1851	1/0/0	1.1349
Panel # 4	0.97/0/0	1/0/0	1.1490	2/0/0	1.1786
Panel # 5	2.83/0/0.42	3/0/0	1.0455	3/0/0	1.0622
Panel # 6	5.32/0/0	5/0/0	0.9753	5/0/0	1.0220
Panel # 7	13.82/0/0	14/0/2	1.0008	14/0/0	1.0270
Panel # 8	8.56/0/0	9/0/2	1.0389	9/0/0	1.0877
Panel # 9	2.73/0.64/0	3/1/0	1.2618	2/2/0	1.1900

Table 6-13: Comparison of the results of rounded and adjusted designs for nine upper-skin panels between the two-level RS approach and the single-level method with lamination parameters. The upper skin has nine panels.

Two-level (GA with RS)	GENESIS Design $n_0/n_{45}/n_{90}$	Rounded Design $n_0/n_{45}/n_{90}$	λ (Buckling) (Rounded Design)	Adjusted Design $n_0/n_{45}/n_{90}$	λ (Buckling) (Adjusted Design)
Panel # 10	11.67/11.60/11.8	12/12/12	1.0824	11/12/12	1.02384
Panel # 11	6.62/16.37/6.53	7/16/7	1.1200	6/16/7	1.0895
Panel # 12	4.15/12.07/4.82	4/12/5	1.1535	3/12/5	1.0921
Panel # 13	5.03/12.61/5.40	5/13/5	1.0307	5/13/5	1.0782
Panel # 14	5.84/17.32/8.96	6/17/9	0.9747	7/17/9	1.0003
Panel # 15	14.67/13.85/11.7	15/14/12	1.0833	15/14/12	1.0236
Panel # 16	12.06/18.01/13	12/18/13	1.0524	11/18/13	0.9915
Panel # 17	5.91/20.52/6.92	6/21/7	1.0211	6/21/7	1.0134
Panel # 18	4.82/14.58/5.46	5/15/5	1.0310	5/15/5	1.0051
Single-level (Continuous)	GENESIS Design $n_0/n_{45}/n_{90}$	Rounded Design $n_0/n_{45}/n_{90}$	λ (Rounded Design)	Adjusted Design $n_0/n_{45}/n_{90}$	λ (Adjusted Design)
Panel # 10	8.40/10.70/11.97	8/11/12	1.0099	9/11/12	1.0000
Panel # 11	3.86/14.21/6.49	4/15/6	0.9800	7/15/5	1.0332
Panel # 12	1.34/11.44/14.88	1/11/5	0.9374	3/11/5	0.9988
Panel # 13	3.50/12.15/5.74	4/12/6	1.0341	3/12/6	1.0370
Panel # 14	7.21/17.63/8.36	7/18/8	0.9860	7/18/8	1.0691
Panel # 15	17.49/13.91/9.93	17/14/10	0.9613	18/14/10	1.0138
Panel # 16	12.04/18.57/12.97	12/19/13	1.0184	12/19/13	1.0458
Panel # 17	6.95/22.15/6.45	7/22/6	0.9536	8/22/6	1.0781
Panel # 18	6.30/15.62/4.12	6/16/4	1.0254	6/16/4	1.0428

Table 6-12 shows the rounded optima, adjusted optima and their strain failure loads for both approaches for nine lower-skin panels. From Table 6-12, we can observe that the final adjusted optima for both approaches are quite different.

Table 6-13 compares the rounded optima, adjusted optima and their buckling loads for upper-skin panels. We can see from Table 6-15 that the adjusted optima for the two approaches are quite different.

Table 6-14: Summary of rounded and adjusted optima of the two approaches.

Two-level (GA with RS)			Single-level (Continuous)		
GENESIS	Rounded	Adjusted	GENESIS	Rounded	Adjusted
335.44	340	337	319.46	323	328

From Table 6-14, we can observe that for this case the continuous optimization procedure did obtain a 3% lighter design than the two-level approach even after rounding and adjustment. This may be due to the existence of local optima or due to limitations of the final rounding and manual adjustment. Table 6-15 and Table 6-16 show the detail optimal stacking sequence for the rounded and adjusted designs.

From Table 6-15 and Table 6-16, we can see that the adjusted stacking sequences of the two approaches are quite different. Comparing the results of the 8-variable, 24-variable and 72-variable cases from the single-level optimization approach with those of the corresponding 6-variable, 18-variable and 54-variable cases using the two-level optimization approach, the single-level optimization approach obtained the same or better results than the response surface approach. Continuous optimization based on lamination parameters obtained lower bound values of the minimum weight.

Table 6-15: Comparison of stacking sequences of nine upper-skin panels for the rounded design for the two-level RS approach and the single-level method with lamination parameters. The upper skin has nine panels.

Two-level (GA with RS)	GENESIS $n_0/n_{45}/n_{90}$	Adjusted Optima $n_0/n_{45}/n_{90}$	Stacking Sequence	Buckling Load
Panel # 10	11.67/11.60/11.8	12/12/12	$[(\pm45)_{12}/90_2/0_4/90_2/0_2/90_2/(90_2/0_2)_2/(90_4/0_2)_4/90_2/0_2]_S$	1.0824
Panel # 11	6.62/16.37/6.53	7/16/7	$[(\pm45)_{15}/0_4/\pm45/0_4/(90_2/0_2)_3/90_2]_S$	1.1200
Panel # 12	4.15/12.07/4.82	4/12/5	$[(\pm45)_{12}/0_4/(90_4/0_2)_2/90_2]_S$	1.1535
Panel # 13	5.03/12.61/5.40	5/13/5	$[(\pm45)_{13}/0_4/(90_2/0_2)_2/90_4/0_2/90_2]_S$	1.0307
Panel # 14	5.84/17.32/8.96	6/17/9	$[(\pm45)_{17}/0_4/(90_4/0_2)_4/90_2]_S$	0.9747
Panel # 15	14.67/13.85/11.7	15/14/12	$[(\pm45)_{13}/90_2/\pm45/90_4/(0_2/90_2)_2/90_2/(0_4/90_2)_6/0_2]s$	1.0833
Panel # 16	12.06/18.01/13.0	12/18/13	$[(\pm45)_{17}/90_2/\pm45/(90_4/0_2)_3/0_2/90_2/0_2/90_4/0_2/(0_2/90_2/0_2)_3]_S$	1.0524
Panel # 17	5.91/20.52/6.92	6/21/7	$[(\pm45)_{20}/0_2/\pm45/0_4/(90_4/0_2)_3/90_2]_S$	1.0211
Panel # 18	4.82/14.58/5.46	5/15/5	$[(\pm45)_{15}/0_2/(0_2/90_2)_3/90_2/0_2/90_2]_S$	
Single-level (Continuous)	GENESIS $n_0/n_{45}/n_{90}$	Adjusted Optima $n_0/n_{45}/n_{90}$	Stacking Sequence	Buckling Load
Panel # 10	8.40/10.70/11.97	8/11/12	$[(\pm45)_{11}/90_4/0_2/(90_2/0_2)_2/90_2/(0_2/90_2/0_2)_2/(90_4/0_2)/90_2]_s$	1.0099
Panel # 11	3.86/14.21/6.49	4/15/6	$[(\pm45)_{15}/0_2/90_2/0_2/(90_4/0_2)_2/90_2]_s$	0.9800
Panel # 12	1.34/11.44/14.88	1/11/5	$[(\pm45)_{10}/90_4/\pm45/90_4/0_2/90_2]_s$	0.9374
Panel # 13	3.50/12.15/5.74	4/12/6	$[(\pm45)_{12}/0_2/90_2/0_2/(90_4/0_2)_2/90_2]_s$	1.0341
Panel # 14	7.21/17.63/8.36	7/18/8	$[(\pm45)_{17}/0_2/\pm45/0_4/90_2/0_2/(90_4/0_2)_3/90_2]_s$	0.9860
Panel # 15	17.49/13.91/9.93	17/14/10	$[(\pm45)_2/90_4/(\pm45)_8/90_2/(\pm45)_3/0_4/\pm45/(0_4/90_2)_7/0_2]_s$	0.9613
Panel # 16	12.04/18.57/12.97	12/19/13	$[(\pm45)_{17}/(90_2/\pm45)_2/(90_4/\pm45)_3/(90_2/0_4)_4/90_2/0_2)_5]_s$	1.0184
Panel # 17	6.95/22.15/6.45	7/22/6	$[(\pm45)_{21}/0_4/\pm45/0_4/90_2/0_2/(90_4/0_2)_2/90_2]_s$	0.9536
Panel # 18	6.30/15.62/4.12	6/16/4	$[(\pm45)_{15}/0_2/\pm45/(0_4/90_2)_2/90_2/0_2/90_2]_s$	1.0254

Table 6-16: Comparison of stacking sequences of the nine upper-skin panels for the adjusted design between the two-level RS approach and the single-level method with lamination parameters. The upper skin has nine panels

Two-level (GA with RS)	GENESIS $N_0/n_{45}/n_{90}$	Adjusted Optima	Stacking Sequence	Buckling Load
Panel # 10	11.67/11.60/ 11.8	11/12/12	$[(\pm45)_{12}/90_4/0_2/(90_2/0_2)_5/(0_2/90_4)_2$ $/0_4/90_2/0_2]_s$	1.02384
Panel # 11	6.62/16.37 /6.53	6/16/7	$[(\pm45)_{15}/0_2/\pm45/0_4/(90_4/0_2)_3/90_2]_s$	1.0895
Panel # 12	4.15/12.07 /4.82	3/12/5	$[(\pm45)_{12}/(0_2/90_4)_2/0_2/90_2]_s$	1.0921
Panel # 13	5.03/12.61 /5.40	5/13/5	$[(\pm45)_{12}/0_2/\pm45/0_4/(90_4/0_2)_2/90_2]_s$	1.0782
Panel # 14	5.84/17.32 /8.96	7/17/9	$[(\pm45)_{16}/0_2/\pm45/0_2/(0_2/90_4)_4/0_2/90_2]_s$	1.0003
Panel # 15	14.67/13.85/ 11.7	15/14/12	$[(\pm45)_{11}/90_2/(\pm45)_2/90_2/\pm45/90_2/$ $(90_2/0_2)_3/(0_2/90_2/0_2)_6]_s$	1.0236
Panel # 16	12.06/18.01/ 13.0	11/18/13	$[(\pm45)_{16}/(90_2/\pm45)/(90_4/0_2)_3/$ $(90_2/0_2)_2/(0_2/90_2/0_2)_3]_s$	0.9915
Panel # 17	5.91/20.52/ 6.92	6/21/7	$[(\pm45)_{20}/0_2/\pm45/0_4/(90_4/0_2)_3/90_2]_s$	1.0134
Panel # 18	4.82/4.58/ 5.46	5/15/5	$[(\pm45)_{15}/0_4/(90_2/0_2)_2/90_4/0_2/90_2]_s$	1.0051
Single-level (Continuous)	GENESIS $N_0/n_{45}/n_{90}$	Adjusted Optima $n_0/n_{45}/n_{90}$	Stacking Sequence	Buckling Load
Panel # 10	8.40/10.70/ 11.97	9/11/12	$[(\pm45)_{11}/90_4/0_2/(90_2/0_2)_3/(90_4/0_2)_3$ $/0_2/90_2/0_2]_s$	1.0000
Panel # 11	3.86/14.21/ 6.49	7/15/5	$[(\pm45)_{14}/0_4/\pm45/0_2/(0_2/90_2)_3/90_2/$ $0_2/90_2]_s$	1.0332
Panel # 12	1.34/11.44/ 14.88	3/11/5	$[(\pm45)_{11}/(0_2/90_4)_2/0_2/90_2]_s$	0.9988
Panel # 13	3.50/12.15/ 5.74	3/12/6	$[(\pm45)_{12}/90_2/0_2/(90_4/0_2)_2/90_2]_s$	1.0370
Panel # 14	7.21/17.63/ 8.36	7/18/8	$[(\pm45)_{17}/0_2/\pm45/0_4/90_2/(0_2/90_4)_3/$ $0_2/90_2]_s$	1.0691
Panel # 15	17.49/13.91/ 9.93	18/14/10	$[(\pm45)_4/(90_2/\pm45)_2/\pm45/90_2/(\pm45)_4/(90_2/$ $0_2)_2/(0_2/\pm45/0_2)_2/0_2/90_2/0_4/\pm45/0_2/(0_2/90$ $_2/0_2)_4]_s$	1.0138
Panel # 16	12.04/18.57/ 12.97	12/19/13	$[(\pm45)_{15}/90_2/\pm45/(\pm45/90_2)_2/90_2/$ $\pm45/(90_4/0_2)_2/(0_2/90_2/0_2)_5]_s$	1.0458
Panel # 17	6.95/22.15/ 6.45	8/22/6	$[(\pm45)_{21}/0_4/\pm45/(0_4/90_2)_2/(90_2/0_2/$ $90_2)_2]_s$	1.0781
Panel # 18	6.30/15.62/ 4.12	6/16/4	$[(\pm45)_{15}/0_2/\pm45/0_4/90_2/0_4/90_4/0_2/$ $90_2]_s$	1.0428

In terms of computational cost, the approach based on W_1^*, W_3^* can calculate buckling load instead of using response surface. From different optimal stacking sequences of three cases for the two approaches, we can conclude that the final adjusted optima around continuous optima are multiple. Even though contiguity constraints cannot be included into wing optimization, those constraints can be enforced in the final rounding and adjustment design procedures; for the examples, this worked well.

Concluding Remarks

In this chapter, we investigate the continuous variable optimization approach based on W_1^*, W_3^* for maximization of buckling loads for composite laminates and single-level optimization based on W_1^*, W_3^* for minimization of weight of a composite wing. Comparing the results of the current approach to the results of available approaches using GA and two-level optimization, the continuous variable optimization approach based on W_1^*, W_3^* is feasible and efficient.

However, the single-level optimization based on flexural lamination parameters is only useful for this simple structure. In practice, complex composite structures usually consist of stiffened panels and buckling load analysis normally requires a refined finite element analysis. So a single-level approach may not be feasible. Therefore, the two-level optimization approach will still be used and response surfaces of buckling loads may be constructed by using flexural lamination parameters.

CHAPTER 7
CONCLUDING REMARKS

In this study, we investigated optimization methodology for designing composite laminates and a composite wing with many composite panels simultaneously. A two-level optimization procedure using response surfaces fitted to genetic panel optimizations was developed. The procedure allows the use of continuous optimization for the overall design, avoiding the high computational cost associated with combinatorial optimization of all panels simultaneously.

The research made the following four contributions:

1. Developed an efficient permutation genetic algorithm named Gene-Rank for stacking sequence optimization of composite laminates. In this permutation GA, equality constraints of fixed integer number of 0°, ±45° and 90° plies, which are imposed by wing-level optimization, are incorporated into permutation gene coding. The Gene-Rank permutation GA was shown to be more effective than a standard GA, and marginally better than an existing permutation GA. In addition, repair strategies were shown to significantly reduce computational cost for both standard and permutation GAs.
2. Developed a two-level optimization algorithm that allows use of continuous optimization at the upper level by using a response surface of maximal panel failure loads. The response surfaces are fitted to the results of many panel optimizations for use by the wing-level optimization for minimization of wing weight. Results of test cases showed that the response surfaces could be used effectively to allow the wing-level optimization to find near optimal wing designs. Some constraint violation due to rounding could be fixed by manually adjusting rounded optima with very small increase in total weight.
3. Developed measures of material composition and stacking sequence continuity for adjacent panels and studied tradeoff between weight and continuity requirements. The results showed that substantial improvements in continuity could be first obtained with little weight penalty. However, beyond a certain point, additional increases in continuity measures required large increases in weight.
4. Developed a single-level continuous optimization by using flexural lamination parameters as design variables for panel and wing optimization. The single-level continuous optimization approach was used to verify the near optimality of

the two-level optimization results. Based on the work, it is recommended that future research will explore minimization of overall wing weight with ply stacking sequence continuity constraints for adjacent panels. We will construct continuity constraints of ply stacking sequence between two adjacent laminates by comparing flexural lamination parameters of adjacent panels. These constraints can then be included in the overall single-level wing optimization.

APPENDIX A
TUNING GENETIC PARAMETERS

The efficiency of genetic algorithm is often sensitive to parameters, such as population size, probabilities of crossover, mutation, etc. We used numerical experiments to tune these parameters. The evaluation measure is number of analyses required for obtaining optimum averaged over case 4 and case 5 in Chapter Three. Typically, the coefficients of variation (standard deviation over mean value) were below 5%. Here we only tune three genetic parameters: population size, probability of crossover and probability of mutation.

From three figures, we can observe that the optimal population size should be below 10 for GR GA and PMX GA, and that the optimal probabilities of crossover and mutation are around 1.0.

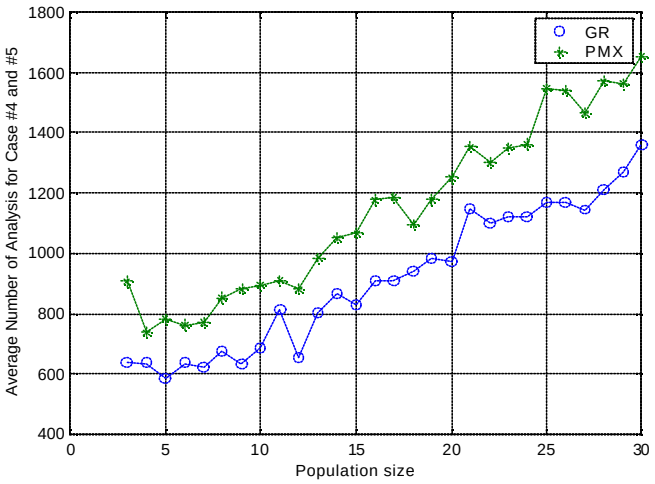

Figure A-1: Tune GA operator parameters: (A) shows the effect of population size.

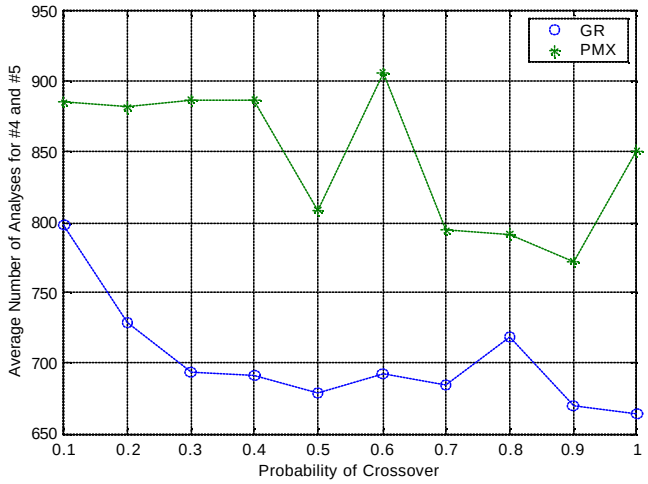

Figure A-1: Tune GA operator parameters: (B) displays effect of probability of crossover.

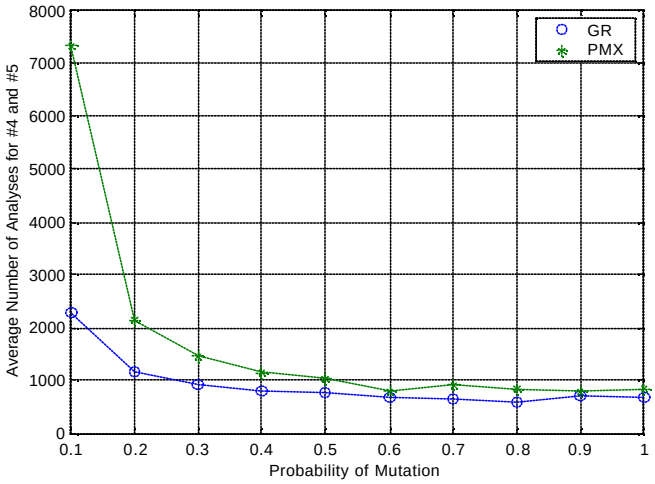

Figure A-1: Tune GA operator parameters: (C) shows effect of probability of mutation.

APPENDIX B

Constitutive relations for Orthotropic Lamina (HaFTKA and Gürdal 1993)

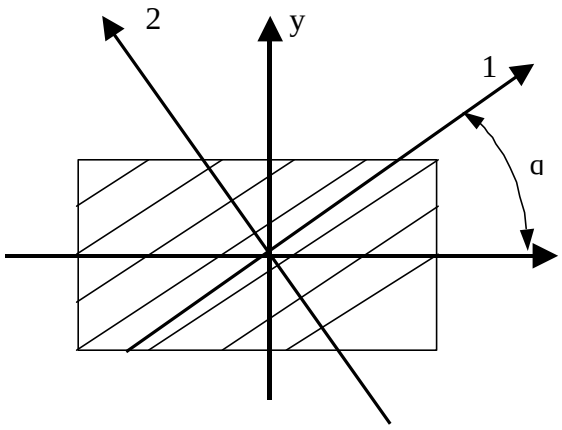

Figure B-1: An Orthotropic lamina with off-axis principal material directions

For a laminate made of an orthotropic material under plane stress conditions, the stress-strain relation is

$$\begin{Bmatrix} \sigma_1 \\ \sigma_2 \\ \tau_{12} \end{Bmatrix} = \begin{bmatrix} Q_{11} & Q_{12} & 0 \\ Q_{12} & Q_{22} & 0 \\ 0 & 0 & Q_{66} \end{bmatrix} \begin{Bmatrix} \varepsilon_1 \\ \varepsilon_2 \\ \gamma_{12} \end{Bmatrix} \tag{B-1}$$

where Q_{ij}'s are called the reduced stiffenesses and are given in terms of four independent engineering material constants in principle material directions as

$$\begin{aligned} Q_{11} &= \frac{E_1}{1 - \nu_{12}\nu_{21}} \\ Q_{22} &= \frac{E_2}{1 - \nu_{12}\nu_{21}} \\ Q_{21} &= \frac{\nu_{12}E_2}{1 - \nu_{12}\nu_{21}} = \frac{\nu_{21}E_1}{1 - \nu_{12}\nu_{21}} \\ Q_{66} &= G_{12} \end{aligned} \tag{B-2}$$

Since the orthotropic layers are generally rotated with respect to reference coordinate axes, the stress-strain relations given in the principle directions of material orthotropy Equation B-2 must be transformed to these axes. This transformation produces

$$\begin{Bmatrix} \sigma_x \\ \sigma_y \\ \tau_{xy} \end{Bmatrix} = \begin{bmatrix} \overline{Q}_{11} & \overline{Q}_{12} & \overline{Q}_{16} \\ \overline{Q}_{12} & \overline{Q}_{22} & \overline{Q}_{26} \\ \overline{Q}_{16} & \overline{Q}_{26} & \overline{Q}_{66} \end{bmatrix} \begin{Bmatrix} \varepsilon_x \\ \varepsilon_y \\ \gamma_{xy} \end{Bmatrix} \tag{B-3}$$

where the transformed reduced stiffnesses $\overline{Q}_{11}$ are related to the Q_{ij} by

$$\begin{aligned}
\overline{Q}_{11} &= Q_{11}\cos^4\theta + 2(Q_{12} + 2Q_{66})\sin^2\theta\cos^2\theta + Q_{22}\sin^4\theta \\
\overline{Q}_{12} &= (Q_{11} + Q_{22} - 4Q_{66})\sin^2\theta\cos^2\theta + Q_{12}(\sin^4\theta + \cos^4\Phi) \\
\overline{Q}_{22} &= Q_{11}\sin^4\theta + 2(Q_{12} + 2Q_{66})\sin^2\theta\cos^2\theta + Q_{22}\cos^4\theta \\
\overline{Q}_{16} &= (Q_{11} - Q_{12} - 2Q_{66})\sin\theta\cos^3\theta + (Q_{12} - Q_{22} + 2Q_{66})\sin^3\theta\cos\theta \\
\overline{Q}_{26} &= (Q_{11} - Q_{12} - 2Q_{66})\sin^3\theta\cos\theta + (Q_{12} - Q_{22} + 2Q_{66})\sin\theta\cos^3\theta \\
\overline{Q}_{26} &= (Q_{11} + Q_{22} - 2Q_{12} - 2Q_{66})\sin^2\theta\cos^2\theta + Q_{66}(\sin^4\theta + \cos^4\theta)
\end{aligned} \tag{B-4}$$

Equation (B-4) can be put into a simpler form as follows:

$$\begin{aligned}
\overline{Q}_{11} &= U_1 + U_2\cos 2\theta + U_3\cos 4\theta \\
\overline{Q}_{12} &= U_4 - U_3\cos 4\Phi \\
\overline{Q}_{22} &= U_1 - U_2\cos 2\theta + U_3\cos 4\theta \\
\overline{Q}_{16} &= -\frac{1}{2}U_2\sin 2\theta - U_3\sin 4\theta \\
\overline{Q}_{26} &= -\frac{1}{2}U_2\sin 2\theta + U_3\sin 4\theta \\
\overline{Q}_{26} &= U_5 - U_3\cos 4\theta
\end{aligned} \tag{B-5}$$

where the U_i's are Tsai and Pagano (1968) material invariants expressed as follow:

$$U_1 = \frac{1}{8}(3Q_{11} + 3Q_{22} + 2Q_{12} + 4Q_{66})$$

$$U_2 = \frac{1}{2}(Q_{11} - Q_{22})$$

$$U_3 = \frac{1}{8}(Q_{11} + Q_{22} - 2Q_{12} - 4Q_{66}) \qquad \text{(B-6)}$$

$$U_4 = \frac{1}{8}(Q_{11} + Q_{22} + 6Q_{12} - 4Q_{66})$$

$$U_5 = \frac{1}{8}(Q_{11} + Q_{22} - 2Q_{12} + 4Q_{66})$$

APPENDIX C

Domain of Variation of Flexural Lamination Parameters for Given Amounts of Plies

This appendix shows that for symmetric and balanced composite laminates with given amounts of 0°, ±45° or 90° stacks, the domain of variation of the lamination parameters W_1^*, W_3^* is a hexagon.

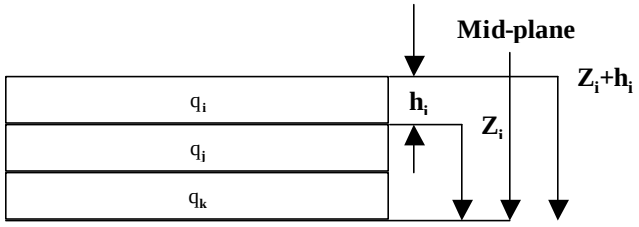

Figure C-1: Ply geometry of laminate $[(\theta_i)n_i/(\theta_j)n_j/(\theta_k)n_k]_s$

In the above laminate, ***(i, j, k)*** is permutation of ***(0, 45, 90)***; n_i, n_j, n_k are number of 0°, 45° and 90° stacks; h_i is thickness of θ_i stacks; Z_i is coordinate measured from middle plane as shown in Fig. C-1. Total number of this type of laminates is six. For these laminates like $[(0°)n_0/(\pm45°)n_{45}/(90°)n_{90}]_s$, equations (6-1) (6-2) can be expressed in following simple forms:

$$W_1^* = \frac{24}{h^3}\int_0^{h/2}\cos 2q\; Z^2 dZ = \sum_1^3 \left(\frac{2Z_i}{h}\right)^3 - \left(\frac{2Z_{i-1}}{h}\right)^3 \cos(2q_i) =$$
$$\sum_1^3 \frac{8}{h^3}\left(3Z_i^2 h_i/2 + 3Z_i h_i^2/4 + h_i^3/8\right)\cos(2q_i) = \sum_1^3 \frac{12}{h^3} a_i \cos(2q_i) \qquad \text{(C-1)}$$

$$W_3^* = \frac{24}{h^3}\int_0^{h/2}\cos 4q\; Z^{*2} dZ = \sum_1^3 \left(\frac{2Z_i}{h}\right)^3 - \left(\frac{2Z_{i-1}}{h}\right)^3 \cos(4q_i) =$$
$$\sum_1^3 \frac{8}{h^3}\left(3Z_i^2 h_i/2 + 3Z_i h_i^2/4 + h_i^3/8\right)\cos(4q_i) = \sum_1^3 \frac{12}{h^3} a_i \cos(4q_i) \qquad \text{(C-2)}$$

where $\boldsymbol{h}$ is total thickness of the laminate and a_i is given as follows:

We consider following integral, which relates to equations (C-1), (C-2).

$$a_i = 2\int_{Z_i}^{Z_i+h_i/2} Z^{*2} dZ^* = \frac{2}{3}(3Z_i^2 h_i/2 + 3Z_i h_i^2/4 + h_i^3/8), \quad i = 0, 45, 90 \qquad \text{(C-3)}$$

by dividing (C-3) by $h^3/12$,

$$a_i^* = 12\frac{Z^2}{h^2}v_i + 6\frac{Z}{h}v_i^2 + v_i^3 \qquad \text{(C-4)}$$

where v_i is the volume fraction of 0°, ±45°, 90° stacks in the laminate.

$$v_i = \frac{h_i}{h}, \qquad \text{i=0, 45, 90} \qquad \text{(C-5)}$$

After simplifying equations (C-1, C-2), we have

$$W_1^* = \cos(2*0^\circ)a_0^* + \cos(2*45^\circ)a_{45}^* + \cos(2*90^\circ)a_{90}^* = a_0^* - a_{90}^* \qquad \text{(C-6)}$$

$$W_3^* = \cos(4*0^\circ)a_0^* + \cos(4*45^\circ)a_{45}^* + \cos(4*90^\circ)a_{90}^* = a_0^* - a_{45}^* + a_{90}^* \qquad \text{(C-7)}$$

Add a_0^*, a_{45}^* and a_{90}^*, we can get

$$a_0^* + a_{45}^* + a_{90}^* = 1 \qquad \text{(C-8)}$$

from (C-6) ,(C-7), we get

$$W_1^* = 1 - 2a_{45}^* \qquad \text{(C-9)}$$

from (C-6), (C-7), we get

$$(W_3^* + 1)/2 = a_0^* + a_{90}^* \qquad \text{(C-10)}$$

So with (C-8), we can find following relationship of W_1^*, W_3^*

$$2W_1^* + W_3^* = 4a_0^* - 1 \qquad \text{(C-11)}$$

$$-2W_1^* + W_3^* = 4a_{90}^* - 1 \qquad \text{(C-12)}$$

a_0^* can has its minimum value when all 0° stacks are stacked innermost, like laminate $[(\theta_i)n_i/(\theta_j)n_j/(0°)n_0]_s$

$$a_{0\min}^* = \nu_0^3. \tag{C-13}$$

In the laminate, (i, j) is permutation of (90, 45). a_0^* can also have its maximum value as follows when 0 stacks are stacked outermost, like laminate $[(0°)n_o/(\theta_j)n_j/(0_i)n_i]_s$

$$a_{0\max}^* = 12\frac{Z_i^2}{h^2}\nu_0 + 6\frac{Z_i}{h}\nu_0^2 + \nu_0^3 \tag{C-14}$$

where Z_i is $Z_i=(h_{45}+h_{90})$. Same as the above, (i, j) is permutation of (90, 45).

Similarly, a_{90}^* can has its minimum and maximum values as follow

$$a_{90\min}^* = \nu_{90}^3 \tag{C-15}$$

$$a_{90\max}^* = 12\frac{Z_i^2}{h^2}\nu_{90} + 6\frac{Z_i}{h}\nu_{90}^2 + \nu_0^3 \tag{C-16}$$

where Z_i is $Z_i=(h_{45}+h_0)$.

Laminates associated with maximum and minimum values of a_{90}^* are $[(\theta_i)n_i/(\theta_j)n_j/(90°)n_0]_s$ and $[(90°)n_{90}\,(\theta_i)n_i/(\theta_j)n_j]_s$.

Therefore, from (B-8), (B-9), we can have four equations as follow

$$4a_{0\min}^* - 1 \le 2W_1^* + W_3^* \le 4a_{0\max}^* - 1 \tag{C-17}$$

$$4a_{90\min}^* - 1 \le -2W_1^* + W_3^* \le 4a_{90\max}^* - 1 \tag{C-18}$$

From (C-4), we have

$$a_{45}^* = 12\frac{Z^2}{h^2}\nu_{45} + 6\frac{Z}{h}\nu_{45}^2 + \nu_{45}^3 \tag{C-19}$$

When all of ±45° layers are stacked together in the top of laminates, Z reaches maximum measure from midplane of laminates. So does a_{45}^{*}.

From (C-19),

$$a_{45\max}^{*} = 12\frac{Z_{\max}^{2}}{h^{2}}v_{45} + 6\frac{Z_{\max}}{h}v_{45}^{2} + v_{45}^{3} \tag{C-20}$$

where Z_{max} is $Z_{max}=(h_0+h_{90})$.

When a_{45}^{*} reaches its maximum, W_3^{*} has minimum.

$$W_{3\min}^{*} = 1 - 2a_{45\max}^{*} = 1 - 2(12\frac{Z_{\max}^{2}}{h^{2}}v_2 + 6\frac{Z_{\max}}{h}v_2^{2} + v_2^{3}) \tag{C-21}$$

When all of ±45° layers are stacked in the inner position of laminates, a_{45}^{*} reaches a minimum value at Z=0.

$$a_{45\min}^{*} = v_{45}^{3} \tag{C-22}$$

$$W_{3\max}^{*} = 1 - 2a_{45\min}^{*} \tag{C-23}$$

Equations (C-17), (C-18) plus Equations (C-21) (C-23) bound hexagon domain of W_1^{*} and W_3^{*} as shown in Fig. 6-5. for the laminates with only 0°, ±45° and 90° specified layers.

LIST OF REFERENCES

Alexandrov, N.M., and Kodiyalam, S., " Initial results of an MDO method evaluation study", 7th AIAA/USAF/NASA/OAI Symposium on Multidisciplinary Analysis and Optimization, September, 1998, pp.701-721.

Alexandrov, N. M., and Lewis, R. M., " Analytical and computational aspects of collaborative optimization ", *NASA/TM-2000*,-210104, April, 2000.

Balabanov, V., Giunta, A.A., Golovidov, O., Grossman, B., Mason, W.H., Watson, L.T., and Haftka, R.T., " Reasonable design space approach to response surface approximation", *Journal of Aircraft, Vol.36, No.1*, January-February, 1999, pp308-315.

Barthelemy , J.-f., M., " Engineering design applications of multilevel optimization methods." *Computer-Aided Optimum Design of Structures: Applications* (eds. C.A. Brebbia and S. Hernandez), Springer-Verlag, 1989, pp.113-133.

Bartheelemy, J-F M., " Engineering application of heuristic multilevel optimization methods", *NASA technical memoraddum 101504*, October, 1988.

Bean, J.C., "Genetic Algorithms and random keys for sequencing and optimization," *ORSA Journal on Computing*, 6(2) , spring, 1994, pp. 154-160.

Bloebaum, C.L., Hajela, P., and Sobieszczanski-Sobieski, J., "Non-hierarchic system decomposition in structural optimization", *Engineering Optimization*, *Vol. 19*, pp. 171-186, 1992.

Braun, R.D., and Kroo, I.M., " Development and application of the collaborative optimization architecture in a multidisplinary design environment" *International Congress on Industrial and Applied Mathematics*, Humburg, Germany, August, 1995.

Braun, R.D., Gage, P.J., Kroo, I.M. and Sobieski, I., " Implementation and performance issues in collaborative optimization", *sixth AIAA/USAF/NASA/ISSMO Symposium on Multidisplinary Analysis and Optimization*, Bellevue, Washington, AIAA Paper No. 96-4017, September 4-6, 1996.

Braun, R.D., Moore, A.A, and Kroo, I.M., " Use of the collaborative optimization architecture for launch vehicle design", *Proceedings of the 6th AIAA/NASA/USAF/ISSMO Symposium on Multidisciplinary Analysis and Optimization*. Bellevue, WA, Sept. 4-6, 1996, AIAA Paper 96-4018.

Bremermann, H.J., "Optimization through evolution and recombination," in M.C. Yovits, G.Tl Jacobi and G.D. Goldman (Eds), *Self-organizing systems*, pp. 93-106, Spartan Books, Washington, D.C., 1962.

Burgee, S., Giunta, A. A., Balabanov, V., Grossman, B., Mason, W. H., Narducci, R. N, Haftka, R. T., and Watson, L. T., "A coarse-grained parallel variable-complexity

multidiscipliary optimization paradigm," *The International Journal of supercomputing applications and high performance computing*, vol. 10, pp. 269-299, 1996.

Bushnell, D., "PANDA2-Program for minimum weight design of stiffened, composite, locally buckled panels." *Computers & Structures*, 25(4), 1987, pp. 469-605.

CSA/NSATRAN, *User Manual*. Computerized Structural Analysis & Research Corporation, CA91301, 1995.

DeJong, K.A., " An analysis of the behaviour of a class of genetic adaptive systems", *Doctoral Dissertation, University of Michigan, Dissertation Abstract International*, 36(10), 5140B, (University of Microfilms No. 76-9381), 1975

DOT Users Manual, Version 4.20, *Vanderplaats Research and Development*, Inc., 1995.

Eldred, M. S. and Schimel, B. D., "Extended parallelism models for optimization on massively parallel computers," *Proceedings of 3rd World Congress of Structural and Multidisciplinary Optimization*, Buffalo, New York, pp. 215-217, 1999.

Fullmer, B. and Mkkulainen, R.," Using marker-based genetic encoding of neural networks to evolve finite-state behaviour*", Proceedings of the First European Conference on Artificial Life (ECAL-91)*, Paris, 1991.

Fukunaga, H., Sekine, H., "Stiffness design metod of symmetrical laminates using lamination parameters," *AIAA Journal*, Vol 30, No. 11, 2791-2793, 1992

Fukunaga, H., Sekine, H., A., "Laminate design for elastic properties of symmetric laminates with extension-shear or bending-twisting coupling," *Journal of Composite Materials*, Vol. 28, No. 8, 708-731, 1994.

Furuya, H., and Haftka, R.T., " Genetic algorithms for placing actuators on space structures." *Proceeding of Fifth International Conference of Genetic Algorithms*. University of Illinois at Uabana-Champaign, 17-21 July,1993, Morgan Kaufmann, Fairfax, pp. 536-542.

Gallagher, K., Sambridge, M., and Drijkoningen, G., " Genetic algorithms: an evolution from Monte Carlo Methods for Strongly Nonlinear Geophysical Optimization", *Geophysical Research Letters*, 18(3), May-June 1992, pp. 735-740

Gerard, G. " Minimum weight analysis of orthotropic plates under compressive loading", *Journal of Aerospace Science(27)*, 21-26, 1960.

Giles, G.L., "Procedure for automating aircraft wing structural design," *Journal of the Structural Divison , ASCE, Vol. 97*, January, 1971, pp. 99-113.

Goldberg, D. E., and Lingle, R., Jr. " Alleles, loci, and traveling salesman problem". Grefenstette, J.J. (Editor), *Proceedings of the First International Conference on Genetic Algorithms*, Lawrence Erlbaum Associates, Hillsdale, NJ, 1985, pp 154-159.

Goldberg, D.E., and Samtani, T.A., "Engineering optimization by a genetic algorithm". *Proceeding of 9th Conference of Electronic Computation*, ASCE. 1987, pp 471-482.

Greene, D.P., and Smith, S.F., " A genetic system for learning models of consumer choice", *Proceedings of the Second International Conference on Genetic Algorithms*, MIT, Cambridge, MA, July 28-31, 1987, pp. 217-223.

Grenestedt, J.L., Gudmundson, P., "Layup optimization of composite material structures," *Optimal Design with Advanced Materials*, editor P.Pedersen, 311-336, 1993.

Haftka, R.T. and Walsh, J.L., " Stacking sequence optimization for buckling of laminated plates by integer programming", *AIAA Journal* , 30(3), 1992, pp. 814-819.

Haftka, R. T. and Gürdal, Z., " Elements of structural optimization", Third Revised and Expanded Edition, Kluwer Academic Publishers, 1993.

Hajela, P., " Genetic search-An approach to the nonconvex optimization problem." *AIAA J.* 26(7), 1990, pp. 1205-1210.

Hajela, P., " Optimal design of viscoelastically damped beam structures", *Applied Mechanic Review*, 44(1), part 2, supplement, Nov. 1991, pp. S96-106.

Hajela, P. and Lin, C.Y., " Genetic search strategies in multicriterion optimal design", *Structural Optimization*, 4, 1992, pp.199-107.

Hinton, G.E, and Nowlan, S.J, "How learning can guide evolution", *Complex Systems*, 1(3), June 1987, pp495-502.

Holland, J.H., "Adaptation in natural and artificial systems", *University of Michigan Press*, Ann Arbor, MI, 1975.

Kaufman, M., Balabanov, V., Burgee, S.L., Giunta, A. A., Grossman, B., Hafkta, R.T., Mason, W.H. and Watson, L.T., "Variable-complexity response surface approximations for wing structural weight in HSCT design", *Computational Mechanics*, Vol.18, 1996, pp.112-126.

Kim, H., Papila, M., Mason W. H., Haftka, R. T., Watson, L. T., and Grossman, B., "Detection and correction of poorly converged optimizations by iteratively reweighted least squares," *AIAA/ASME/ASCE/AHS/ASC Structures, Structural Dynamics and Material Conference Paper AIAA-00-1525*, Atlanta, GA, April 3-6, 2000.

Kodiyalam, S., " Evaluation of methods for multidisciplinary design optimization", *Phase I, Tech. Rep. NASA/CR-1998-208716, NASA* Langley Research Center, September 1998.

Kogiso, N., Watson, L.T., Gürdal, Z., Haftka, R.T., " Genetic algorithms with local improvement for composite laminate design ", *Structural Optimization, 7(4)*, 207-218, 1994.

Kogiso, N., Watson, L.T., Gürdal, Z., Haftka, R.T., and Nagendra, S., "Design of composite laminates by a genetic algorithm with memory," *Mechanics of Composite Materials and Structures*, 1(1), September 1994, pp. 95—117.

Krasteva, D. T., Watson, L. T., Baker, C., Grossman, B., Mason, W. H. and Haftka, R. T., "Distributed control parallelism in multidisciplinary design," *Concurrency: Practice and Design*, vol. 11, pp. 435-459, 1999.

Kristinsdottir, B.P., Zabinsky, Z.B., Tuttle, M.E. and Neogi, S, " Optimal design of large composite panels with varying loads", *Composite Structures*, 51 (2001) 93-102.

Kristinsson, K.K. and Dumount, G.A., " Systems identification and control using genetic algorithms," *IEEE Transactions on Systems, Man and Cybernetics*, 22(5), September, 1992, pp. 1033-1046.

Kroo, I., " Decomposition and collaborative optimization for large-scale aerospace design ". In Multidisciplinary Design Optimization: *State of the Art, SIAM*, September, 1995.

Lansing, W., Dwyer, W., Emerton, R., and Ranalli, E., " Application of fully stressed design procedures to wing and empennage structures", *Journal of Aircraft*, Vol. 8 (9), September, 1971, pp.683-688.

Le Riche, R. and Haftka, R.T., "Optimization of laminate stacking sequence for buckling load maximization by genetic algorithm ", *AIAA J.*, 31(5), May, 1993, pp.951-956.

Le Riche, R. and Haftka, R.T., " Improved genetic algorithm for minimum thickness composite laminate design," *Composite Engineering*, 5(2), pp. 1995, 143-161.

Lekhnitskii, S.G., Anisotropic Plates, Translated by S.W. Tsai and T. Cheron, *Gordo and Breach Sci. Publ. Inc*., 1968.

Liu, B., Haftka, R.T., and Akgün, M. A.," Permutation genetic algorithm for stacking sequence optimization." *Proceedings of the 39th AIAA/ASME/ASCE/AHS/ASC Structures, Structural Dynamics and Material Conference*, Long Beach, CA, April 20-23, 1998. AIAA Paper 98-1830.

Liu, B., Haftka, R.T., and Akgün, M. A., " Composite wing structural optimization using genetic algorithms and response surfaces", *7th AIAA/USAF/NASA/ISSMO Symposium on Multidisciplinary Analysis a Optimization*, St. Louis, MO, September 2-4,1998, AIAA Paper 98-4854.

Liu, B., R.T. Haftka, M. Akgün, and A. Todoroki, "Permulation genetic algorithm for stacking sequence design of composite laminates." *Computer Methods in Applied Mechanics and Engineering*, Special issue edited by David Goldberg and Deb Kalyanmoy, Vol. 186, Elsevier Science Ltd, June, 2000.

Liu, B., R.T. Haftka, and M. Akgün, "Two-level composite wing structural optimization using response surfaces." *Journal of Structural Multidisciplinary Optimization*, Vol. 20, pp. 87-96, Springer & Verlag, 2000.

Lucasius, C.B., Blommers, M.J., Buydens, L.M.C. and Kateman, G., " A genetic algorithm for conformational analysis of DNA", *in Handbook of Genetic Algorithms*, L. Davis (Ed.), van Nostrand Reinhold Publ., New York, 1991, pp. 251-281.

McCullers, L. A., "Aircraft configuration optimization including optimized flight profiles" *Proceedings of a Symposium on Recent Experiences in Multidisciplinary Analysis and Optimization*, J. Sobieski, compiler, NASA CP-2327, pp. 395-412, 1984.

McCullers, L. A., "Flight optimization system release 5.92", *NASA Langley Research Center*, 1997.

Mesquita, L. and Kamat, M.P., " Optimization of stiffened laminated composite plate with frequency constraints", *Engineering Optimization*, 11, 1987, pp. 77-88

Michalewicz, Z., " Genetic Algorithms + Data structure = Evolution Programs". *Springer-Verlag*, 1992.

Miki, M., " Optimum design of fibrous laminated composite plates subject to axial compression." *Proceeding of the. 3rd Japan-US Composite Material Conference*, Tokyo, Technomic Publishing Co., Lancaster, 1979 , pp.1017-1019

Miki, M., " Optimum design of laminated composite plates subject to axial compression ", *Composites' 86: Recent Advances in Japan and the United States*, Eds., Kawata, K., UmeKawa, S., and Kobayashi, A., Proc, Japan-U.S. CCM-III, Tokyo, pp. 673-680, 1986.

Miki, M. and Sugiyama, Y., "Optimum design of laminated composite plates using lamination parameters," *Proc. Of the AIAA / ASME/ ASCE/ AHS/ ASC 32nd Structures, Structural Dynamics and Materials Conference*, Washington, DC. USA. AIAA Paper AIAA-91-0971, 275-283, 1991

Miki, M. and Sugiyama, Y., "Optimum design of laminated composite plates using lamination parameters," *AIAA Journal*, Vol 31, No 5, 921-922, 1993

Nagendra, S., Haftka, R.T., and Gürdal, Z., "Stacking sequence optimization of simply supported laminates with stability and strain Constraints," *AIAA Journal*, Vol. 30, No. 8, pp. 2132--2137, 1992.

Nagendra, S., Haftka, R.T. and Gürdal, Z., " Design of blade stiffened composite panel by a genetic algorithm." *Proceeding of 34th Structures, Structural Dynamics and Material Conference*, La Jolla, California, April 19-21, 1993, pp. 2481-2436, *AIAA-93-1584-CP*,

Nagendra, S., Haftka, R.T., Gürdal, Z., "PASCO-GA: a genetic algorithm based design procedure for stiffened composite panels under stability and strain constraints," In *Proc. of the Tenth DOD/ NASA/ FAA Conference on Fibrous Composites in Structural Design*, Hilton Head, South Carolina, Nov. 1-4, 1994.

Nagendra, S., Jestin, D., Gürdal, Z., Haftka, R.T., and Watson, L.T., "Improved genetic algorithms for the design of stiffened composite panels," *Computers & Structures*, Vol. 58, No. 3, pp. 543-555, 1996.

Orvosh, D. and Davis, L. " Using a genetic algorithm to optimize problems with feasibility constraints", *Proceedings of The First IEEE Conference On Evolutionary Computation, Vol. 2*, pp548-553, Orlando, Florida, June 27-29, 1994.

Papila, M. and Haftka, R. T., "Response Surfaces for optimal weight of cracked composite panels: noise and accuracy," *8th AIAA/USAF/NASA/ISSMO Symposium on Multidisciplinary Analysis and Optimization*, September 6-8, 2000, AIAA-2000-4755.

Potter, W.D., Tonn, B.E., Hilliar, M.R., Liepens, G.E., Goeltz, R.T. and Purucker, S.L., " Diagnosis, parsimony and genetic algorithms", *Proceedings of the Third Conference on Industrial and Engineering Applications of Artificial Intelligence and Expert Systems*, 1990, pp. 1-8.

Powell, D., and Skolnick, M.M., " Using genetic algorithms in engineering design optimization with nonlinear constraints", *Proceeding of the Fifth International Conference of. Genetic Algorithms*, University of Illinois of Urbana-Champaign, Morgan Kaufmann, Fairfax., 17-21 July, 1993, pp. 424-431.

Ragon, S.A., Gürdal, Z., Haftka, R.T., and Tzong, T.J., " Global/local structural wing design using response surface techniques." *Proceedings of the 38th AIAA/ASME/ASCE/AHS/ASC Structures, Structural Dynamics and Material Conference*, Kissimmee, FL, April 7-10, 1997, Part 2, pp. 1204-1214, AIAA Paper 97-1051.

Rao, S.S., Pan, T.S., and Venkayya, V.B., "Optimal placement of actuators in actively controlled structures using genetic algorithms", *AIAA Journal, 28(6)*, 1990, pp.942-943.

Rechenberg, J., " Cyhernetic solution path of an experimental problem," *Royal Aircraft Establishment*, Library Translation 1122, Farnborough, England, UK, 1965.

Renaud, J.E., and Gabriele, G.A., " Improved coordination in nonhierarchic system optimization", *AIAA Journal, Vol. 31, No. 12*, December 1993, pp2367-2373.

Renaud, J.E., and Gabriele, G.A., " Approximation in nonhierarchic system optimization", *AIAA Journal, Vol. 32, No. 1*, January 1994, pp198-205.

Schmit, L. A., and Farshi, B., " Optimum design of laminate fiber composite Plates ", *International Journal for Numerical Methods in Engineering*, 1977, pp. 623-640.

Schmit, L.A., and Ramannathan, R.K., " Multilevel approach to minimum weight design including buckling constraints", *AIAA J., 16(2)*, 1978, pp.97-104.

Schmit, L.A., and Mehrinfar, M.," Multilevel optimum design of structures with fiber-composite stiffened panel components", *AIAA J., 20(1)*, 1982, pp. 138-147.

Schoenauer, M and Xanthakis, S.," Constrained GA optimization", *Proceeding of the Fifth Int. Conference of Genetic Algorithms*, University of Illinois at Urbana-Champaign, Morgan Kaufmann, Fairfax, 17-21, July, 1993, pp. 573-580.

Shanley, F. R.," Weight-Strength analysis of aircraft structures", Second Edition, New York, Dover publications, Inc. 1960.

Shankar, J., Ribbens, C.J., Haftka, R.T, and Watson, L.T.,"Computational study of a non-hierarchical decomposition algorithm", *Comput. Optim. Appl., 2* (1993) 273--293.

Sharma, A.K., Skies, G.D., Loikkanen, M.J., and Tzong, T.J.," Aeroelastic design optimization program (ADOP) user manual version 1.1", *McDonnell Douglas Report Number MDC92K0408*, January, 1993.

Shin, Y. S., Haftka, R. T., Watson, L. T. and Plaut, R. H., "Design of laminated plates for maximum buckling load," *Journal of Composite Materials*, 1989, pp. 348-370.

Sobieski, I., and Kroo, I., " Collaborative optimization applied to an aircraft design problem ", *AIAA Paper96-0715*, Jan. 1996.

Sobieszazanski-Sobieski, J., Leondorf, D., "A mixed optimization method for automated design of fuselage structures," *Journal of Aircraft, Vol. 9*, December, 1972, pp. 805-811.

Sobieszczanski-Sobieski, J., Jame, B.B., and Dovi, A.R., " Structural optimization by multilevel decomposition ", *AIAA Journa*l, 28(3), 1985, pp1775-1782.

Sobieszczanski-Sobieski, J., Jame, B.B., and Riley, M.F., " Structural sizing by generalized, multilevel optimization ", *AIAA Journal*, 25(1), 1987, pp139-145.

Sobieszczanski-Sobieski, J., " Optimization by decomposition : a Step from hierarchic to non-Hierarchic systems." *Presented at the Second NASA/Air Force Symposium on Recent Advances in Multidisciplinary Analysis and Optimization (Held in Hampton), NASA CP-3031*, Part 1, 1988.

Sobieszczanski-Sobieski, J., " Sensitivity of complex, internally coupled systems." *AIAA Journal, Vol. 28, No.1*, January 1990.

Sobieszczanski-Sobieski, J. and Hatka, R.T., " Multidisplinary aerospace design optimization: survey of recent development", *Structural Optimization*, 14, p1-23, 1997.

Stroud, W.J., and Anderson, M.S.: *PASCO: Structural Panel Analysis and Sizing Code, Capability and Analytical Foundations*, NASA TM-80181, Nov. 1981.

Thareja, R., and Haftka, R.T., "Numerical difficulities associated with using equality constraints to achieve multilevel decomposition in structural optimization", *Proceedings of the 27th AIAA/ASME/ASCE/AHS/ASC Structures, Structural Dynamics and Material Conference*, San Antonio, Texas, May 1986, pp21-28, AIAA Paper 86-0854.

Todoroki, A., and Haftka, R.T., "Stacking sequence optimization by a Genetic Algorithm with a New Recessive Gene Like Repair Strategy " *Composite Part B*, 29(3), 1998, pp.277-285

Todoroki, A., and Haftka, R. T., "Lamination parameters for efficient genetic optimization of the stacking sequences of composite panels," *Proc. of the 7th AIAA/USAF/NASA/ISSMO Multidisciplinary Analysis and Optimization Symposium, St. Louis MO*, AIAA-98-4816, p870-879, 1998.

Torenbeek, E., " Development and application of a comprehensive, design-sensitive weight prediction method for wing structures of transport category aircraft ", *Delft University of Technology*, September 1992, Report LR-693.

Tsai, S.W., and Hahn, H.T., Introduction of composite materials, *Technomic, Lancaster*, PA, 1980.

Tsai, S.W. , and Pagano N. J., " Invariant properties of composite materials," *in Composite Materials Workshop, (Eds. Tsai, S.W., Halpin, J.C., Pagano, N.J.) Technomic Publishing Co.*, Westport, pp. 233-253, 1968.

Vanderplaats Research & Development , Inc., *DOT User Manual*, Version4.20, May,1995

Vanderplaats, Miura and Associates, Inc., *GENESIS User Mannual*, Version 4.0, Dec. 1997.

Vanderplaats, G.N., Yang, Y.J., and Kim, D.S., " Sequential linearization method for multilevel optimization", *AIAA Journal, 28(2),* 1990, pp. 290-295.

Watabe, H. and Okino, N., “A Study on genetic shape design”. *Proc. Fifth Int. Conf. Genetic Algorithms, University of Illumes at Urbana-Champaign*, pp. 445-450, Morgan Raufmann, Fairfax., 17-21, July, 1993.

Whitney, J.M, “ Structural analysis of laminated anisotropic Plates”, *Technomic Publishing Company*, Lancaster, 1985.

Yamazaki, Koetsu, “ Two-level optimization technique of composite panels by genetic algorithm”, *Proceedings of the 37th AIAA/ASME/ASCE/AHS/ASC Structures, Structural Dynamics and Material Conference*, Salt Lake City, UT, April15-17,1996, Part 4, pp. 1882-1886, AIAA Paper 96-1539

Z. Michalewicz, "Genetic Algorithms + Data Structure = Evolution Programs". *Springer-Verlag*, 1992.

BIOGRAPHICAL SKETCH

Boyang Liu was born in Baotou, Inner Mongolia (Nei Mong·Gol) Autonomy Region, China, in 1966. In 1988, he graduated from the Mechanics department of the Lanzhou University, Lanzhou, Gansu province, China, with a Bachelor of Science degree in Engineering Mechanics. In 1991, he graduated from Xian University of Architecture and Technology, Xian, Shaanxi province, China, with a Master of Engineering Science degree. From 1991 to 1996, he was an assistant professor and lecturer in Xian University of Architecture and Technology. In the summer of 1996, he joined the Multidisciplinary and Design Group of Distinguished Professor Haftka at the department of Aerospace Engineering, Mechanics and Engineering Science of the University of Florida. He earned his Doctor of Philosophy degree in Engineering Mechanics in May 2001.

.